

Università degli Studi di Padova

Dipartimento di Ingegneria Industriale



CORSO DI LAUREA MAGISTRALE IN  
INGEGNERIA AEROSPAZIALE

Tesi di laurea magistrale

**Strategia di ottimizzazione vibroacustica per un  
gearbox di turbina eolica**

Vibroacoustic optimisation strategy for a wind turbine gearbox

Relatore: Ch.mo Prof. Mirco Zaccariotto  
Correlatore: Ir. Frederik Vanhollebeke

Laureando: Piva Marco

Anno accademico 2012 – 2013



# Contents

<b>Premessa</b>	<b>5</b>
<b>Abstract</b>	<b>7</b>
<b>1 Introduction</b>	<b>9</b>
1.1 Worldwide wind energy production	9
1.2 State-of-the-art wind turbines	12
1.2.1 Extracting energy from wind with different types of wind turbines	12
1.2.2 Description of a wind turbine	17
1.2.2.1 Blades	18
1.2.2.2 Nacelle	20
1.2.2.3 Tower	21
1.2.3 Wind turbine acoustic noise	22
1.2.3.1 Mechanical noise	23
1.2.3.2 Aerodynamic noise	24
1.3 State-of-the-art gearboxes	26
1.3.1 Types of gear stages	27
1.3.2 Components of the gearbox	30
1.4 State-of-the-art in gearbox modelling	31
1.4.1 Models for gearbox dynamical behaviour	32
1.4.2 Models for gearbox NVH behaviour	32
<b>2 Simplified reproduction of the gearbox with beam and shell elements</b>	<b>39</b>
2.1 Beam and shell elements and consequences of their use	40
2.2 Simplification of the geometry	41
2.2.1 Torque arm geometry	42
2.2.2 Geometry of the gearbox without the high speed stage housing	46
2.2.3 Geometry of the gearbox	53
<b>3 Comparison with full geometry</b>	<b>65</b>
3.1 Modal assurance criterion	66
3.2 Comparison of the torque arm	67

3.3	Comparison of the gearbox without the high speed stage housing	71
3.4	Comparison of the complete gearbox	77
<b>4</b>	<b>Sensitivity analysis of the torque arm</b>	<b>87</b>
4.1	Sensitivity analysis of the torque arm	88
4.2	Influence of the suspension system	93
<b>5</b>	<b>Optimization</b>	<b>97</b>
5.1	Sensitivity analysis of the gearbox	98
5.2	Campaign of simulations	101
5.2.1	Illustration of the configurations	102
5.2.2	Results of the simulations	106
5.3	Verifications of the tolerance of any geometrical errors	111
5.3.1	First verification	111
5.3.2	Second verification	114
5.4	Final comparison	118
<b>6</b>	<b>Conclusions</b>	<b>121</b>
6.1	Building a simplified model: considerations	121
6.2	Conclusions about comparison phase in three different building steps	124
6.3	Considerations about optimisation results	126
	<b>Bibliography</b>	<b>131</b>
	<b>Ringraziamenti</b>	<b>135</b>

# Premessa

Nell'ambito dell'ingegneria delle turbine eoliche, le vibrazioni ed il rumore delle turbine costituiscono una problematica sulla quale attualmente ci si sta concentrando molto. Questo problema diventa di primaria importanza quando le turbine si trovano installate vicino ad aree urbanizzate. Portare e mantenere i livelli ed i limiti di vibrazioni a valori accettabili è un'operazione che eliminerebbe quella che probabilmente è una delle maggiori problematiche connesse all'installazione di nuove turbine eoliche, favorendo in questo modo la diffusione di una tecnologia che mai come oggi sembra essere di vitale importanza per poterci avvicinare ad un mondo più pulito e meno soggetto all'ingente quantità di problemi e rischi causati dall'inquinamento atmosferico globale.

Le procedure che predicono ed ottimizzano il comportamento vibrazionale di un gearbox di turbina eolica solitamente richiedono una geometria completa e particolareggiata. Tuttavia, nel corso dello sviluppo del gearbox di turbina eolica, tale dettagliata geometria è disponibile solamente al termine della progettazione, quando le modifiche sono quasi impossibili od oltremodo costose. Nel presente lavoro di tesi, è studiato un diverso processo, costituito da una prima fase in cui viene creata una geometria semplificata del gearbox, la quale viene poi modificata nella fase dedicata all'ottimizzazione. La leggerezza del modello semplificato permette di compiere una campagna di simulazioni, propria della fase di ottimizzazione, con un bassissimo dispendio di spazi e tempi di calcolo.

Questa tesi è il risultato di una collaborazione con ZF Wind Power, al fine di studiare l'approccio per ottenere una geometria semplificata di un gearbox di turbina eolica, in stato dell'arte, e per ottimizzare quest'ultimo in termini di rumore e vibrazioni.

Il lavoro consiste in 4 diverse fasi, ad ognuna delle quali è stato dedicato un capitolo:

- Capitolo 2.  
Sviluppo del modello semplificato, costituito da un ridotto numero di elementi beam e shell, consentendo rapidi tempi di calcolo.
  
- Capitolo 3  
Accertamento dell'accuratezza del modello semplificato per quanto riguarda il suo comportamento vibrazionale. Tale processo è stato svolto in 3 diversi momenti dello sviluppo della geometria del gearbox, in modo da facilitare un'immediata identificazione delle correzioni da apportare.
  
- Capitolo 4.  
Una fase di sensitivity analysis al fine di analizzare lo shifting della prima frequenza naturale del torque arm.
  
- Capitolo 5.  
L'ottimizzazione delle caratteristiche di NVH del gearbox, in cui le frequenze naturali sono state rimosse dal range [70 Hz - 150 Hz]. Tale ottimizzazione è guidata dalla scelta del posizionamento, della quantità e delle dimensioni di nervature in modo tale da raggiungere il suddetto obiettivo, cercando di non provocare un pesante aumento della massa della struttura.

La riproduzione della geometria semplificata, il calcolo delle frequenze naturali dei modelli full e semplificato, e le modifiche relative all'ottimizzazione sono state sviluppate tramite i software FEM MSC Patran/Nastran Student Edition 2012 ([www.mscsoftware.com](http://www.mscsoftware.com)).

Le analisi di correlazione con l'impiego delle matrici MAC sono state eseguite utilizzando il software LMS Virtual LAB.

# Abstract

In the field of the wind turbines, vibrations and noise are a problem which is getting more focus lately. This becomes an issue of primary importance when wind turbines are installed closer to urbanised areas. Bringing and keeping the vibrational and noise levels within acceptable values would solve this problem, promoting the growth and diffusion of a technology which today more than ever is of vital importance in order to approach towards a cleaner world as well as less prone to the large amount of issues and risks due to global air pollution.

Procedures which predict and optimise the noise and vibration behaviour of a wind turbine gearbox, typically require that full geometry is available. However, during the development of a wind turbine gearbox this full geometry is only available at the end of the design when modifications to this geometry are almost impossible or extremely expensive. In this thesis a different method is investigated, by building a simplified geometry of the gearbox, that afterwards is modified in the optimisation phase. The size of the simplified model allows performing a simulation campaign that is needed for the optimisation, characterised by a very low costs in terms of time and space of computation.

This thesis is the result of a collaboration with ZF Wind Power, to investigate the approach to derive a simplified geometry of a state-of-the-art gearbox of a wind turbine, and to optimise this for noise and vibration.

The work consists of 4 different phases, and a chapter is dedicated to each of them:

- Chapter 2.  
Development of the simplified model, composed of a low amount of beam and shell elements resulting in fast computation times.

- Chapter 3.  
Verification of the accuracy of the simplified model with respects to its vibrational behaviour. This process was accomplished at 3 different steps during the creation of the gearbox geometry, so as to make the identification of the corrections needed easy and quick .
  
- Chapter 4.  
A sensitivity analysis to investigate the shifting of the first natural frequency of the torque arm.
  
- Chapter 5.  
Optimisation of the NVH behaviour, based on shifting of natural frequencies out of the frequency range [70 Hz - 150 Hz]. This optimisation was driven by the choice of positioning the amount and the dimensions of ribs which reach this goal, also taking account not to heavily increase the mass of the structure.

The reproduction of the simplified geometry, the computing of the natural frequencies of the full and simplified models and the changes aimed to the optimisation were performed with the FEM software MSC Patran/Nastran Student Edition 2010 ([www.mscsoftware.com](http://www.mscsoftware.com)).

Correlation investigation using MAC matrices was performed using LMS Virtual.LAB software.



# 1 Introduction

## 1.1 Worldwide wind energy production

In a world where environmental and energetic issues are increasing, renewable energies are taking a leading role on global scenario. In the last 3 centuries mankind for every aspect of its life has developed a dependence on non renewable and polluting source of energy like fossil fuels. Now we are in a particular and crucial historical phase. The WorldWatch Institute reports in [1.1] that not only we are facing the so called peak oil, that is the time in which, due to limited natural stocks, the fossil fuels extraction ends its growth and starts to decrease. In addition to this, we are facing an historical moment in which the amount of fossil fuels burned in the world is such as to be harmful to ourselves, and to globally cause huge environmental issues.

For those reasons now more than ever the development of renewable and clean energies is of vital importance. The need for develop and improve technologies for the exploitation of such a kind of energy sources arises from the need to placate the harm which global climate has undergone, and from the need to exploit sure and inexhaustible energy sources.

The renewable source which is experiencing the fastest growth after solar PV, and is characterised by the greatest installed capacity after the hydroelectric power is wind power [1.2]. This is one of the renewable sources of most ancient conception. However, only in the recent decades the huge potential of such an energetic source has been considered. After the oil crisis of 70s

indeed, several national research programmes for the development of renewable sources were started, as reported by Arsuffi in [1.3]. Rave [1.4] describes as in the last two decades there has been an exponential growth of installed wind power, as shown in figure 1.1, overcoming each annual development forecast previously estimated by relevant international institutions, as European Wind Energy Association. The technological development that such machines have undergone has been from rotors with diameter of less than 20 meters and delivering about 50 kW, typical in the 80s, to modern rotors with about 130 meters of diameter, which supplies between 3.6 MW and 6 MW today [1.5].

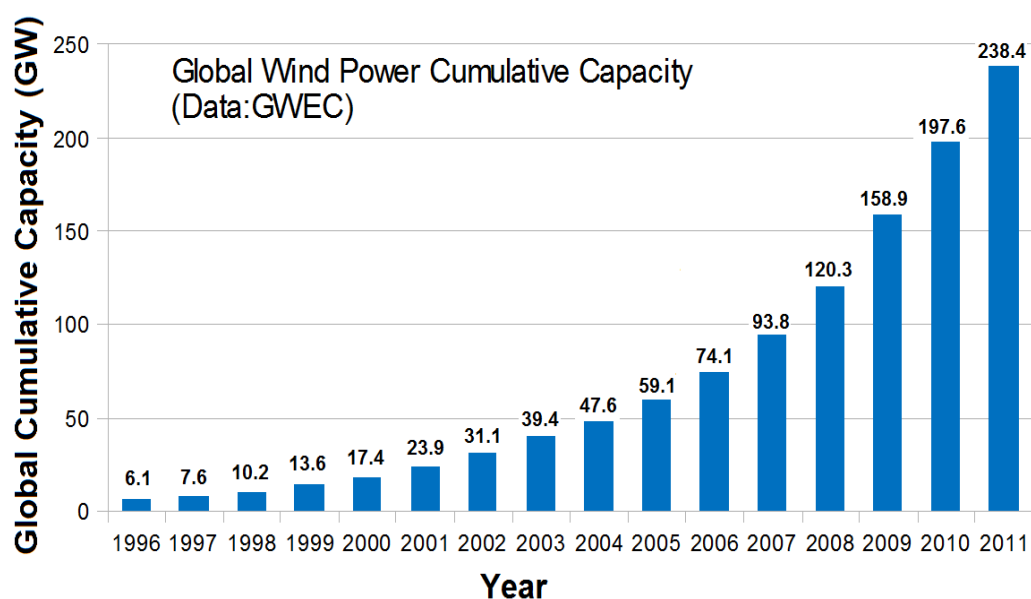


Figure 1.1. Global wind power cumulative capacity from 1996 to 2011.

From en.wikipedia.org

Presently EU is the area characterised by the highest concentration of installed wind power. However, China is the Country that has the role of major wind power producer, followed by USA, as shown in table 1.1.

Position	Country	Total Capacity by June 2012	Added Capacity first half 2012	Total Capacity end 2011	Added Capacity first half 2011	Total Capacity end 2010
		[MW]	[MW]	[MW]	[MW]	[MW]
1	China	67'774	5'410	62'364	8'000	44'733
2	USA	49'802	2'883	46'919	2'252	40'180
3	Germany	30'016	941	29'075	766	27'215
4	Spain	22'087	414	21'673	480	20'676
5	India	17'351	1'471	15'880	1'480	13'065
6	Italy*	7'280	490	6'787	460	5'797
7	France**	7'182	650	6'640	400	5'660
8	United Kingdom	6'840	822	6'018	504	5'203
9	Canada	5'511	246	5'265	603	4'008
10	Portugal	4'398	19	4'379	260	3'702
Rest of the World		35'500	3'200	32'227	3'200	29'500
Total		254'000	16'546	237'227	18'405	199'739

\* till end of May 2012 \*\* till end of April 2012

© WWEA 2012

Table 1.1. Wind power capacity of major producer Countries in the last years.

From 2012 Half-year Report, [www.wwindea.com](http://www.wwindea.com)

Presently there are different scenarios which aim to predict the future expansion of use of wind power; some are moderate, other are optimistic. Arsuffi [1.3] lists the guidelines of the new multi-megawatt machines:

- Optimisation with respect to wind features of the site
- Compatibility of the constraints imposed by the electricity network
- Optimisation of acoustic performance
- Optimisation of aerodynamic performance
- Suitability for offshore use

Although in the last decades great progress has been made regarding the performance and efficiency of wind turbines, there is still room for improvement for the most classical type of wind turbine, that is the horizontal-axis wind turbine. Ponta [1.5] suggests improvements such as: a further increase of the rotor diameter dimensions, the introduction of adaptive-blades to reduce aerodynamic loads, the concept of modular blades which allow to obtain easy-to-handle modules, as well as the use of advanced materials and manufacturing techniques.

## 1.2 State-of-the-art wind turbines

### 1.2.1 Extracting energy from wind with different types of wind turbines

A wind turbine captures the kinetic energy of the wind in a rotor which consists of some blades. These blades are coupled to an electrical generator. In order to enhance the energy capture, the turbine is mounted on a tall tower. There are two possible configurations for the turbine: horizontal, shown on the left of figure 1.2, and vertical axis, on the right of figure 1.2 (this one is called Darrieus rotor, named after its inventor).

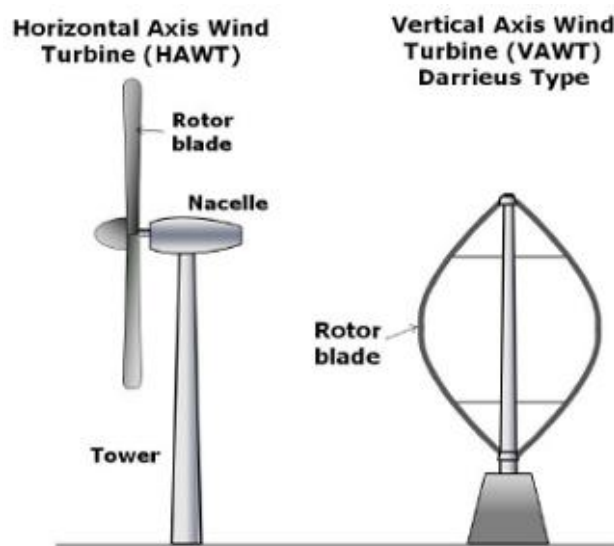


Figure 1.2: Horizontal (left) and vertical (right) axis wind turbines configurations.

From [www.people.bu.edu](http://www.people.bu.edu).

Patel [1.6] confirms that modern wind turbines use the horizontal axis design. The incoming wind in the rotor swept area is crucial for the power production of the wind tower, of course. Ackermann [1.7] shows that the kinetic energy of a cylinder of radius  $R$  (coinciding with the rotor radius) travelling at the speed  $V_W$  provides a total wind power of:

$$P_W = 0.5 \rho_a \pi R^2 V_W^3$$

With:

$\rho_a$  density of air.

R Radius of the rotor

$V_W$  Average wind speed

Extracting all the kinetic energy from the wind would imply to zero the wind speed after the rotor; this is however not possible. The wind speed is only reduced by the rotor, which extracts only a fraction of the wind power. This fraction is named power efficiency coefficient  $c_p$  of the wind turbine. Therefore, the mechanical power of the wind turbine is:

$$P_M = c_p P_W$$

The forces which act on the blade section depend on the angle incidence  $\varphi$  between the relative wind speed  $V_{rel}$  (seen from the blades) and the plane of moving rotor blades. If the wind turbulence created by the blade tip is ignored, a simple geometrical consideration can show that the incoming wind speed and the speed of the blade define the angle of incidence. Indeed, considering the equivalence

$$V_{tip} = \omega_t R$$

where  $V_{tip}$  is the speed of the blade tip and  $\omega_t$  is the turbine rotational speed, the angle of incidence can be calculated as :

$$\varphi = \arctan(V_W / \omega_t R)$$

In figure 1.3 the described parameters, as well as the angle of attach  $\alpha$  and the blade angle  $\beta$  (named pitch angle as well), are shown.

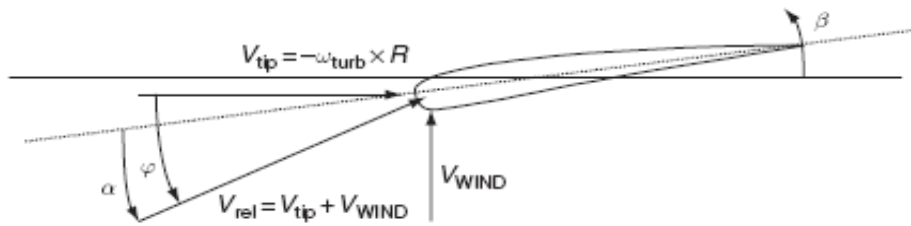


Figure 1.3. Representation of wind conditions around a moving blade.

From *Wind Power in Power Systems*. T. Ackermann.

The forces acting on the blade by the relative wind, and thus the energy extraction as well, depend on the  $\alpha$  angle. For that reason,  $c_p$  can be expressed as a nonlinear function of  $\lambda$  and  $\beta$  as follows:  $c_p = f(\beta, \lambda)$ , where parameter  $\lambda$  is the tip-speed ratio:

$$\lambda = R \omega_t / V_W$$

Older wind turbines were characterised by a fixed blade angles, thus a constant  $\beta$  angle ( $\beta_{\text{const}}$ ). In such case blades stall at high wind speeds and therefore spontaneously reduce the lift. Stall is the reduction of lift determined by the exceeding of the critical angle of attack. For angles of attack higher than the critical one, air becomes turbulent and separates from the blade, leading to a dramatic loss of lift.

Now, assuming a constant wind speed,  $\lambda$  will vary proportionally to the rotational speed of the rotor  $\omega_t$ . Thus, if the curve  $c_p - (\lambda)$  for a specific wind turbine is known, the curve  $c_p - (-\omega_t)$  will be of identical shape for different wind speeds, but widening along the rotational speed axis, as shown in figure 1.4.

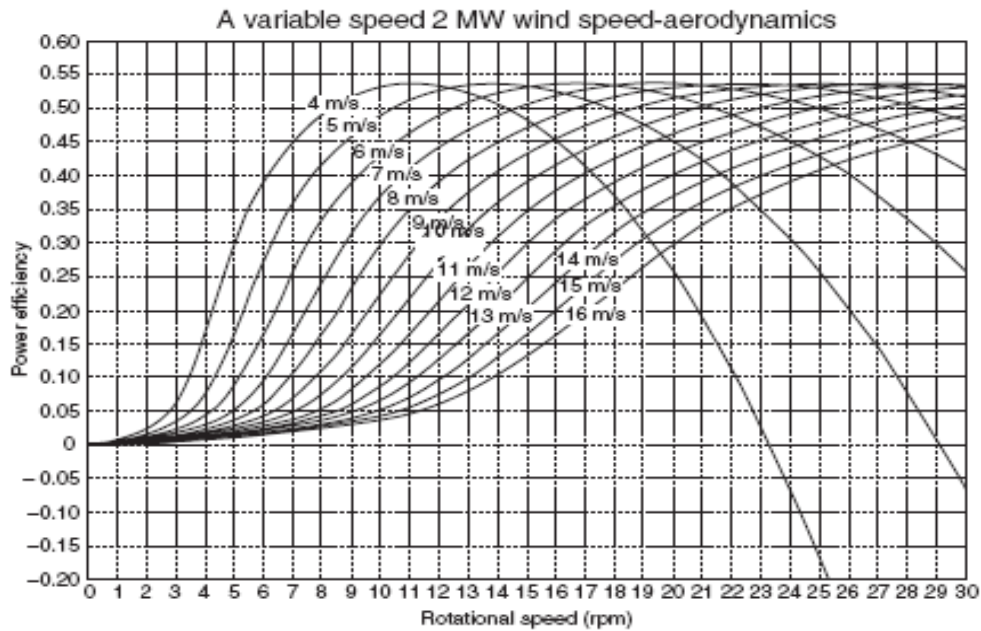


Figure 1.4. Power efficiency coefficient in function of rotational speed for wind speeds from 4 to 16 m/s.

From *Wind Power in Power Systems*. T. Ackermann.

The optimal operational point for the wind turbine is defined by identifying the point  $\lambda_{opt}$ , and consequently determining the optimal value of  $\omega_t$  as follows:

$$\omega_{t, opt} = V_W \lambda_{opt} / R$$

Such equations indicate that the fixed-speed wind turbines have to be designed so that the rotational speed match the most likely speed in the area where they are installed, while at all other wind speeds it won't be able to operate with optimised power efficiency.

As an improvement for fixed-speed wind turbines, variable-speed wind turbines were developed. In this case the turbine blades can be pitched (blade pitching means changing of the angle of attack), and the rotational speed can be adjusted to match a wide range of wind speeds, making the tip-speed ratio  $\lambda$  follow the optimal value  $\lambda_{opt}$ . Therefore, the power efficiency

coefficient  $c_p$  reaches its maximum. For that reason, the mechanical power output of a variable-speed wind turbine is higher than the one of a similar fixed-speed wind turbine, as shown in figure 1.5.

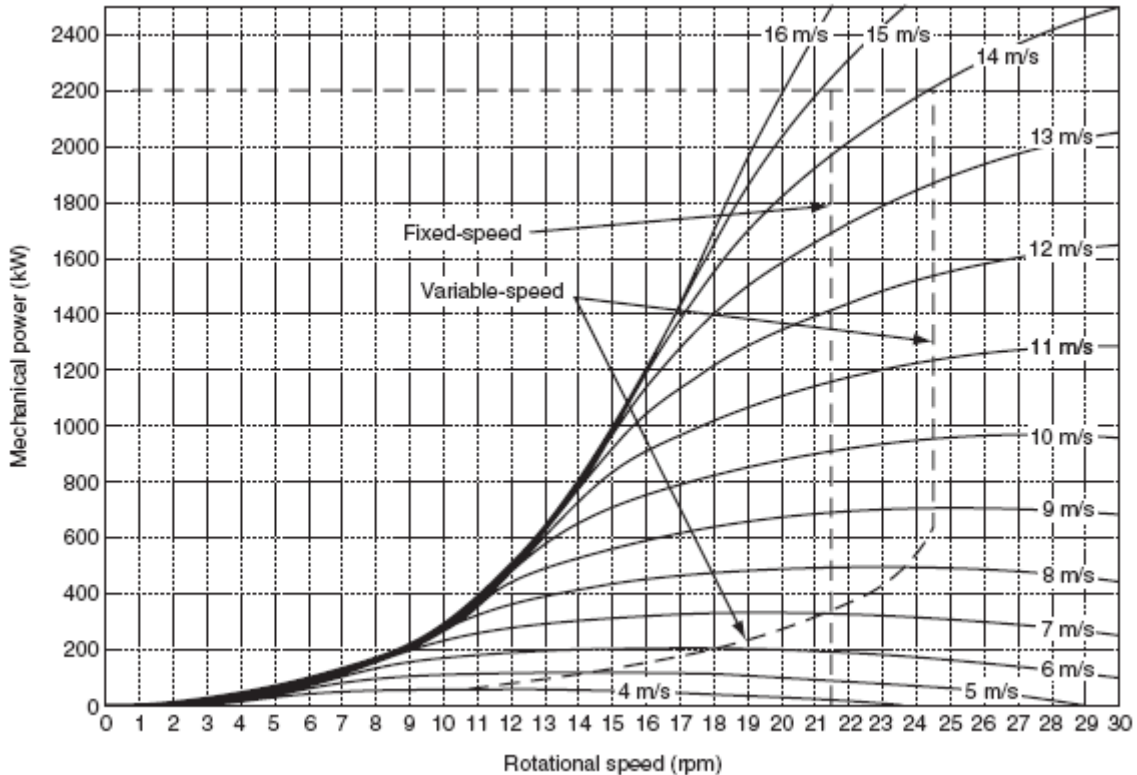


Figure 1.5. Mechanical power curves for fixed-speed and variable speed wind turbines, for speeds from 4 to 16 m/s.

From *Wind Power in Power Systems*. T. Ackermann.

This is a remarkable advantage, in addition to a better quality of power delivered to the grid and a better system stability, as remarked in [1.8]. However, these good qualities have to face some complications which cause the high costs of power electronics, control systems and generator designs. Carlin [1.9] explains that for many wind turbines developers, variable-speed operations have a key role on the wind generator of the future, given the attractive prospect of increase of performances and decrease of costs.



## 1.2.2 Description of a wind turbine

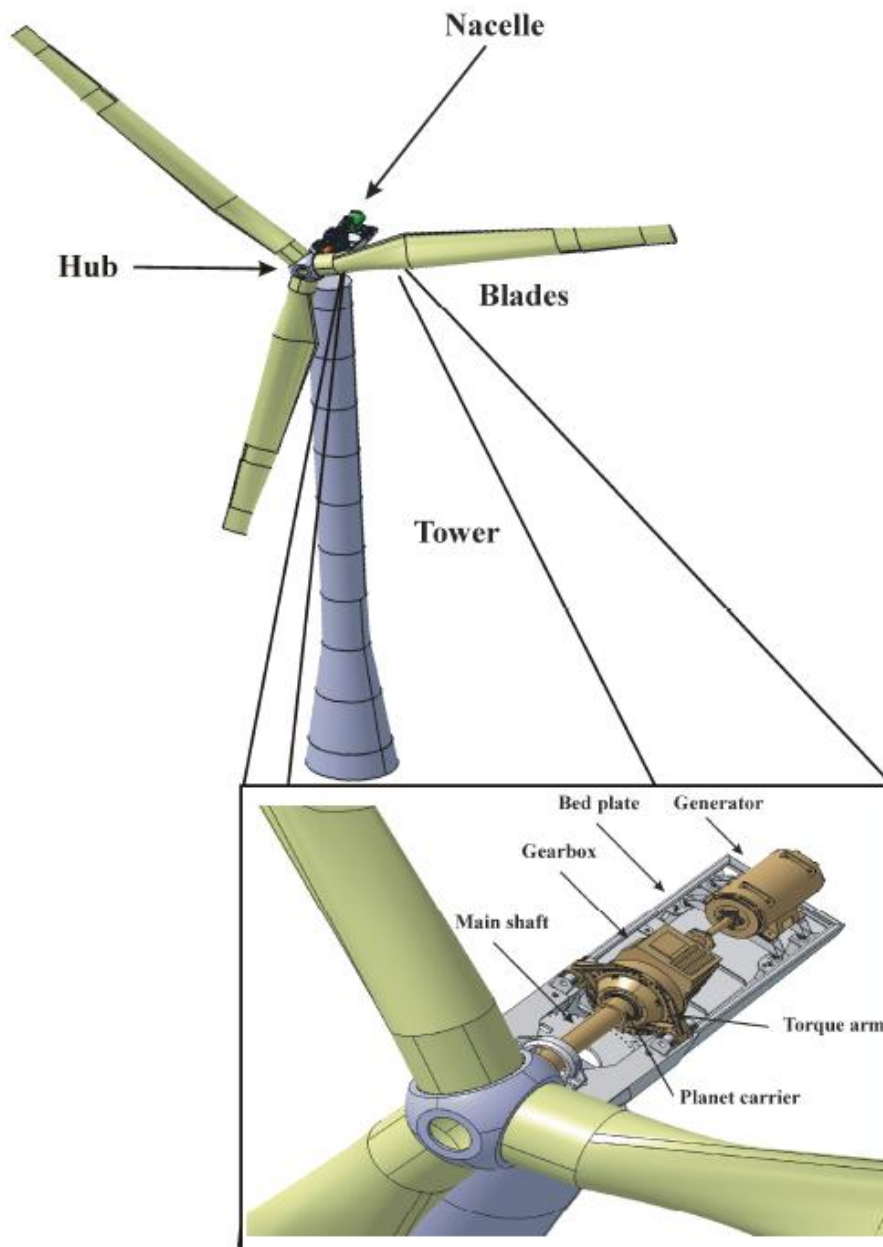


Figure 1.6. Wind turbine main components.

From: J. Helsen: *The dynamics of high power density gear units with focus on the wind turbine application*. PhD dissertation.

Horizontal-axis and vertical-axis wind turbine both have their advantages and disadvantages, but the typical kind of wind turbine is the horizontal-axis one, and this one will be considered and described. It is constituted by three main parts: the rotor blades, the nacelle and the tower, as shown in figure 1.6.

### **1.2.2.1 Blades**

Modern wind turbines have two or three blades. Peeters [1.10] observes that the configuration featured by three blades is more used because at the same power obtained and rotor diameter, such a wind turbine type needs less rotational speed. This feature lowers the issues related to noise radiation and load fluctuations.

The mechanical stress due to centrifugal forces and continuous vibrations make the design of blades a difficult task. However, such a stress is kept under a certain allowable limit, by controlling the rotor speed. This kind of control can be obtained through two ways:

- Stall control with fixed blade angle. This control is based on the stall principle: the blade is designed with a certain  $\beta$  angle. The increase of wind speed leads to an increase of the angle of attack, which can overcome the critical angle of attack. This determine stall, and thus a power decrease. This is a self-regulating control.
- Pitch control with controllable blade angle. This system has the ability to control the blade angle so as to determine a power decrease according to the wind speed. In this way, the angle of attack is determine by the control. Power can be decreased both by increasing the angle of attack (leading the blade to stall) and by decreasing the angle of attack in order to obtain power

values lower than the maximum.

Wind turbines have another control, with a different scope. Yaw control allows positioning the turbine completely on the wind, in case wind changes direction, or out of the wind, in case of failures, storms or other critical events.

Given the exposed issues, blades require to be made by light and resistant materials. Such features are met by fibre reinforced composites, which is the favourite group of materials for the blade construction, especially with glass and carbon fibres. Similarly to the aircraft wings, wind turbine blades need to be built of external panels supported by internal webs, as shown in figure 1.7. They carry the shear load and part of the bending load and restrain the cross section from deformation and the external shells from buckling.

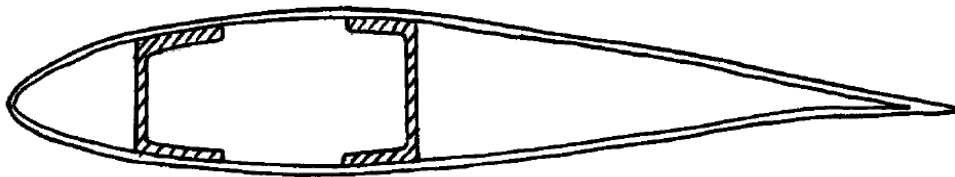


*Figure 1.7. Section of a wind turbine blade.*

*From: Guidelines for Design of Wind Turbines. Risø and DNV. [1.11]*

The blade is twisted along its axis, so as to allow it to follow the change of the resulting wind along the blade, experienced by the same blade when it rotates, as described by Risø and DNV [1.11]. Blades are fixed to the rotor shaft through the hub, as indicated in figure 1.7.

Patel [1.6] reports that the blade cost is generally kept below 10 percent of the total installation cost.

### 1.2.2.2 Nacelle

The nacelle is the set of the components installed on the top of the tower, except for the rotor blades and hub. The nacelle, as illustrated in the lower part of figure 1.6, contains the majority of the components of the wind turbine, like the low and high speed shafts, the gearbox, the generator, which are the core of the conversion from mechanical to electrical energy and are called the drive train, and it contains the blade pitch control and the yaw drive as well [1.12]. The nacelle enclosure has the function to protect these parts against the external environment, and it is usually made of fibreglass. The bed plate is the sustaining surface on which all components are supported. Such a support can rotate around the longitudinal axis of the tower. This rotation is the yawing, and is driven by the yaw drives to allow the turbine to follow the wind direction.

A detailed description of the drive train is provided by Peeters [1.10]. The drive train is composed by the generator, the gearbox, the shafts and the array of secondary components as bearings and break disk. Drive train allows to have a low rotational speed of the blades in spite of a high rotational speed at the generator. The gearbox, which will be described more in detail in paragraph 1.3, enable such a change of speed from the rotor to the generator.

The rotor introduces the mechanical energy into the drive train as a 6-components load vector. However, only the torque one is needed to produce the electricity, while the other loads are transferred towards the tower. The unnecessary loads are carried by the bearings supporting the main shaft, and the reaction torque is carried by the suspension of the gearbox.

For safety reasons, the wind turbine has always to be provided with a mechanical emergency brake, in order to be able to stop the wind turbine in case of emergency. Usually this is a brake disk with callipers, mounted at the

output of the gearbox.

### **1.2.2.3 Tower**

The tower of the wind turbine provides the necessary elevation of the rotor, in order to allow it to work at the height where the wind resource satisfies the design of the wind turbine. Usually towers of large wind turbines have tubular shape, and in some cases lattice towers are also used. They are mostly made of steel. Towers are connected to the foundation by means of a bolted connection or a weld.

Most of the towers for large wind turbines are featured by a tubular shape, with sections of 20-30 meters length. More precisely, the towers are conical, with a larger diameter at the base, where obviously the load response to the wind loading is bigger, and smaller at the top. Generally, the design of the maximum limits for the length of the tower sections and the outer diameter, has to consider the requirements to allow for transportation.

In order to calculate section loads, Risø and DNV [1.11] consider the tower as a cantilever beam, where the external loads are applied at the top of the tower.

The foundation depends on the type of site where the wind turbine is placed. Onshore wind turbines are supported by either a pile foundation or a slab foundation. Such a choice is determined by the type of soil and its particular features [1.11]. When offshore wind turbines are considered, the foundation includes a separate structure that transfer loads from the bottom of the tower to the supporting soil, through the water. This foundation has to carry loads from marine waves and current as well. Different types of foundations for

offshore wind turbine are well described by S. Malhotra in [1.13]

Recently, a floating offshore wind turbine concept has been investigated. Such a possibility is highly attractive because much of the offshore wind resource potential is available in water deeper than 30 meters. Obviously, this is the only case in which the foundations are not needed, and the basis of the tower is featured by innovative concepts, as described by J. M. Jonkman in [1.14].

### **1.2.3 Wind turbine acoustic noise**

Rogers et al. [1.15] classifies four kinds of sound which a wind turbine can generate:

1. Tonal sound. This is noise at a discrete frequency which is louder than the background noise. Tonalities can be caused by aerodynamic phenomena, but also by mechanical phenomena, such as gear meshing.
2. Broadband sound. It is usually determined by the wind turbulences interacting with the blades. It is featured by a constant sound pressure distribution with frequencies up to 100 Hz.
3. Low frequency sound. It is a kind of sound characterised by frequencies within the range [20 – 100 Hz], and is usually related to a particular type of wind turbine which has the rotor at the downwind side.
4. Impulsive sound. As suggested by the name, this type of sound is caused by short acoustic impulses, which are typical for a downwind turbine, and occurs

when the air flow is disturbed around the tower and interacts with the blades.

The noise sources emitted from wind turbines can be classified into two types:

1. mechanical noise
2. aerodynamic noise

Mechanical sounds originates from the vibrations of mechanical parts such as generator, gearbox, yaw drives and auxiliary equipment and their dynamic response. Aerodynamic sound is due to the interaction between air flow, blades and tower.

### **1.2.3.1 Mechanical noise**

Mechanical noise is determined by the relative motion of mechanical components and their dynamic response. This noise is associated to the rotational motion of the parts mentioned above and it tends to be tonal (although it can have a broadband component).

A. L. Rogers et al. reports in [1.15] an example of a 2 MW wind turbine represented in figure 1.8, that the gearbox is the main source of mechanical sounds.

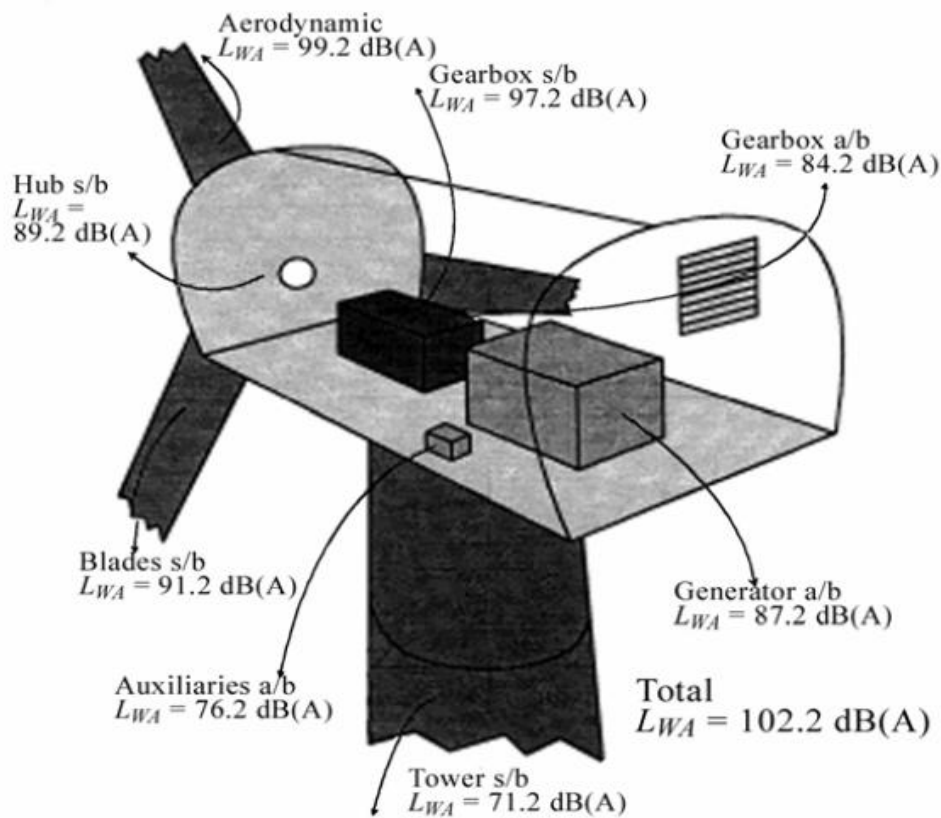


Figure 1.8. Illustration of the sound power level and its components of a wind turbine, underlining the difference between structure-borne (s/b) and air-borne (a/b) transmission path.

From: Rogers. *Wind Turbine Acoustic Noise*. [1.15]

### 1.2.3.2 Aerodynamic noise

Aerodynamic noise can be divided into three types:

- Low frequency noise. This kind of noise is related to the low frequency part of the sound spectrum, and originates from the interaction between the rotating blade and localised flow deficiencies. Flow deficiencies can be determined by wind speed variations or flow around the tower for example.
- Inflow turbulence noise. It is related to atmospheric turbulence, which result in



local pressure fluctuation around the blade.

- Airfoil self-noise. This is typically of a broadband nature, although tonal components may be produced because of blunt trailing edges or the presence of slits on the blade.

Generally, aerodynamic noise increases with the rotor speed.

The perception of wind turbine generated sound depends on some environmental factors like wind speed, distance between the wind turbine and the noise measurement location, ambient sound levels, atmospheric conditions, the surroundings,.... Wind turbine generated sound depends on some wind turbine design features. Such features can be related to the rigid attach to the hub, and thus to the shaft, the upwind or downwind configuration, the difference between rotor speed and wind speed over time. However, lower rotational speed for blades implies lower sound generation, generally. Speed of tip at blades has great influence on aerodynamic sound generation. In order to limit aerodynamic sound emissions, variable speed wind turbines are often kept at low rotor speed.

A fundamental factor to predict the perception of the wind turbine generated sound is the distance from the wind turbine. The assumption about the way that sound waves propagates is crucial for the determination of the sound pressure at certain distances from the source. It is reasonable to assume a spherical or hemispherical propagation, given the ratio between the height of the turbine (from 50 to 100 meters) and the distances sensible to higher sound levels (until 400-600 meters). Assuming spherical propagation, Rogers et al. [1.15] establish that sound pressure level decreases by 6 dB per doubling of distance from the wind turbine. At a certain distance, assuming hemispherical propagation, sound level is 3 dB higher than the one obtained with spherical propagation.

Rogers et al. [1.15] list the factors which have to be considered by an accurate sound propagation model, like source features, distance as well as ground effects and shape of the land, weather effects and particular obstacles.

Furthermore, he represents the sound spread along the distance, through a simple model based on hemispherical propagation hypothesis, as regards a wind turbine with a source sound power level of 102 dB, and 50 meters high, reported in figure 1.9.

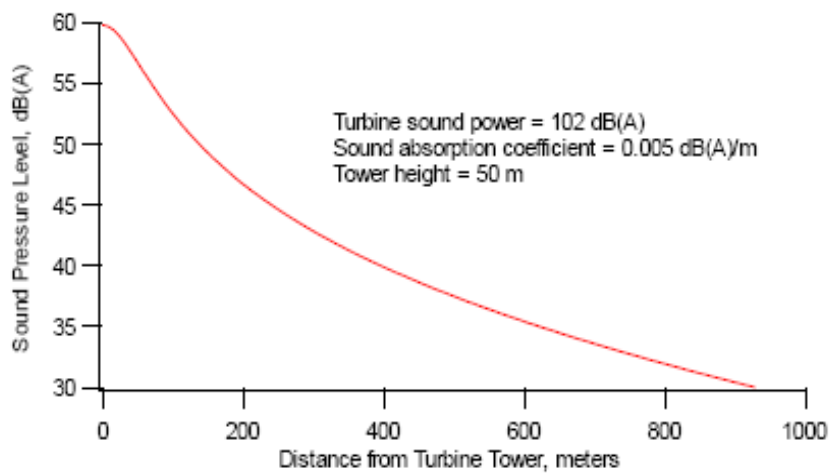


Figure 1.9. Example of the sound propagation from a wind turbine.

From Rogers. [1.15]

### 1.3 State-of-the-art gearboxes

As mentioned above, the function of the gearbox is to increase the rotational speed from the rotor to the generator, which works at about 1000 to 1500 revolution per minute (rpm). For this purpose it is placed between the main shaft and the generator, as shown in figure 1.10. Gears as well as bearings

and other parts supporting gears, are the internal components of the gearbox.

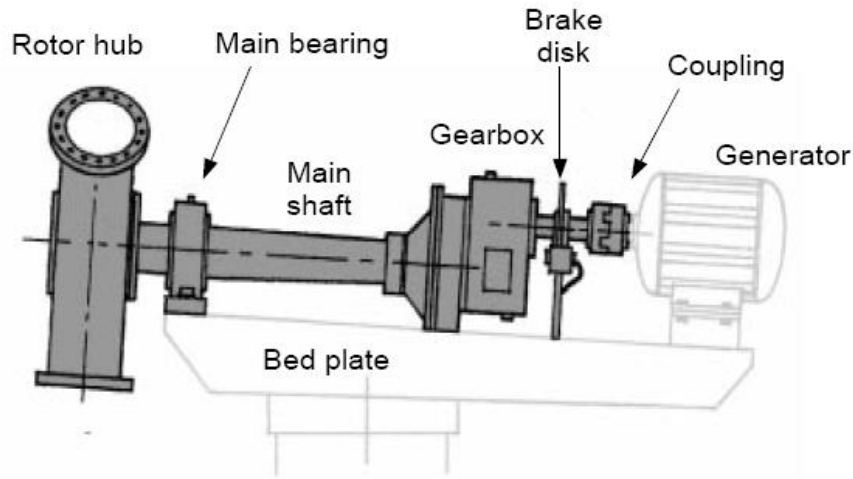


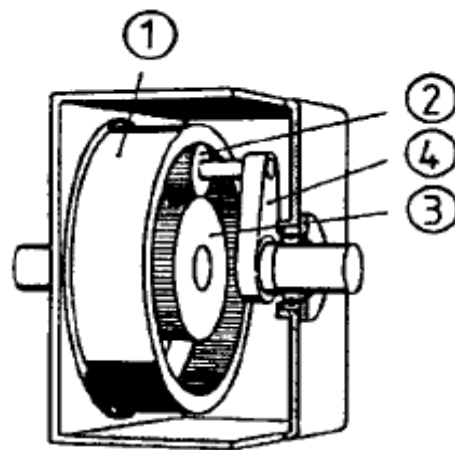
Figure 1.10. Drive train main components.

Reproduced from Bonus. Bonus-Info Newsletter. 1998.

### 1.3.1 Types of gear stages

The different dimensions of gears allows the change of rotational speed between the shafts associated to the relative gears. If the difference between the size of the wheels is 1:5, thus the shaft attached to the smaller wheel will rotate 5 times while the greater wheel accomplishes one revolution. Usually the ratio between 2 gears is kept below 1:6. Therefore, to achieve the performance which allows to pass from the typical rotor speed rotation (from 10 to 15 rpm, depending on the dimensions of the wind turbine) to the generator speed rotation, mostly a three gear stage gearbox is needed, in order to provide transmission ratios of approximately 100. Indeed, if two sets of gears are combined, and each of them is characterised by a 1:5 ratio respect to the previous stage, the global ratio resulting will be 1:25, determining the need of a third gear stage, characterised by a 1:4 or 1:5 ratio

respect the previous one, for example. In this way the output rotational speed results in 100 or 125 times the input one, getting rotational speeds typical for the generator. Given such numerical example, is easy to notice that the use of less than one or two gear stages is quite rare. H Stiesdal in [1.16] describes as wind turbines providing more than 450 kW need a planetary gearbox, that is a gearbox which contains a planetary gear stage. The planet gear is made by a wheel with interior teeth, that is the ring wheel and is stationary, three gear wheels named planet wheels, which are set on a common planet carrier. Finally, there is a central toothed gear, named sun gear wheel, around which the planet wheels rotate. The planet gearbox layout is shown in figure 1.11.



- 1 Ring wheel
- 2 Planet wheel
- 3 Sun wheel
- 4 Planet carrier

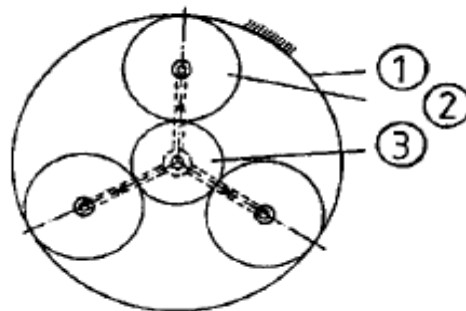


*Figure 1.11. Representation of a planetary stage.*

*From Stiesdal. The Wind Turbine. Components and Operations. Bonus-Info-1998 newsletter.*

As the three planet wheels turn around the sun gear wheel, this one gets a gear ratio of up to 1:5, and it is fixed to a shaft associated to the two normal gear stages. The normal gear stages are positioned at the end of the gearbox, that is at the side near the generator.

An advantage of this kind of gearbox is the possibility to build it compact because the ring wheel does not need to have the same size than a gear

wheel in a standard gearbox, but it can be smaller.

However, according to the needed overall gear ratio, the wind turbine gearbox consists of two planetary stages with one high speed parallel stage, or one low speed planetary stage with two parallel stages. Such a choice is determined by the value of gear ratios which characterise the stages: a parallel stage defines a gear ratio up to five and a planetary stage allows to get a gear ratio up to seven. The typical three gear stages used include one or two planetary gear stages and one or two parallel gear stages.

Hybrid architecture exists as well. It consists of one or more typically two planetary gear stages and they are used with a slow speed generator.

Usually, given the high loads they carry, teeth undergo a hardening process which is described in detail by Stiesdal in [1.16]

### **1.3.2 Components of the gearbox**

Now that the type of gears have been briefly explained and motivated, the components of the gearbox have to be described, and they are illustrated in figure [1.12]. A large wind turbine will be considered, where one or two planet stages can be found.

Starting from the input side, that is the main shaft side, the first part of the gearbox is the torque arm. Its function is dedicated to fix the gearbox to the nacelle and to prevent it from the rotating with the main shaft.

After the torque arm there is the first planetary stage.

Each planetary stage is followed by a set of bearings, collected in a bearing housing, holding the main shaft steady. In order to satisfy such a functionality, tight tolerances are required.

At the end of the gearbox, toward the generator, there is the high speed stage (there can be two high speed stages).

There are different kinds of shaft in the gearbox, as planetary shaft, sun shaft, low and high speed shaft. They have to be characterised by high strength and hardness.

The components like shafts, gears and bearings are accommodated in the gearbox housing.

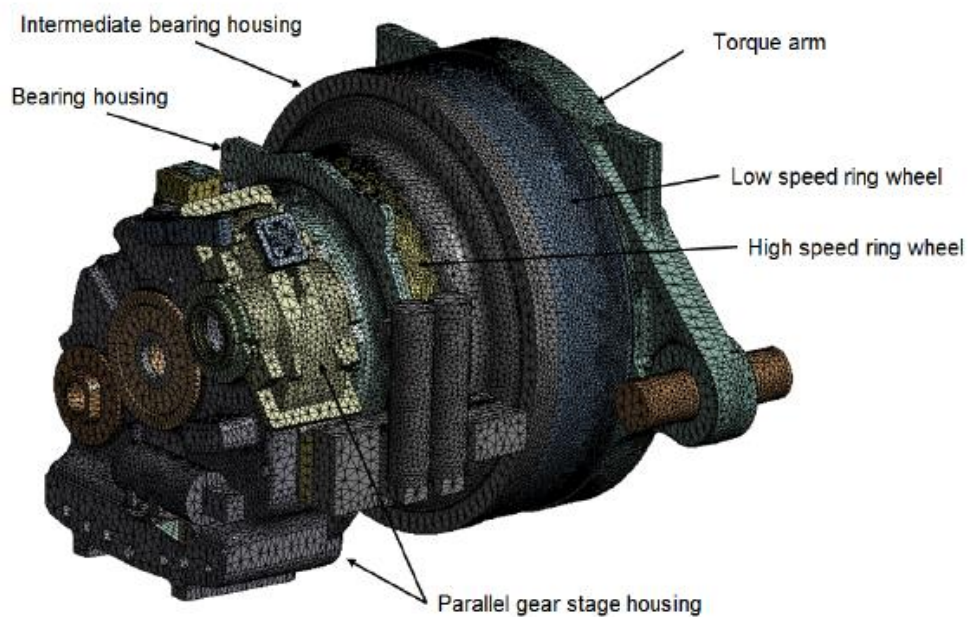


Figure 1.12. Components of the gearbox, in a FE representation.

From Vanhollebeke. Combining multibody and acoustic simulation models for wind turbine gearbox NVH optimisation. ZF Wind Power Antwerpen NV. Belgium.

## 1.4 State-of-the-art in gearbox modelling

The complex dynamics of gearbox and more widely of the entire drive train

and wind turbine is the subject of a lively research currently. Different kind of models can be used to investigate gearbox from different points of view. In this section some of the most recent strategies to study the dynamical and the NVH behaviour of a gearbox are described.

#### **1.4.1 Models for gearbox dynamical behaviour**

The interactions between the parts of a gearbox suggest the use of the multibody technique, a method especially suitable to study the dynamical behaviour of a connected array of bodies. As explained by Helsen in [1.18], such an approach allows to describe the motion of the bodies through their kinematics, and by means of elements as joints or springs connecting the bodies. Mostly those bodies are considered rigid. Precisely this consideration can be quite weighty, as it leaves no room to investigate the deformation of all internal gearbox components.

Another possibility would be modelling the entire system in finite element. Such approach accounts for structural components deformations. However, this advantage has a high price to pay, as the times for calculations are overly high.

Helsen in [1.18] investigates flexible multibody models, that is the study of the effects due to introduction of flexibility in the model, where this is considered necessary. In his work the flexible multibody technique is considered the best for the wind turbine drive train modelling, and the solutions to each issue typical of this technique are discussed.



Helsen et al. in [1.19] as well, investigate the influence of the flexibility associated to the structural components of a whole wind turbine drive train, comparing the achieved results with measurements.

This thesis investigates the implications of using a finite elements model for a gearbox housing, and seeks the needed devices to construct a simplified gearbox housing that can be considered well-representing the full model, but with quick calculation times.

#### **1.4.2 Models for gearbox NVH behaviour**

The sources of noise and vibrations for wind turbines concern the fluid turbulences occurring because of the aerodynamics of blades, the imperfections of shafts, the gear contacts, the bearings and the generator. There are two kinds of sound propagation paths: air-borne and structure-borne. Structure-borne sound is propagated through structural parts before being radiated into the air. Air-borne indicates a direct radiation from the structural component to the air.

Most of the structure-born noise originates from the vibrations occurring in gears. These vibrations propagate to the housing and determine acoustic noise. This noise propagates in the nacelle and then vibrations spread outside the nacelle.

Vibrations involve the bedplate as well, and from there propagate to nacelle, tower and blades. In this way, acoustic noise is spread to the external environment.

A widely used method in the industry in general is the FEM-BEM approach. Citarella in [1.21] indicates Finite Elements Method as suitable to study the structural behaviour, and Boundary Elements Method as fit for the acoustic estimation. However, he describes the classical approach with this method as time-consuming, because of the complex way to get the BEM solution for different frequencies and load cases.

As regards the optimisation of the helicopters gearbox NVH behaviour, Seybert in [1.22] reports that BEM technique can analyse the consequences of strategies for eventual changes in the structure, as thickness variations and changes of the housing material properties.

In the previous paragraph (1.3.1) the flexible multibody model was described as the best way to model the whole drive train including the gearbox. This is true for the calculation of the structure-borne sound as well. As regards the air-borne transfer path, there are some methods like simplified acoustic techniques and other more advanced methods as the finite element method. Such methods are characterised by a different nature. However, an efficient combination between them is crucial in order to obtain a good prediction of the sound levels.

Vanhollebeke [1.23] investigated such a combination. He assumed the gear excitation as the only excitation source inside the gearbox, as bearings take a secondary role among the excitation sources. Furthermore, he considered two transfer paths, which are represented in figure 1.13: the structural transfer path, which uses gear excitations for the calculations of the structural deformations; and the acoustic transfer path, that uses the deformations as input, and provides the total radiated sound power as output.

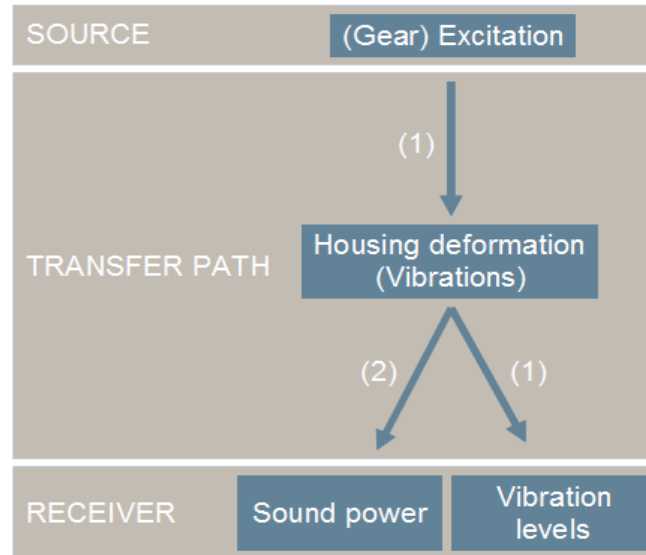
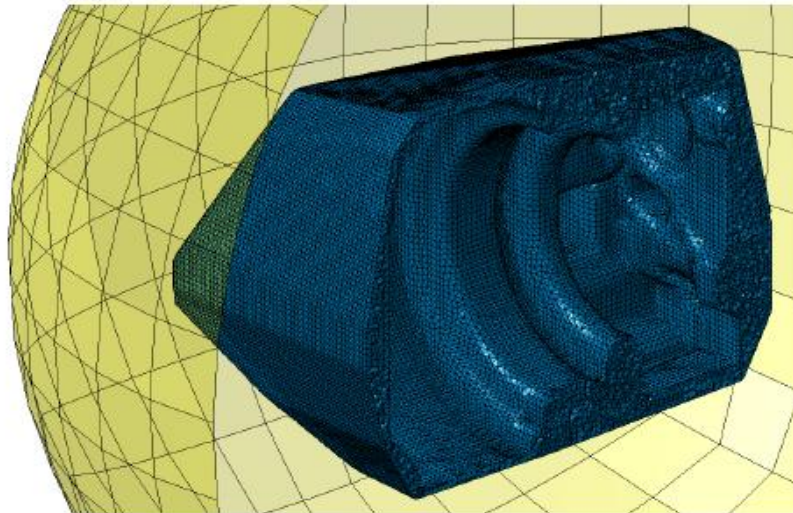


Figure 1.13. General approach used by Vanhollebeke, with the two transfer path: (1) structural and (2) acoustic.

From: Vanhollebeke. *Combining multibody and acoustic simulation models for wind turbine gearbox NVH optimisation*. ZF Wind Power Antwerpen NV. Belgium.

The acoustic transfer path was calculated using acoustic finite elements, in which the surrounding air is modelled in finite elements (see figure 1.14). By using this model, he also showed the advantages of the MATV (modal acoustic transfer vectors) as a way to link the multibody model and the acoustic model. Indeed, MATV expresses the linear relation between a certain vibrational mode and the pressure in a certain point of the studied field and are the direct output of a flexible multibody calculation. One of the results of Vanhollebeke's investigation was the identification of the gearbox parts which mostly contribute to the overall sound level.



*Figure 1.14. View of the acoustic Finite Elements mesh built by Vanhollebeke.  
From Vanhollebeke: Combining multibody and acoustic simulation models for wind turbine gearbox NVH optimisation. ZF Wind Power Antwerpen NV. Belgium.*

By considering the possibility to study the gearbox internal excitations coming from gears and other external components, and accomplishing separately such an investigation, thus the need to investigate the modal behaviour of the external gearbox parts arises. For external gearbox parts the gearbox deprived of its movable parts as gears, bearings and shafts. The resulting structure comprises: torque arm, ring wheels, bearing housing and high speed stage housing. Given a certain set of natural frequencies of this overall structure, the possibilities to remove such eigenfrequencies from the range in which there is the probability of resonance can be investigated. Such kind of study has the aim of optimising the NVH behaviour of the gearbox and is the object of this thesis. However, this approach by splitting interior and exterior parts is only related to the frequency range in which the optimisations are performed. In higher frequency ranges the dynamics of housing and internal parts will couple and won't be separable.

In this work, a wind turbine gearbox with two planetary stages and a parallel (high) speed stage is investigated. The gearbox is deprived of the internal

movable parts like shafts, gears and bearings. Investigations regarding the modal behaviour of the structure are studied through the finite elements method. The structure is built with 1D and 2D geometry, (only beam and shell elements) for the purposes exposed in chapter 2.

This thesis will continue with the description of the building of the simple model in chapter 2, in which the geometrical features as well as the approximations made with respect to the full model are reported. Afterwards, accuracy of the simplified model will be investigated in chapter 3. Chapters 2 and 3 will be articulated mostly by the multi-step strategy chosen for the building of the simple model and for the accuracy assurance process. These two chapters will deal with the first goal of this thesis, that is the investigation of the approach to derive a simplified geometry of the wind turbine gearbox. Then the sensitive analysis of the torque arm will be performed and discussed in chapter 4. In chapter 5 the optimisation of the NVH behaviour of the gearbox will be investigated, attaining the second goal of this thesis. Finally, in chapter 6 the conclusions of this work will be exposed and the results achieved will be discussed as regards the two goals as well as some considerations about further investigations.



## 2 Simplified reproduction of the gearbox

The starting point as well as the first goal of this work is to derive a basic geometry of the gearbox which represents the full model in terms of vibrational modes. Afterwards, such a model will be considered as well-representing the full one after getting a good result from the comparison process described in chapter 3. Thus, the simplified model will be used in the optimisation phase which will be explained in chapter 5.

The first aim of this thesis is to provide an investigation about which are the fundamental geometrical features, and which are negligible, in order to obtain a simplified representation of the structure that has to be characterised by a certain level of faithfulness with respect to the full model as well.

The development of a simple basic geometry is motivated by the need to produce structural changes on the gearbox. Indeed, in order to understand the kind and the entity of changes that, if brought to the structure, would allow to reach the NVH goals, a great amount of simulations are needed. Currently, building a fine mesh on a structure makes the computation a cumbersome task, that can be unsustainable if it is finalised to support a simulation campaign.

Having a simple model which corresponds to the full model in a certain frequency range would greatly increase this process. It would allow to predict the effect of certain modifications without having to modify both the detailed CAD and FE model.

For that reason an investigation into effects of the structural simplification is mandatory. The structure of the gearbox was developed in each step with beam and shell elements, whose features are described in the following paragraph.

## 2.1 Beam and shell elements

The elements used in the simplified model are beam and shell elements. In Patran, beam property uses the theory of the Timoshenko beam. While the full model is a solid and thus consists of 3D elements, building the simplified model with beam and shell elements allow to obtain a gearbox structure fully made by 1D and 2D elements. The difference between such two cases is very strong in terms of heaviness of the mesh, but not very marked in terms of functionality of finite elements. Taking for example the building of a bar, if it is a solid which consists of 3D elements, it will need an amount of finite elements which covers the geometry in the three dimensions. On the contrary, if the bar is built as a 1D structure, and consists of beam elements, these are 1D elements and their amount is very low with respect to the needed amount of 3D elements.

As regards the accuracy, although beam and shell elements bring a certain degree of approximation on 3D solid structures, the concept that 2D and 1D elements can be considered special cases of 3D elements, has to be taken into account, as considered by Falzon [2.1].

The greatest conceptual difference is between 3D elements and shell elements. While the first are characterised by 6 degrees of freedom for each node, shell elements have only 5 degrees of freedom for each node. The lacking one regards torque, that is the torsion around the normal vector of shell element. There are some devices to get a remedy in case of a structure whose main problem is the torque of some shell elements. However, this deficiency is overcome by the introduction of a physically reasonable stiffness parameter, which allows the element resists to loads at this 6<sup>th</sup> degree of freedom as well.

For that reason, the use of beam and shell elements is more efficient than the creation of 3D elements, which are much more demanding on computation resources. Indeed, Falzon [2.1] suggests that when a structure can be



approximated into a 1D or 2D structure within acceptable tolerances, a rule of thumb is to do such approximation. The lightness of beam and shell elements allowed to get a simplified gearbox model whose structure can be quickly modified and analysed in the scope of the optimisation of its vibrational behaviour.

Building of the model was done in several steps. Section 2.2.1 describes the modelling of the torque arm. Section 2.2.2 describes the modelling of the subsequent parts of the gearbox except the high speed stage housing. Finally, section 2.2.3 describes the addition of this last part, completing the characterisation of the gearbox.

## **2.2 Simplification of the geometry**

An understanding of the simplifications brought to the basic geometry of the gearbox is possible without describing the technical details of the full geometry provided by ZF Wind Power.

The key aspect of the simplified model is its building through beam and shell elements, and the absence of 3D elements.

The building process of the gearbox started from the torque arm, ending at the high speed stage housing. Pictures extracted from Patran show the 3D features assigned to the properties of the beams, but do not display thickness of the shells. For that reason the surfaces appear plate, unlike the beams. While the surfaces are characterised only by their thickness, each beam is featured by the two dimensions of its section and by the offset, which is the distance between the neutral axis of the beam and the curve that supports the beam. Except for a particular beam in the high speed stage housing, all

designed offset values were along axial dimension (that is the z dimension represented in figure 2.1, 2.4 and 2.9).

### **2.2.1 Torque arm geometry**

The torque arm geometry is the most complex among the parts of the gearbox, after the high speed stage housing.

In the full model, surfaces have several details and are characterised often by a inhomogeneous thickness. In some cases they are even curved. Thus, a certain thickness value that represents the best possible the one of the full model, was assigned to each surface of the simplified model. Then, such a value was often modified in order to obtain a good correlation with the vibrational behaviour of the full model, through the comparison process described in chapter 3.

The parameters which define the torque arm are illustrated in figures 2.1 and 2.2, and their values are collected in table 2.1.

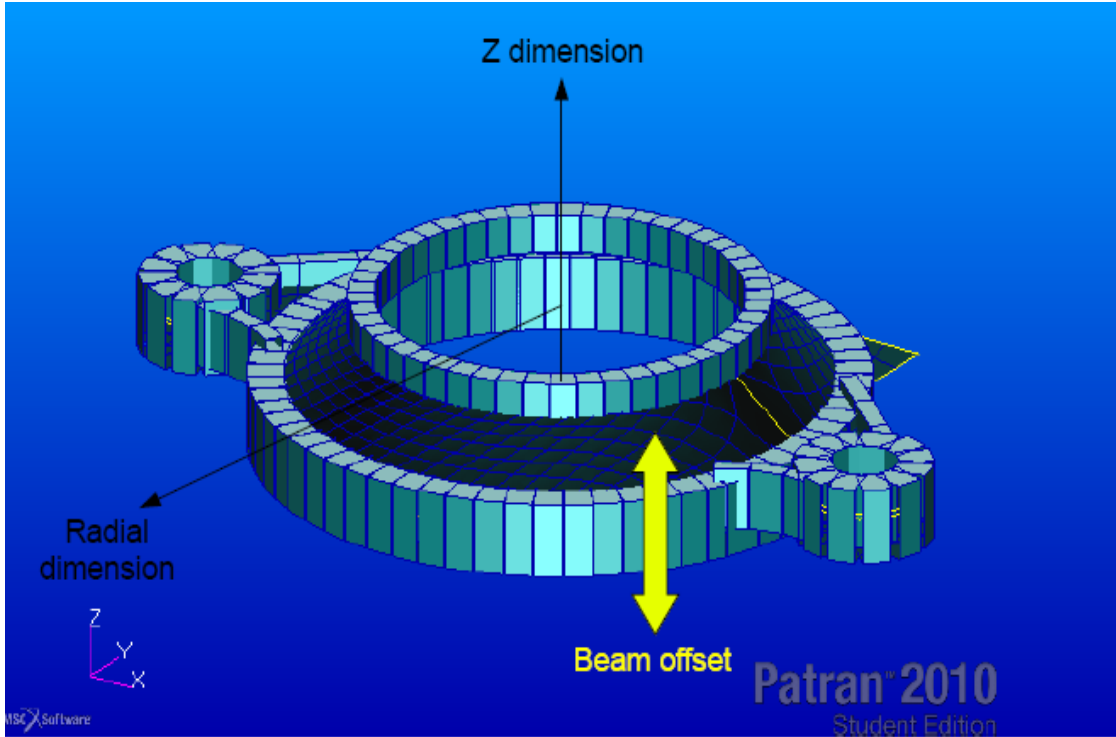


Figure 2.1: Some parameters of the torque arm

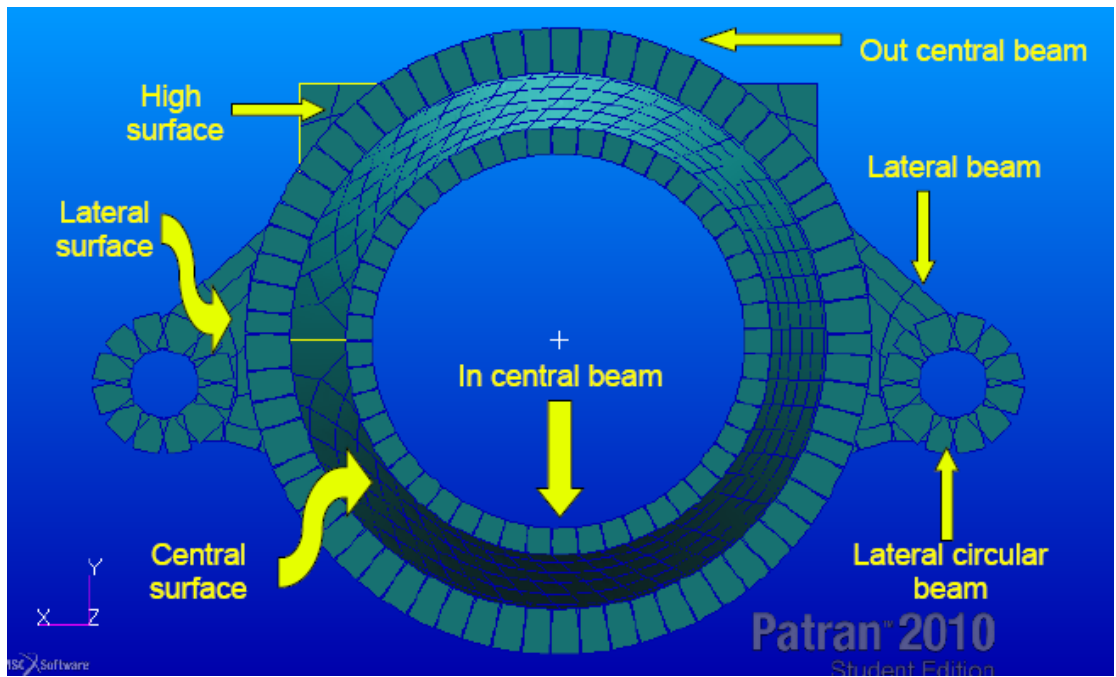
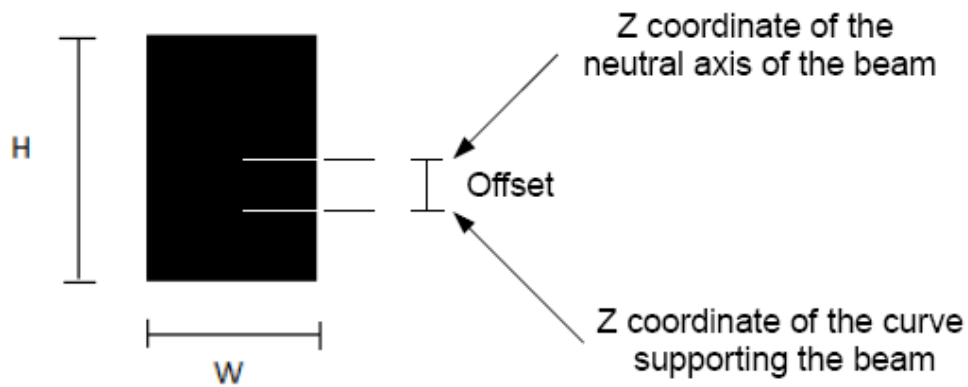


Figure 2.2: Some parameters of the torque arm

<b>Torque arm parameters</b>	<b>Reference value [m]</b>
Central surface: thickness	0,079
Lateral surfaces: thickness	0,129
High surfaces: thickness	0,104
In central beam: radial dimension	0,096
In central beam: z dimension	0,134
In central beam: offset	0,015
Out central beam: radial dimension	0,158
Out central beam: z dimension	0,255
Out central beam: offset	-0,090
Lateral circular beams: radial dimension	0,128
Lateral circular beams: z dimension	0,259
Lateral circular beams: offset	-0,020
Lateral beams: W dimension	0,066
Lateral beams: z dimension	0,209
Lateral beams: offset	-0,025

*Table 2.1: Values of the torque arm parameters*

Sections of each beam present in the torque arm are rectangular, with their two dimensions represented in figure 2.3, where H and W are the dimensions of the section requested by Patran. In figures 2.1 and 2.2 and in table 2.1 such dimensions were translated respectively in z dimension and either W or radial dimension, depending on the non-circular or circular shape of the beam.



*Figure 2.3: Section of beams present in the torque arm, with dimensions and offset indicated. In this case the  $H$  dimension of the section is supposed following the  $z$  coordinate of the reference system, and the offset is referred to the direction along  $H$  dimension of the section.*

In order to build the simplified torque arm showed in the figures above, some approximations were made. They are:

- Neglect the slight variation of the central surface thickness and its slightly curved shape
- Neglect three little circular ribs present on the central surface. Two of them have a hole in their centre, penetrating the surface.
- Neglect the irregular thickening of a few areas belonging to the lateral surfaces. Thus, an equivalent average thickness was attributed to the lateral surfaces, searching an as good as possible correspondence with the actual irregular one.
- Shape of the lateral beams was simplified from a slightly more complex shape to a straight segment or to an arc.
- The edges are sharp, while in the full model they are blunt.

Such a simplified model attained the needed good results, as regards the vibrational behaviour.

### **2.2.2 Geometry of the gearbox without the high speed stage housing**

The subsequent step in the gearbox building process was the creation of the first stage ring wheel, intermediate bearing housing, second stage ring wheel and bearing housing. The two ring wheels were modelled with a surface representing the main structure and many beams with T section, representing the teeth. This can be noted through a comparison between figures 2.5 and 2.6. Including the teeth in the simplified model have the purpose to well represent the stiffness of the two rings with respect to the full model, without increasing the thickness of the surface of each ring wheel, and thus avoiding a considerable increase of their overall mass. When the parts listed above were built, the comparison of the natural frequencies did not show a good correspondence between the full and the simplified model. For that reason many parameters were changed both in the new 4 parts and in the already built torque arm. Indeed, the variation of some parameters already defined through a previous comparison phase was found to be the easier way to approach the vibrational behaviour of the simplified model to the full one. After bringing the variations at the new 4 parts listed in table 2.2, and testing several other changes, the variations of the torque arm parameters collected in the same table showed an immediate improvement of the vibrational behaviour. Such changes allowed to obtain a well-related model, according to the comparison process.

In figure 2.4 parameters and parts of the simplified model are illustrated. In

red colour, the inner surface of the intermediate bearing housing is showed, and it is bordered by the mid and internal circular beams. Such parameters were underlined with red colour in order to make them noticeable despite their internal position. The mid circular beam is the lower border of the internal surface, and the internal beam is the upper border.

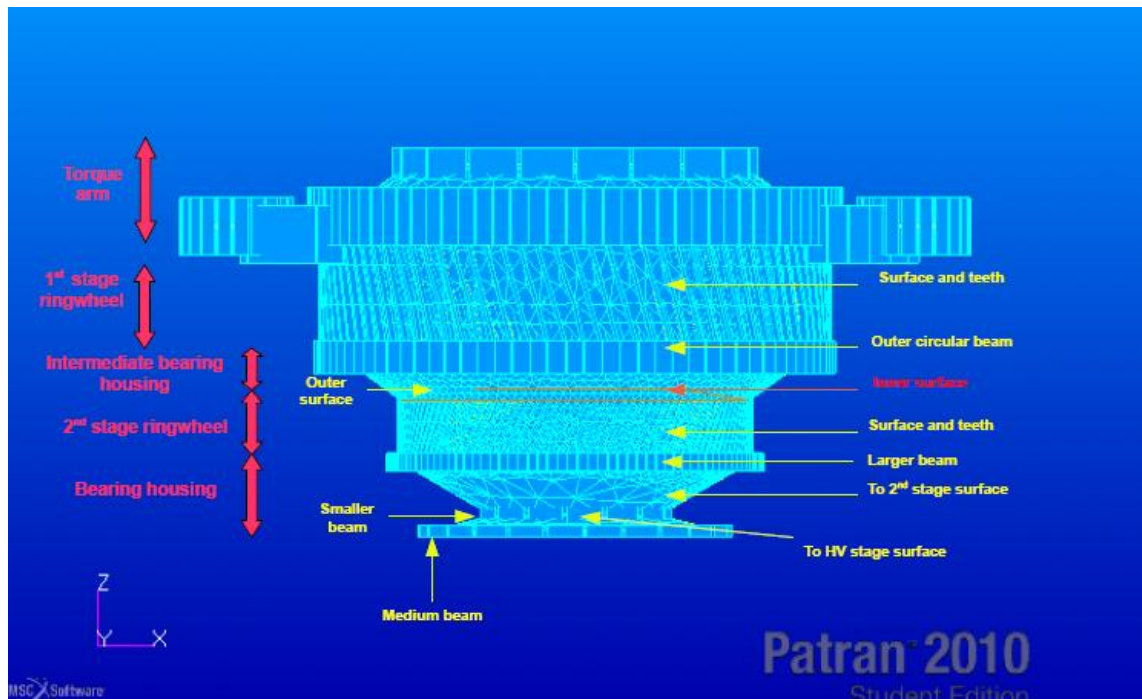


Figure 2.4: Parameters composing the 1<sup>st</sup> and 2<sup>nd</sup> stage ring wheel, intermediate bearing housing and bearing housing.

Figures 2.5 and 2.6 are the shaded representations of this part of the gearbox, respectively without and with the 3D display of the beams.

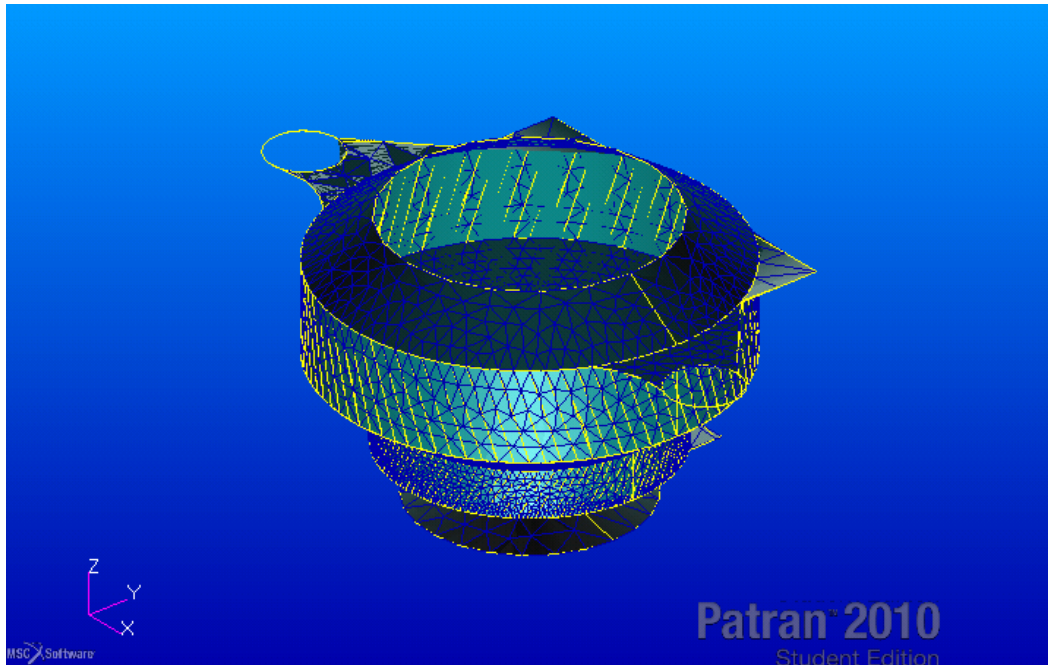


Figure 2.5: Shaded representation of gearbox without high speed stage housing, without 3D beams display.

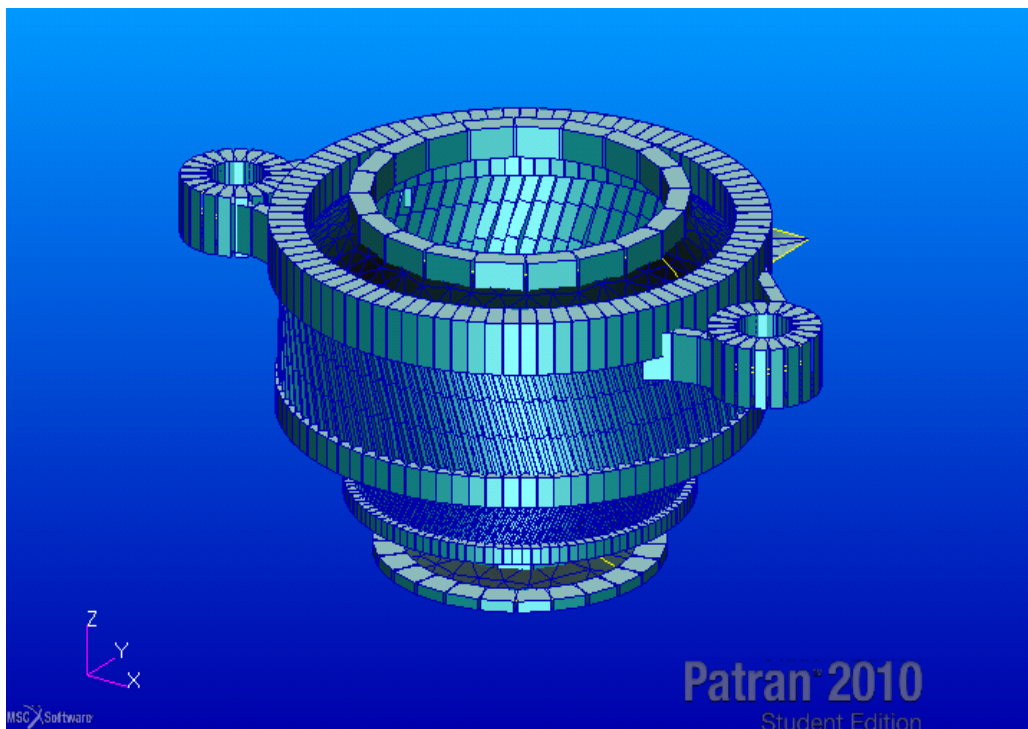
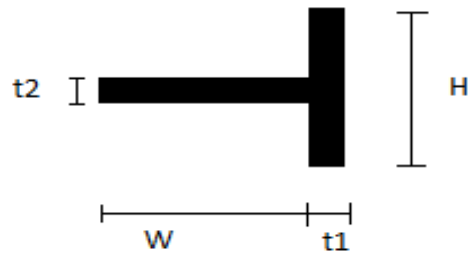


Figure 2.6: Shaded representation of gearbox without high speed stage housing, with 3D beams display.



The section of the teeth beams is showed in figure 2.7, with references to the used dimensions. All other beams have the section represented in figure 2.3, with the same names of dimensions.



*Figure 2.7: Section and dimensions of beams composing the teeth of 1<sup>st</sup> and 2<sup>nd</sup> stage ring wheel.*

In table 2.2 the changed parameters from the first to the second version of this gearbox building step are underlined. Some of the greatest variations are offset of beams, but this can be motivated by the fact that the offset of beams is the most difficult parameter to define by the only observation and dimensioning from the CAD model. The largest percentage of variation from the first version of the simplified model was given to the outer surface thickness of the intermediate bearing housing. Such surface, like other surfaces of the bearing housing and intermediate bearing housing as well, is characterised by a very irregular thickness and shape and some imperfections as holes. For that reason the great entity of the change was considered possible.

**Values of the parameters [m]**

<b>Part</b>	<b>Parameter</b>	<b>1<sup>st</sup> version model</b>	<b>2<sup>nd</sup> version model</b>	<b>Difference from the 1<sup>st</sup> version</b>	<b>Percentage of change from the 1<sup>st</sup> version</b>
1 <sup>st</sup> stage ring wheel	surface thickness	0,212	0,172	-0,040	-18,8
	beams (teeth): W dimension	0,023	0,033	0,010	41,6
	beams (teeth): t1 dimension	0,023	0,013	-0,010	-45,3
	beams (teeth): t2 dimension	0,016	0,016	0,000	0,0
	beams (teeth): H dimension	0,059	0,059	0,000	0,0
2 <sup>nd</sup> stage ring wheel	surface thickness	0,103	0,073	-0,030	-29,1
	beams (teeth): W dimension	0,012	0,018	0,006	47,4
	beams (teeth): t1 dimension	0,012	0,006	-0,006	-52,6
	beams (teeth): t2 dimension	0,010	0,010	0,000	0,0
	beams (teeth): H dimension	0,031	0,031	0,000	0,0
Bearing housing	to 2 <sup>nd</sup> stage surface thickness	0,377	0,058	-0,319	-84,6
	to HV stage surface thickness	0,068	0,078	0,010	14,7
	high surfaces (ears) thickness	0,052	0,035	-0,017	-32,7
	smaller beam: W dimension	0,073	0,103	0,030	41,3
	smaller beam: H dimension	0,085	0,085	0,000	0,0
	medium beam: W dimension	0,110	0,160	0,050	45,5
	medium beam: H dimension	0,049	0,059	0,010	20,4
	larger beam: W dimension	0,114	0,114	0,000	0,0
	larger beam: H dimension	0,072	0,072	0,000	0,0

Intermediate bearing housing	inner surface	0,082	0,062	-0,020	-24,4	
	outer surface	0,071	0,190	0,119	168,0	
	inner circular beam: W dimension	0,056	0,056	0,000	0,0	
	inner circular beam: H dimension	0,117	0,117	0,000	0,0	
	mid circular beam: W dimension	0,076	0,076	0,000	0,0	
	mid circular beam: H dimension	0,219	0,219	0,000	0,0	
	outer circular beam: W dimension	0,100	0,100	0,000	0,0	
	outer circular beam: H dimension	0,130	0,130	0,000	0,0	
	outer circular beam: offset	-0,045	-0,045	0,000	0,0	
	Torque arm	central surface thickness	0,089	0,095	0,006	7,1
		lateral surfaces thickness	0,179	0,155	-0,024	-13,5
		high surfaces (ears) thickness	0,104	0,094	-0,010	-9,6
outer circular beam: W dimension		0,158	0,148	-0,010	-6,3	
outer circular beam: H dimension		0,225	0,235	0,010	4,4	
outer circular beam: offset		0,095	0,035	-0,060	-63,2	
lateral beams: W dimension		0,066	0,070	0,004	6,1	
lateral beams: H dimension		0,209	0,232	0,023	11,0	
lateral beams: offset		-0,025	-0,035	-0,010	40,0	
circular lateral beams: offset		0,128	-0,005	-0,133	-103,9	
circular lateral beams: W dimension		0,128	0,094	-0,034	-26,6	
circular lateral beams: H dimension		0,259	0,230	-0,029	-11,2	
circular lateral beams: offset		-0,020	-0,005	0,015	-75,0	

inner circular beam: W dimension	0,096	0,096	0,000	0,0
inner circular beam: H dimension	0,134	0,134	0,000	0,0
inner circular beam: offset	0,015	0,015	0,000	0,0

*Table 2.2: Values of parameters of the gearbox without the high stage speed housing. The changed parameters from the first to the second version are underlined.*

The simplifications brought in the building of such parts of the gearbox are:

- Neglect the several holes which characterise intermediate bearing housing and bearing housing.
- Neglect the small ribs in the surfaces of intermediate bearing housing and bearing housing.
- Neglect the protrusions present in beams of intermediate bearing housing and bearing housing.
- Neglect the variation of thickness which characterise the surfaces of intermediate bearing housing and bearing housing.
- Neglect the blunt shape of edges which characterises the full model, by making them sharp in the simplified model.
- Approximate the trapezoidal section of the teeth of first and second stage ring wheel to the T section showed in figure 2.7.

First and second stage ring wheel are easy to faithfully represent in the simplified model, because of their regular shape. The teeth section was the feature submitted to the greatest approximation among the two ring wheels, but inclination and distance between teeth of the full model were respected in

the simplified model.

Intermediate bearing housing and bearing housing underwent the heaviest geometrical approximations because of their complexity. This complexity allowed to justify a marked variation of value of some parameters of intermediate bearing housing and bearing housing. These marked variations were necessary in the phase of the research of a good correspondence between the models in terms of vibrational behaviour. However, such variations were not so big to leave a realistic geometrical correspondence with the full model.

### **2.2.3 Geometry of the gearbox**

Once the second version of the gearbox configuration without the high speed stage housing was completed, and satisfied the accuracy assurance process which will be described in chapter 3, the last building step of the gearbox started. Such a step is based on the creation of the high speed stage housing, which has the most complex geometry of the gearbox. It consists of surfaces with several little and big holes and ribs, with a very complex internal geometry as well. However, globally it has a boxy shape, and such a feature was particularly used. Indeed, the high speed stage housing was approximated to a box, outlining the features which mainly characterise its geometry and vibrational behaviour.

A first approach which searches a heavy simplification of the high speed stage housing by reducing it to almost a box was examined, and the result is shown in figure 2.8. It consists of a box that is almost a half parallelepiped at the front side, and a half cylinder at the back side. At the upper surface, the high speed stage housing is adjacent to the bearing housing, without internal surfaces or any other elements which are not visible in the representation of

figure 2.8. At the lower surface a hole with diameter of 0.48 m was built. All circular holes built until this point in the gearbox are concentric along the z axis. These are all features which characterise the simple first version of the high speed stage housing.

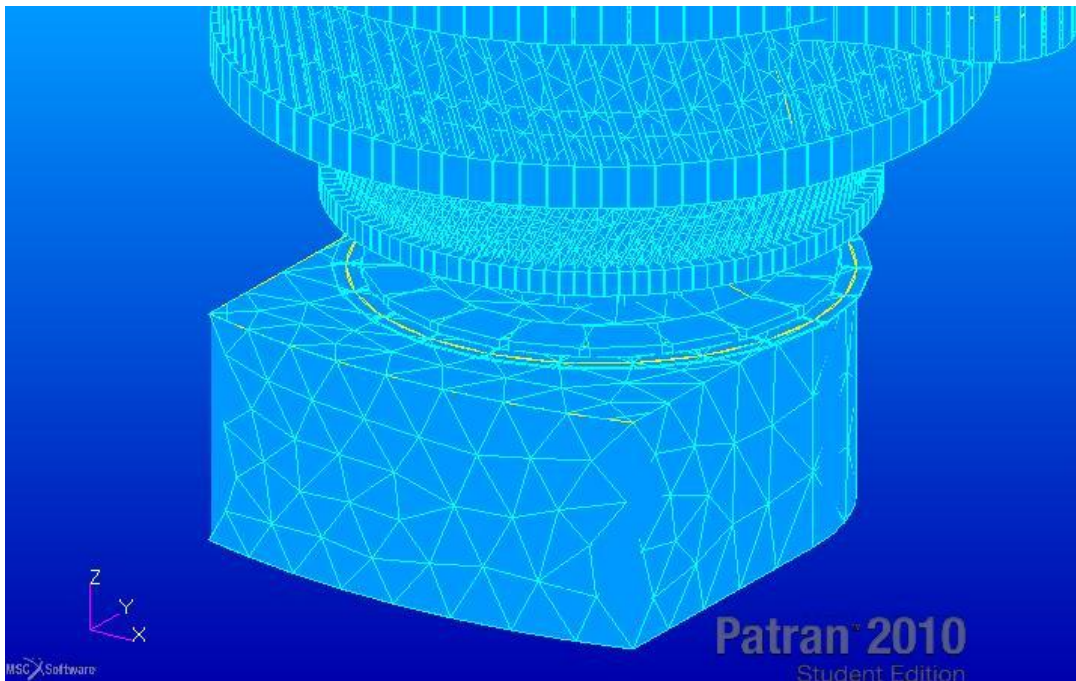


*Figure 2.8: First building approach to the high speed stage housing, with a heavy simplification.*

This first very simple version was useful to test the effects of such a heavy simplification of the high speed stage housing. However, its vibrational behaviour was far from becoming a structure well-related to the full model. In order to obtain values of natural frequencies which satisfy the comparison phase, thickness of the surfaces of the bearing housing had to be increased too much (until the values expressed in table 2.7 as parameters of the first version model) for keeping a realistic geometrical correspondence with the full model. For that reason a second and more accurate version of the high speed stage housing was created. The geometrical changes which brought to such a version are:

- 1) Rebuild a smaller high speed stage housing. In table 2.3 the key dimensions of the old and new model are compared. X, y and z dimensions are referred to the coordinate system shown in figure 2.8, 2.9 and 2.10.

	Old model	New model
lateral square surface: x dimension	1.414 m	1.011 m
lateral square surface: y dimension	1.625 m	0.385 m
lateral circular surface: radius	0.707 m	0.650 m
z dimension of high speed stage housing	0.696 m	0.413 m

*Table 2.3: Differences between the geometries of 1<sup>st</sup> and 2<sup>nd</sup> version of high speed stage housing.*

- 2) Create a toroidal surface at the top of the high speed stage housing. Such surface, underlined with red colour in figure 2.9, is internal and adjacent to the medium beam of the bearing housing. The diameter of the hole is 0.48 m, the same of the hole at the lower surface. The two holes are concentric along the z axis.
- 3) Create 2 beams at the front side of the high speed stage housing. Such beams have the geometrical features collected in table 2.4, and in figure 2.9 are indicated as front beams.

Direction of the beams:	parallel to y ax
Distance between the beams:	0.554 m
Section of the beams:	0.03 m x 0.03
Offset of the beams (in y direction):	-0.015 m

*Table 2.4: Geometrical parameters of the two beams created in the 2<sup>nd</sup> version of high speed stage housing.*

- 4) Create 2 holes at the bottom surface, decentralised from the z axis, and with the geometrical features collected in table 2.5. The holes are observable in figure 2.10.

	radius	center position point
1 <sup>st</sup> hole	0.145 m	[0.277, -0.4, -1.157] m
2 <sup>nd</sup> hole	0.145 m	[-0.277, 0.4, -1.157] m

*Table 2.5: Geometrical features of the two holes created at the bottom surface, in the 2<sup>nd</sup> version of high speed stage housing.*

- 5) Distinguish the bottom surface into 2 surfaces, as showed in figure 2.10. Such operation was made in order to give to bottom surface a greater degree of detail in order to be more faithful to the full model geometry. Moreover, the division of this surface allows to have one more parameter available to be changed in view of the vibrational goal. The difference between the old single surface and the two new surfaces are summarised in table 2.6.

Bottom greater surface thickness	0.067 m
Bottom smaller surface thickness	0.033 m
Old model whole surface thickness	0.085 m
Division plan: perpendicular to the y axis, and at the coordinate y=-0.6 m	

*Table 2.6: Differences of bottom surfaces between the 1<sup>st</sup> and 2<sup>nd</sup> version of high speed stage housing.*

Figures 2.9 and 2.10 show the second version of the high speed stage housing, with references to the parameters. Figure 2.10 shows a view from below.



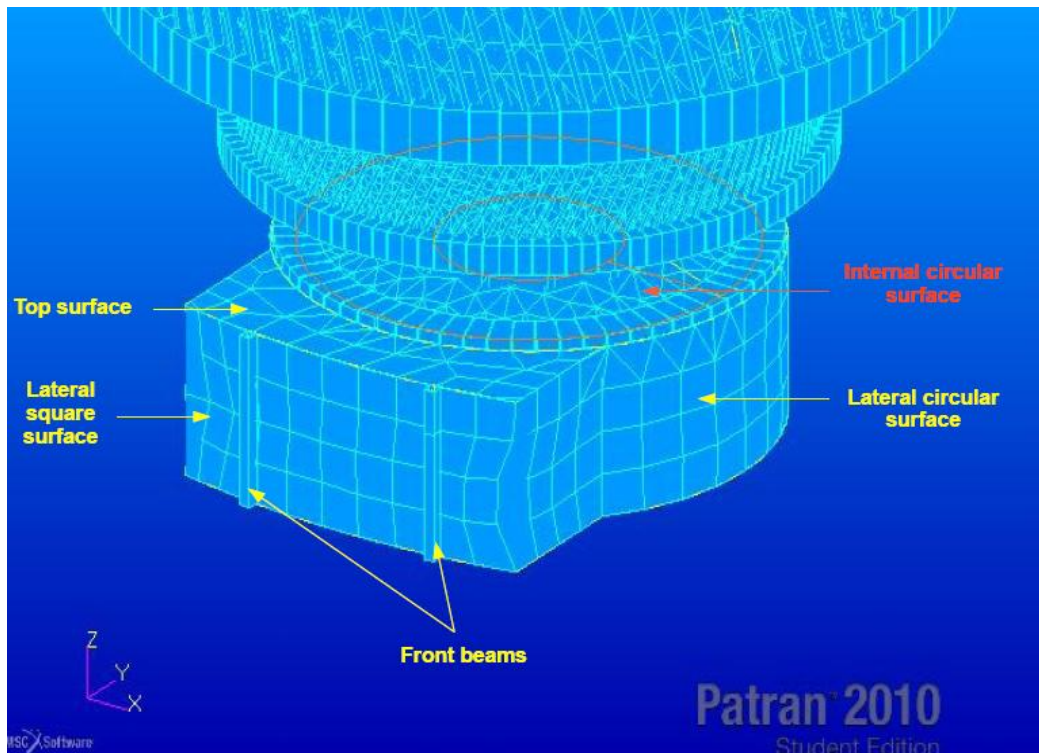


Figure 2.9: View of the 2<sup>nd</sup> high speed stage housing version, with indication of its parameters.

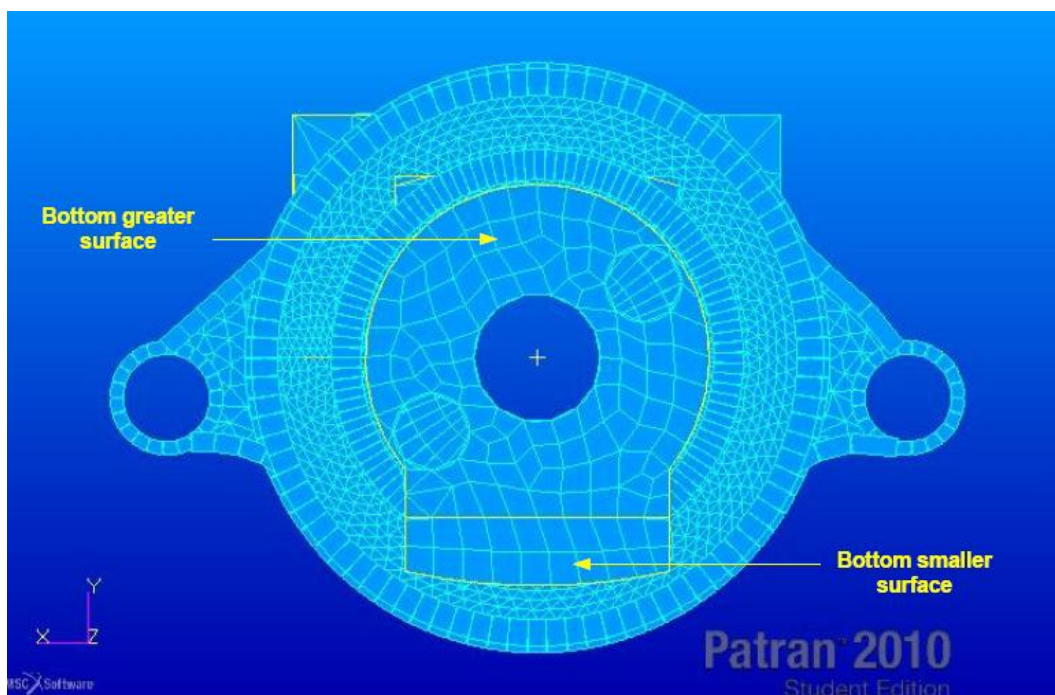


Figure 2.10: Bottom view of the 2<sup>nd</sup> high speed stage housing version, with indication of parameters.

In addition to the geometrical changes of the high speed stage housing described above, the variation of some parameters of other parts of the gearbox was performed to achieve a better correlation in terms of vibrational behaviour. Table 2.7 shows these variation in parameters, while table 3.9 shows the resulting changes in natural frequencies.

Part	Parameter	Values of the parameters [m]			
		2 <sup>nd</sup> version model	1 <sup>st</sup> version model	Variation from old model [m]	Variation percentage from old model
2 <sup>nd</sup> stage ring wheel	surface thickness	0,093	0,073	0,020	27,3
Bearing housing	to 2 <sup>nd</sup> stage surface thickness	0,081	0,146	-0,065	-44,8
	to HV stage surface thickness	0,108	0,190	-0,082	-43,2
	medium beam: W dimension	0,110	0,160	-0,050	-31,3
	medium beam: H dimension	0,049	0,059	-0,010	-16,9
Intermediate bearing housing	outer surface	0,071	0,061	0,010	16,4
Torque arm	lateral beams: H dimension	0,212	0,232	-0,020	-8,6
	lateral beams: offset	-0,005	-0,035	0,030	-86,2
	circular lateral beams: W dimension	0,050	0,094	-0,044	-46,8
	circular lateral beams: H dimension	0,180	0,230	-0,050	-21,7
High speed stage housing	bottom greater surface thickness	0,067	0,085	Different geometry	-21,2
	bottom smaller surface thickness	0,033	0,085		Different geometry
	front beams: W dimension	0,030	Did not exist		
	front beams: H dimension	0,030	Did not exist		
	front beams: y-offset	-0,015	Did not exist		

internal circular surface thickness	0,170	Did not exist		
lateral circular surface	0,050	Unchanged	Different geometry	
lateral square surface	0,090	0,070	Different geometry	28,6
top surface	0,152	Was divided in 2 different surfaces		

**Other values**

Total volume [m3]	2,277	2,712	-0,435	-16,0
Total mass [kg]	16700	19780	-3080	-15,6

*Table 2.7: Variation of parameters to get the final vibrational correlation.*

These changes allowed to get a simplified model that is well-related to the full model, and to obtain the needed basic structure to support the optimisation phase. Such finished model is showed in figure 2.11, with a 3D display of beams.

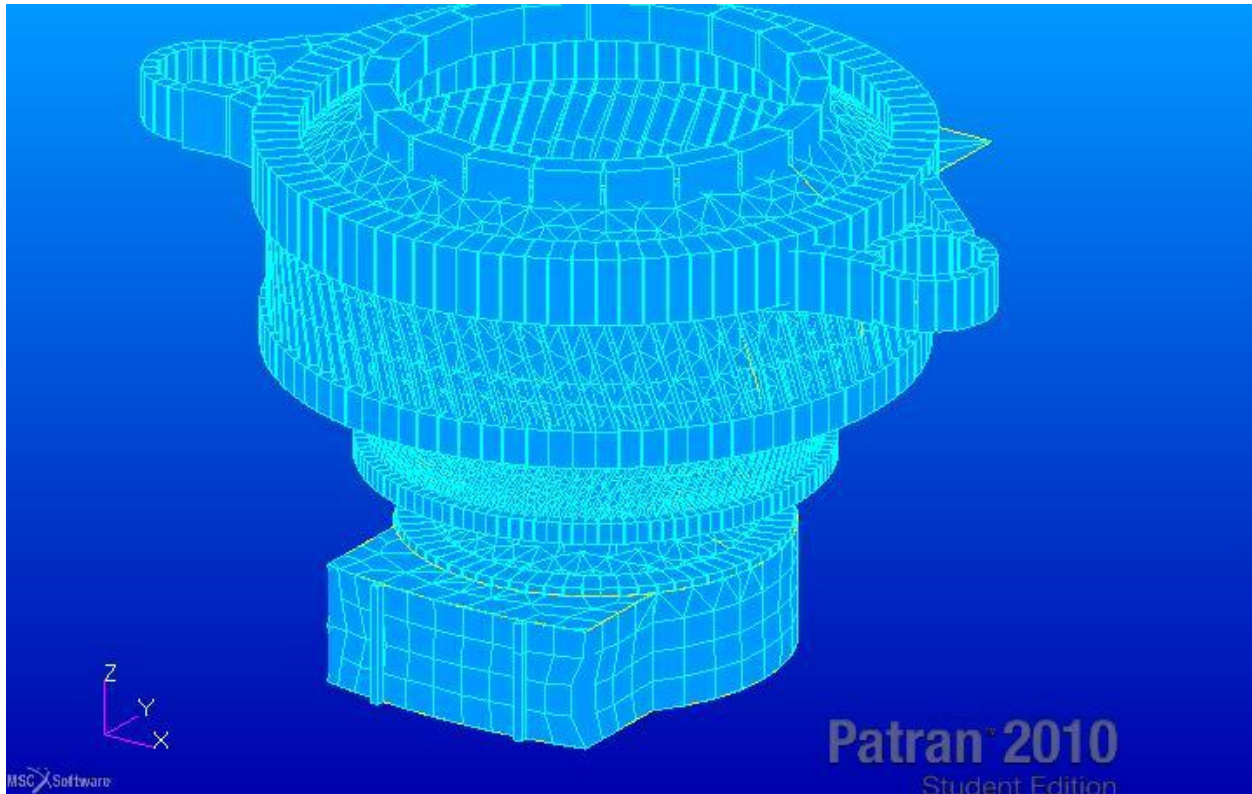


*Figure 2.11: Final version of the simplified gearbox model.*

The simplifications made in the high speed stage housing are very heavy in the second version as well, and are:

- Neglect all complex internal geometry, except the internal circular surface.
- Neglect the minor holes (the main holes were created).
- Neglect the very complex variation of thickness of surfaces.
- Neglect big and small ribs, characterised by a complex geometry, except the front beams.
- Approximate half of the overall structure of the high speed stage housing to a cylinder, and the other half to a parallelepiped. In the full model, there is not such a high definition of these forms, because of several irregularities.

- Neglect the blunt shape of edges typical of the full model, by making them sharp in the simplified model.

The front beams have a very weak function in terms of stiffening of the front part of the lateral square surface. However, they have a considerable effect of adding mass at an end of the structure. This is a non-negligible effect on many natural frequencies, and making such mass a parameter which is independent from the lateral square surface was necessary in order to reach a good correlation with the full model.

In the final model, the main geometrical features were considered. However, other geometrical features, which are considerable in terms of dimensions, were created and evaluated in the tests performed to arrive to the final configuration. Such features are ribs of middle and great dimensions, located at the bottom surface. Nevertheless, their effects were not influential to the vibrational behaviour. For that reason they were neglected, so as to follow the goal of building a simplified structure which considers only the essential geometrical features and well represents the vibrational behaviour of the full model.

Finally, in table 2.8 all parameters of the final simplified gearbox version are collected.

<b>Part</b>	<b>Parameter</b>	<b>Value of the parameter [m]</b>
1 <sup>st</sup> stage ring wheel	surface thickness	0,172
	beams (teeth): W dimension	0,033
	beams (teeth): t1 dimension	0,013
	beams (teeth): t2 dimension	0,016
	beams (teeth): H dimension	0,059

2 <sup>nd</sup> stage ring wheel	surface thickness	0,093
	beams (teeth): W dimension	0,018
	beams (teeth): t1 dimension	0,006
	beams (teeth): t2 dimension	0,010
	beams (teeth): H dimension	0,031
Bearing housing	to 2 <sup>nd</sup> stage surface thickness	0,081
	to HV stage surface thickness	0,108
	high surfaces (ears) thickness	0,035
	smaller beam: W dimension	0,103
	smaller beam: H dimension	0,085
	medium beam: W dimension	0,110
	medium beam: H dimension	0,049
	larger beam: W dimension	0,114
	larger beam: H dimension	0,072
Intermediate bearing housing	inner surface	0,062
	outer surface	0,071
	inner circular beam: W dimension	0,056
	inner circular beam: H dimension	0,117
	mid circular beam: W dimension	0,076
	mid circular beam: H dimension	0,219
	outer circular beam: W dimension	0,100
	outer circular beam: H dimension	0,130
	outer circular beam: offset	-0,045
Torque arm	central surface thickness	0,095
	lateral surfaces thickness	0,155
	high surfaces (ears) thickness	0,094
	outer circular beam: W dimension	0,148

	outer circular beam: H dimension	0,235
	outer circular beam: offset	0,035
	lateral beams: W dimension	0,070
	lateral beams: H dimension	0,212
	lateral beams: offset	-0,005
	circular lateral beams: offset	-0,005
	circular lateral beams: W dimension	0,050
	circular lateral beams: H dimension	0,180
	circular lateral beams: offset	-0,005
	inner circular beam: W dimension	0,096
	inner circular beam: H dimension	0,134
	inner circular beam: offset	0,015
High speed stage housing	bottom greater surface thickness	0,067
	bottom smaller surface thickness	0,033
	front beams: W dimension	0,030
	front beams: H dimension	0,030
	front beams: y-offset	-0,015
	internal circular surface thickness	0,170
	lateral circular surface	0,050
	lateral square surface	0,090
	top surface	0,152
	<b>Other values</b>	
Total volume [m3]		2,277
Total mass [kg]		16700

*Table 2.8: Final simplified gearbox: list and values of all parameters.*





### 3 Comparison with full geometry

The comparison phase of the simplified geometry with the full geometry is crucial for the goal of this thesis. When the building step of the simplified model is accomplished, a good and reliable correlation with the full model is necessary. As this work is aimed at the aspects regarding the natural frequencies of gearbox, noticing just a good correlation between the geometries is not sufficient, and a good correlation between the values of the natural frequencies is needed, in order to assure that the simplified model has a modal behaviour well-related to the full model. When first natural frequencies (the first 4 to 6 or more, according to the complexity of the geometry) of the simplified model are within a 10% range of the respective ones of the full model, from the experience of ZF Wind Power the simplified model is considered well correlated to the full one.

Once this request is satisfied, a verification through the modal assurance criterion (MAC) is needed, because a certain natural frequency of the simplified model could be near the value of a natural frequency of the full model, but this doesn't mean that these two eigenmodes share the same modes shape. Indeed, the modal assurance criterion verifies the correspondence between the mode shapes achieved from two models, instead of the only values of natural frequencies.

The comparison procedure was performed not only at the completed simplified gearbox, but at the 3 different building steps of the gearbox, described in chapter 2. In such a way, the gearbox was checked during 3 steps of its building: only the torque arm, the gearbox without the high speed stage housing, and finally the complete simplified gearbox. By performing the comparison at each of these steps, a methodical, easy and exact construction of the object was reached.

### 3.1 Modal assurance criterion

The Modal Assurance Criterion is a method which indicates the correlation between two different mode shapes, through the quantitative comparison of modal vectors. It allows to determine the consistency between different models, with regard to the mode shapes, as described by Pastor in [3.1]. The MAC is the normalised scalar product of two set of vectors  $\{\varphi_A\}_r$  and  $\{\varphi_X\}_q$ , where the first is the compatible analytical modal vector of the mode  $r$  and the second is the test modal vector of the mode  $q$ . They are the two modal vectors of the respective vibrational modes.  $\{\varphi_A\}_r^T$  and  $\{\varphi_X\}_q^T$  are their respective transpose.

$$MAC(r, q) = \frac{\left| \{\varphi_A\}_r^T \{\varphi_X\}_q \right|^2}{\left( \{\varphi_A\}_r^T \{\varphi_A\}_r \right) \left( \{\varphi_X\}_q^T \{\varphi_X\}_q \right)}$$

Because of the normalization, MAC values are bounded between 0 and 1, where the scalar product equal to 0 indicates the orthogonality of the mode shapes (and therefore no correlation) and 1 indicates the perfectly consistency of the mode shapes. From the experience of ZF Wind Power, a value of 0.8 is considered as a very good correlation.

In this work, MAC had a key role in the phase of comparison between the full and the simplified model, defining with certainty the grade of correlation between the respective mode shapes and thus between the models as well. Its key role is due to the possibility of a misunderstanding about the vibrational modes: the value of a natural frequency of the simplified model can be similar to the one of a natural frequency of the full model, despite their different mode shapes. But different mode shapes denote an incongruity

between the 2 modes, though the values of the natural frequencies are very similar. Through the only comparison of the natural frequencies, such an incongruity can not be identified. For that reason MAC is fundamental.

The resulting scalar values are arranged into the MAC matrix, where each modal vector of first model is compared to all modal vectors of second model, and vice versa. In the present chapter, the correlations between the corresponding mode shapes are gathered into tables, in which the identity of mode shapes and the MAC values resulting from the criterion are collected. Each of such tables is followed by a graphical representation of the MAC matrix, which provides a quicker visualization of how mode shapes of the simplified model (in the horizontal axis) are related with the mode shapes of the full model (in the vertical axis).

Each MAC analysis is coupled to a comparison of natural frequencies. As explained by Pascal in [3.1], this is necessary because MAC does not give information about the frequency correspondence. Indeed, from the graphical representation of MAC matrices, good correlation between vibrating modes which have considerable frequency separation can be observed as well.

In this thesis, the simplified and the full model were submitted to MAC at different steps of the building of the simplified model. Modeshapes were computed using Nastran and MAC matrices were computed using LMS Virtual.LAB by ZF Wind Power. In all cases, the models were submitted to MAC by ZF Wind Power.

### **3.2 Comparison of the torque arm**

The geometry of the torque arm is the most complex among parts of the gearbox after the high speed stage housing. Once it was built according to

real dimensions as far as possible, some little changes were made in the geometrical description of some beams and some surfaces, to improve the correspondence between the respective mode shapes and natural frequencies.

In the case of torque arm, a good result is considered achieved when the first 4 - 5 natural frequencies are within the range of 10% of respective values of the full model, according to the experience of ZF Wind Power.

The correspondences between natural frequencies was achieved, and they are collected in table 3.1.

The rigid body modes were not considered in tables of this chapter, except some rigid body modes reported in the table 3.2. For that reason, the identification number of the natural frequencies starts from the 7<sup>th</sup> eigenfrequency, because of the presence of the 6 rigid body modes before them.

Id	Simplified model	Full model	Freq1-Freq2 [Hz]	Percentage of variation from the full model
	Natural frequencies (1) [Hz]	Natural frequencies (2) [Hz]		
7	80,5	76,7	3,8	5,0 %
8	100	98,3	1,7	1,7 %
9	156,5	176,9	-20,4	-11,5 %
10	189,3	196,9	-7,6	-3,9 %
11	217	224,9	-7,9	-3,5 %
12	265,4	257,8	7,6	2,9 %
13	319,4	342,8	-23,4	-6,8 %
14	335,2	348,2	-13	-3,7 %
15	469,8	462,6	7,2	1,6 %
16	485,4	488,9	-3,5	-0,7 %

*Table 3.1: Torque arm: natural frequencies comparison between full and simplified model.*

Among the first 16 natural frequencies, the only one which in the simplified model exceeds the range of 10% from the respective one in the full model is the 3<sup>rd</sup> natural frequency, but its 11.5% variation from the full model's respective value is tolerated. The comparison of the natural frequencies is in such a way approved.

Such simplified model was submitted to modal assurance criterion. The results are collected in the table 3.2.

Simplified model		Full model		Comparison		
Id	Freq1	Id2	Freq2	MAC Value	Freq2-Freq1 (Hz)	
1	0.0	1	0.0	0.580	0.00	
2	0.0	5	0.0	0.544	0.00	
4	0.0	4	0.0	0.855	0.00	
7	80.5	7	76.7	0.949	3.85	Symmetric flapping mode
8	100.0	8	98.3	0.945	1.62	
9	156.5	9	176.9	0.973	20.43	
10	189.3	10	196.9	0.927	7.61	
11	217.0	11	224.9	0.938	7.91	
12	265.4	12	257.8	0.876	7.59	
13	319.4	13	342.8	0.823	23.37	
14	335.2	14	348.2	0.789	12.96	
15	469.8	15	462.6	0.823	7.20	
16	485.4	16	488.9	0.645	3.58	

*Table 3.2: Torque arm: MAC results. The first two columns are referred to the simplified model, and the 3<sup>rd</sup> and 4<sup>th</sup> columns are referred to the full model. The last two columns regard the comparison of the models in terms of MAC value and difference of frequency between the correlated eigenmodes. On the right of the table is indicated the frequency to which the symmetric flapping mode occurs. This one will be discussed in Chapter 4, and represented in figure 4.1.*

Figure 3.1 is the graphical representation of MAC matrix. Relation between mode shapes is represented by the intensity of red colour: more intense is the red and better is the correlation, whilst the correlation is very weak if colour approaches to green. Again, the first six mode shapes should not be taken into account as they are the rigid body modes.

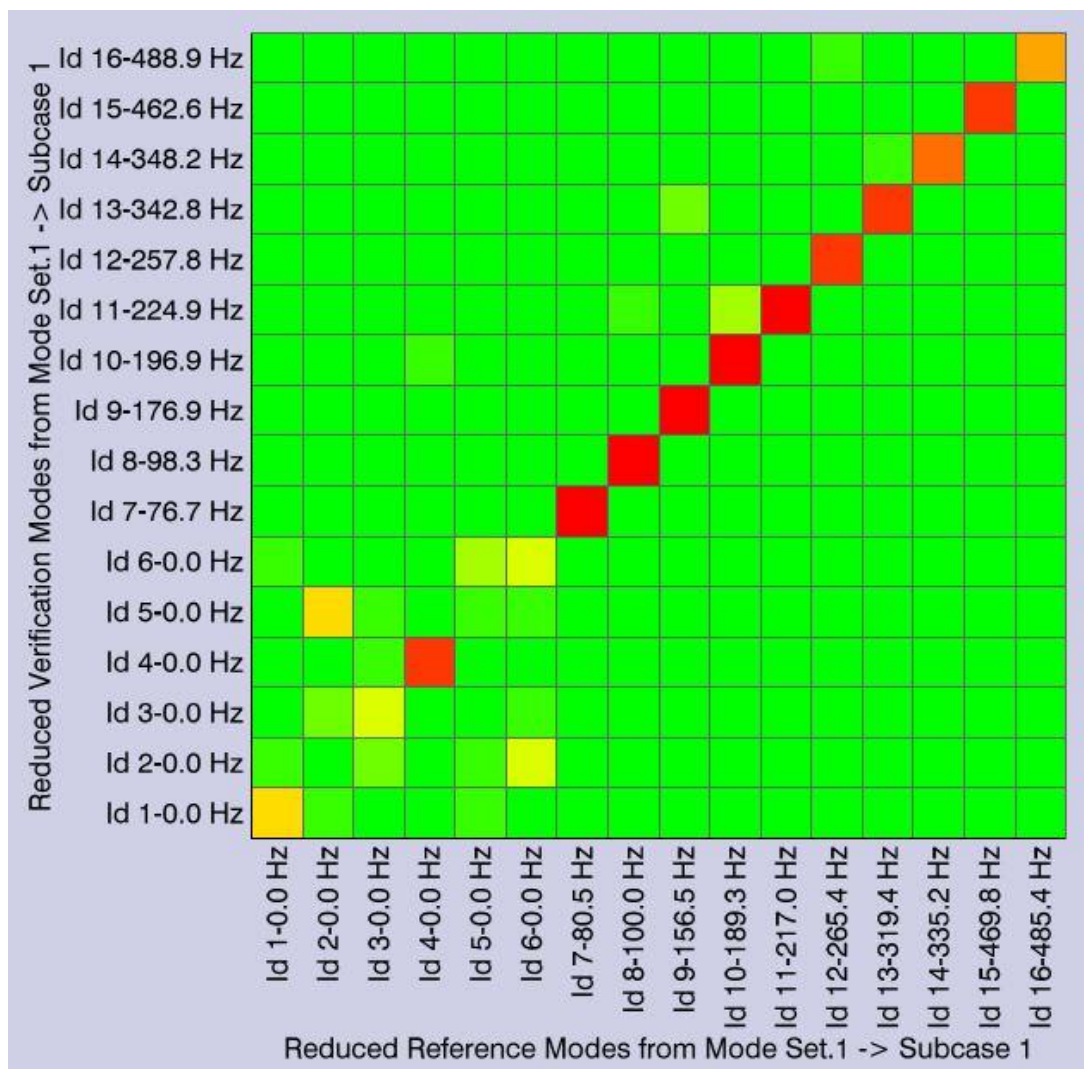


Figure 3.1: Torque arm: MAC graphical representation.

These results show:

- The correspondence between the first 10 vibrational modes.
- The high MAC values of the first 10 mode shapes.

For the first 5 mode shapes the MAC values are above 0.9. The subsequent 4 mode shapes are above 0.8, and the 10<sup>th</sup> mode shape has a MAC value above 0.6. Among the attained results only since the 10<sup>th</sup> mode shape (identified with id 16) the MAC value is lower than 0.8. With these results the simplified torque arm can be considered very well correlated with the full model.

### **3.3 Comparison of the gearbox without the high speed stage housing**

Once a good result was achieved by the comparison of torque arm, the modelling proceeded with the first stage ring wheel, the intermediate bearing housing, the second stage ring wheel and the bearing housing. Then, this configuration of the gearbox without the high speed stage housing was submitted to the comparison procedure.

The correlation between natural frequencies is shown in table 3.3:

	<b>Full model</b>	<b>Simplified model</b>		
<b>Number of natural frequency</b>	<b>Natural frequencies [Hz]</b>	<b>Natural frequencies [Hz]</b>	<b>Difference from the full model [Hz]</b>	<b>Percentage of variation from the full model</b>
7	177,1	168,4	-8,8	-4,9 %
8	193,9	194,8	1,0	0,5 %
9	262,4	209,8	-52,6	-20,0 %
10	270,1	217,1	-53,0	-19,6 %
11	306,9	267,3	-39,6	-12,9 %
12	327,7	268,5	-59,3	-18,1 %
13	332,5	275,4	-57,1	-17,2 %
14	405,1	293,1	-112,0	-27,7 %
15	428,0	306,4	-121,6	-28,4 %
16	450,7	307,9	-142,8	-31,7 %
17	459,0	317,9	-141,1	-30,7 %
18	478,5	325,4	-153,1	-32,0 %
19	495,7	398,6	-97,1	-19,6 %
20	501,0	405,3	-95,7	-19,1 %
21	519,0	435,5	-83,5	-16,1 %
22	550,6	440,8	-109,8	-19,9 %
23	562,8	442,1	-120,7	-21,4 %
24	568,6	451,5	-117,1	-20,6 %
25	579,0	473,6	-105,4	-18,2 %
26	597,1	507,6	-89,5	-15,0 %

*Table 3.3: First version of gearbox without high speed stage housing: natural frequencies comparison between full and simplified model.*

These correlations were not good enough to assume this simplified model as well related to the full model. For that reason, some variations were performed in this preliminary model. These variations are summarised in the table 3.4:



### Adjusted parameters overview

Part	Parameter	Values of the parameters [m]		Variation from the old model [m]	Percentage of variation from the old model
		Old model	New model		
1 <sup>st</sup> ring	surface thickness	0,212	0,172	-0,040	-18,9
	beams (teeth): W dimension	0,023	0,033	0,010	44,3
	beams (teeth): t1 dimension	0,023	0,013	-0,010	-44,3
2 <sup>nd</sup> ring	surface thickness	0,103	0,073	-0,030	-29,0
	beams (teeth): W dimension	0,012	0,018	0,006	51,4
	beams (teeth): t1 dimension	0,012	0,006	-0,006	-51,3
Bearing housing	to 2 <sup>nd</sup> stage surface thickness	0,377	0,058	-0,319	-84,7
	to HV stage surface thickness	0,068	0,078	0,010	14,7
	high surfaces (ears) thickness	0,052	0,035	-0,017	-32,7
	smaller beam: W dimension	0,073	0,103	0,030	41,0
Intermediate bearing housing	inner surface	0,082	0,062	-0,020	-24,4
Torque arm	central surface thickness	0,089	0,095	0,006	6,7
	lateral surfaces thickness	0,179	0,155	-0,024	-13,5
	high surfaces (ears) thickness	0,104	0,094	-0,010	-9,6
	outer circular beam: offset	0,095	0,035	-0,060	-63,2
	outer circular beam: W dimension	0,158	0,148	-0,010	-6,3
	outer circular beam: H dimension	0,225	0,235	0,010	4,4
	lateral beams: offset	-0,025	-0,035	-0,010	39,8
	lateral beams: W dimension	0,066	0,070	0,004	6,1
	lateral beams: H dimension	0,209	0,232	0,023	11,0
	circular lateral beams: offset	-0,020	-0,005	0,015	-75,0
	circular lateral beams: W dimension	0,128	0,094	-0,034	-26,6
circular lateral beams: H dimension	0,259	0,230	-0,029	-11,2	

Table 3.4: Variations of parameters submitted to the first version of gearbox without high speed stage housing.

These variations are aimed at bringing the first 5 natural frequencies of the simplified model within the 10% of the respective natural frequencies of the full model. Results of such variations, in terms of natural frequencies, are collected in the table 3.5. In tables of this paragraph the rigid body modes are removed, and the numbering starts from 1.

Id	Simplified model	Full model	Difference from the full model [Hz]	Percentage of variation from the full model
	Natural frequencies [Hz]	Natural frequencies [Hz]		
1	175,3	177,1	-1,8	-1,0 %
2	194,2	194,1	0,1	0,1 %
3	240,6	261,6	-21	-8,0 %
4	244,6	269,5	-24,9	-9,2 %
5	331	305,9	25,1	8,2 %
6	333,7	326,1	7,6	2,3 %
7	334,4	331,4	3	0,9 %
8	377,1	404,3	-27,2	-6,7 %
9	381,5	426,9	-45,4	-10,6 %
10	409	404,3	4,7	1,2 %
11	413	426,9	-13,9	-3,3 %
15	453,2	458,9	-5,7	-1,2 %
16	461,1	478,5	-17,4	-3,6 %
17	500	478,5	21,5	4,5 %
18	501,1	495,1	6	1,2 %

*Table 3.5: Second version of gearbox without high speed stage housing: natural frequencies comparison between full and simplified model.*

The resulting natural frequencies show a small deviation from the full model, and the only 9<sup>th</sup> natural frequency is slightly out of the 10% range. At this point the correspondence between mode shapes has to be checked through the modal assurance criterion, whose results are given below (see table 3.6). In these results correspondence between the respective natural frequencies of

the two models is shown. Correspondence is good at the first 9 natural frequencies, in which all MAC values are above 0.5 and 3 of them are above 0.8.

Simplified model		Full model			
Id1	Freq1	Id2	Freq2	MAC Value	Freq2-Freq1 (Hz)
1	175,3	1	177,1	0,957	1,88
2	194,2	2	194,1	0,97	-0,11
3	240,6	3	261,6	0,524	20,98
4	244,6	4	269,5	0,557	24,92
5	331	5	305,9	0,719	-25,12
6	333,7	6	326,1	0,667	-7,62
7	334,4	7	331,4	0,651	-3,04
8	377,1	8	404,3	0,837	27,18
9	381,5	9	426,9	0,777	45,34
10	409	8	404,3	0,662	-4,7
11	413	9	426,9	0,769	13,82
15	453,2	11	458,9	0,419	5,68
16	461,1	12	478,5	0,657	17,37
17	500	12	478,5	0,46	-21,46
18	501,1	13	495,1	0,556	-5,99

*Table 3.6: Second version of gearbox without high speed stage housing: MAC results.*

The MAC matrix is graphically represented in figure 3.2, the correspondence between the different natural frequencies is shown, and MAC values reported in table 3.6 are more evident.

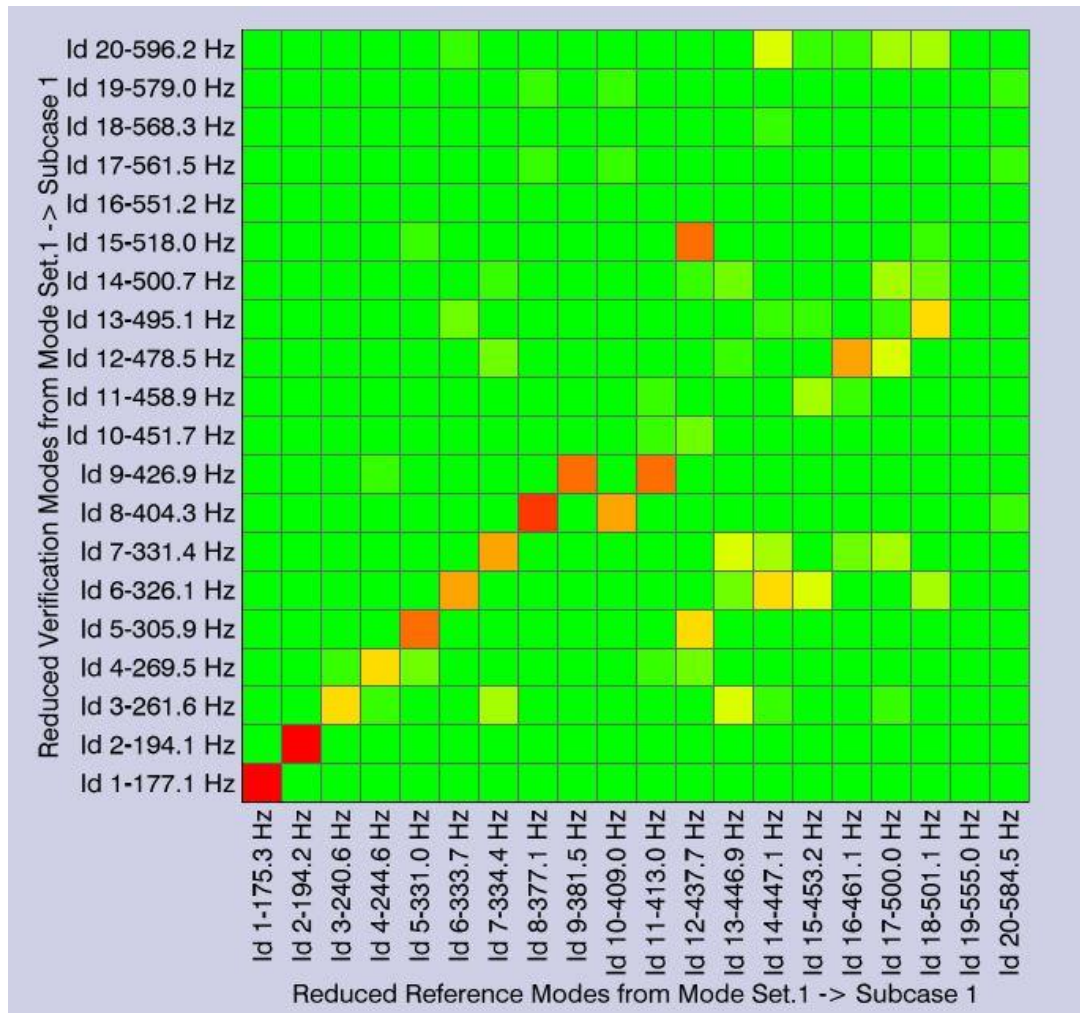


Figure 3.2: Second version of gearbox without high speed stage housing: MAC graphical representation.

This result was considered correlated good enough with the full geometry. Although MAC values are lower than the ones obtained with the torque arm it was not considered as a problem which could degrade the validity of the study. Indeed, the more the geometry is complex and the more it is difficult to achieve high MAC values.

### 3.4 Comparison of the complete gearbox

Once the good result in the simplified gearbox without the high speed stage housing was achieved, the gearbox was completed by building the high speed stage housing.

High speed stage housing is the most complex part of the gearbox housing, as described in chapter 2. Two models of this high speed stage housing were built:

1. A first version of the high speed stage housing as a very simplified structure, almost a box, to understand the grade of geometrical complexity needed by the simplified model to be well related to the full one.
2. A second version of the high speed stage housing, with a superior grade of complexity.

The achieved results from the two high speed stage housing versions, described in the this paragraph, give the quantitative and qualitative idea of the needed degree of geometrical complexity necessary to achieve good correlation with the full model.

After the addition of the first version, a comparison of the first 20 natural frequencies was made, and table 3.7 collects these results.

<b>Id</b>	<b>Full model Natural frequency [Hz]</b>	<b>Simplified model Natural frequency [Hz]</b>	<b>Difference from the full model [Hz]</b>	<b>Percentage of variation from the full model</b>
1	126,3	126,7	0,4	0,3 %
2	161,0	148,2	-12,7	-7,9 %
3	192,1	174,7	-17,4	-9,0 %

4	212,4	194,6	-17,8	-8,4 %
5	225,1	203,3	-21,8	-9,7 %
6	289,6	240,0	-49,7	-17,1 %
7	295,4	244,5	-50,9	-17,2 %
8	298,2	263,8	-34,4	-11,5 %
9	313,6	271,8	-41,9	-13,3 %
10	331,7	345,0	13,3	4,0 %
11	363,2	355,5	-7,6	-2,1 %
12	385,3	383,0	-2,3	-0,6 %
13	417,4	406,7	-10,7	-2,6 %
14	440,6	415,8	-24,8	-5,6 %
15	456,7	422,5	-34,2	-7,5 %
16	466,9	435,5	-31,4	-6,7 %
17	469,3	453,5	-15,8	-3,4 %
18	490,3	460,5	-29,8	-6,1 %
19	493,1	461,8	-31,3	-6,3 %
20	513,6	477,4	-36,1	-7,0 %

*Table 3.7: First version of complete gearbox: natural frequencies comparison between full and simplified model.*

Then the model was submitted to modal assurance criterion, and the results are shown in the table below (3.8), accompanied by the graphical representation of the MAC matrix (figure 3.3).

Simplified model		Full model		MAC Value	Freq2-Freq1 (Hz)
Id1	Freq1	Id2	Freq2		
1	126.7	1	126.3	0.923	-0.35
2	148.2	2	161.0	0.928	12.81
3	174.7	3	192.2	0.942	17.54

4	194.6	4	212.6	0.957	17.95
10	345.0	10	332.0	0.596	-12.99
11	355.5	11	364.3	0.484	8.75
18	460.5	15	457.2	0.420	-3.26
20	477.4	18	490.8	0.656	13.38

Table 3.8: First version of complete gearbox: MAC results

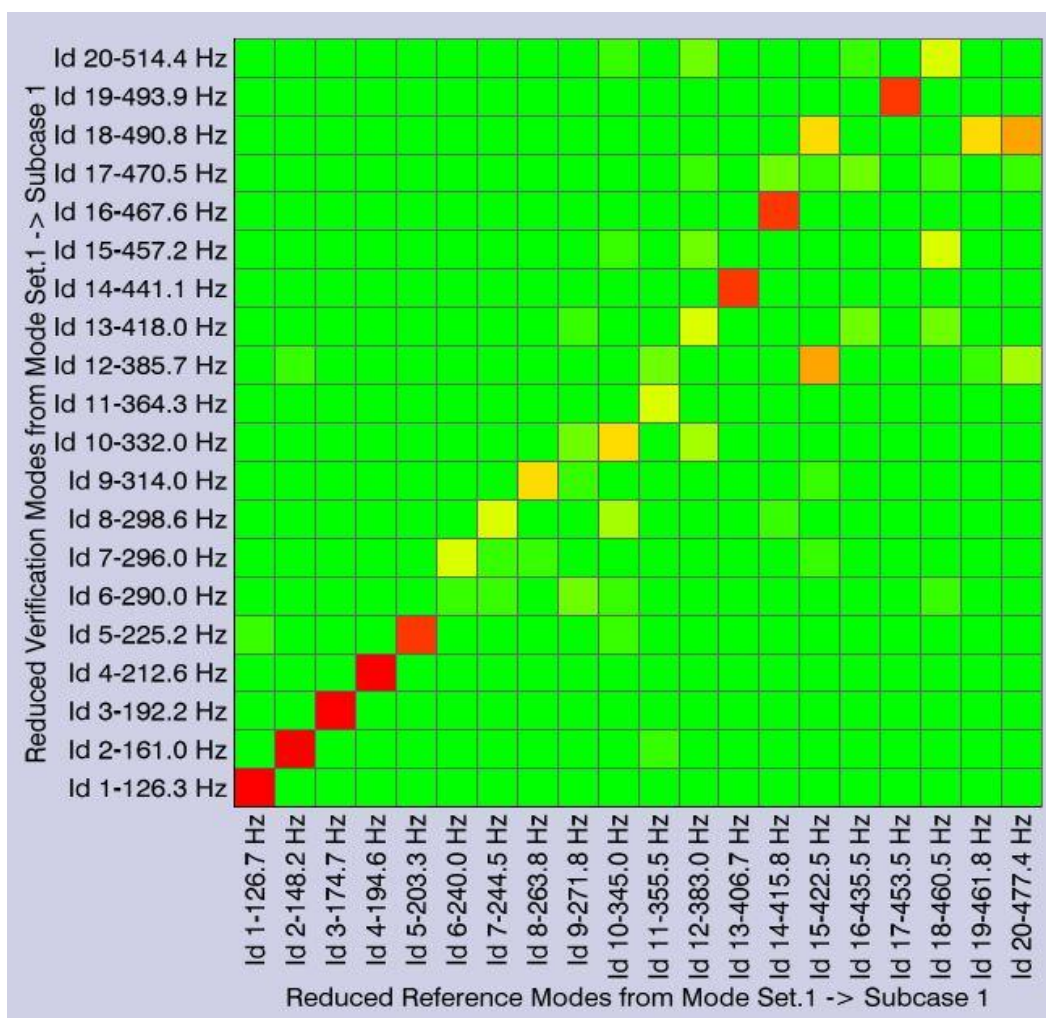


Figure 3.3: First version of complete gearbox: MAC graphical representation.

Results in terms of correspondence of mode shapes are good for the first 5

natural frequencies. In order to get higher MAC values and keep the percentage of variation lower than 10% from the full model, thickness of surfaces which compose the bearing housing were increased. However, to get values of the first eigenfrequencies close to the natural frequencies of the full model, this thickness needed to be increased too much. This change brings the model far from the reality, because really the bearing housing has not a deep sharp cut like the one of this simplified model. This too heavy increase of the thickness of the bearing housing was rejected, and a different reproduction of the high speed stage housing was performed, keeping unchanged the geometry of the rest of the gearbox, but varying some parameters as thickness of some surfaces and dimensions of the section of some beams.

The adjusted parameters of the new model, as well as the unchanged parameters, are collected in table 2.7. These modifications led to a better correlation among the first 6 natural frequencies which is described below.

The effects of the variation of the parameters on the natural frequencies are collected in table 3.9.



		Start	Step 1	Step 2	Step 3	Step 4	Step 5	Step 6	Step 7	Step 8	Step 9	Step 10	Step 11
	Geometry changes	Undone	done	done	done	done	done	done	done	done	done	done	done
High speed stage housing	bottom greater surface thickness [m]	0.085	0.085	0.067	0.067	0.067	0.067	0.067	0.067	0.067	0.067	0.067	0.067
	bottom smaller surface thickness [m]	0.085	0.085	0.033	0.033	0.033	0.033	0.033	0.033	0.033	0.033	0.033	0.033
	lateral square surface thickness [m]	0.070	0.070	0.070	0.070	0.090	0.090	0.090	0.090	0.090	0.090	0.090	0.090
Bearing housing	to 2 <sup>nd</sup> stage surface thickness [m]	0.146	0.146	0.146	0.146	0.146	0.081	0.081	0.081	0.081	0.081	0.081	0.081
	to HV stage surface thickness [m]	0.190	0.190	0.190	0.190	0.190	0.108	0.108	0.108	0.108	0.108	0.108	0.108
	medium beam W dimension [m]	0.160	0.160	0.160	0.160	0.160	0.160	0.110	0.110	0.110	0.110	0.110	0.110
	medium beam H dimension [m]	0.059	0.059	0.059	0.059	0.059	0.059	0.049	0.049	0.049	0.049	0.049	0.049
Intermediate bearing housing	Outer surface thickness [m]	0.061	0.061	0.061	0.061	0.061	0.061	0.061	0.071	0.071	0.071	0.071	0.071
2 <sup>nd</sup> stage ringw heel	Surface thickness [m]	0.073	0.073	0.073	0.073	0.073	0.073	0.073	0.073	0.093	0.093	0.093	0.093
Torque arm	Lateral beams offset [m]	-0.035	-0.035	-0.035	-0.035	-0.035	-0.035	-0.035	-0.035	-0.035	-0.035	-0.005	-0.005
	Lateral beams H dimension [m]	0.232	0.232	0.232	0.232	0.232	0.232	0.232	0.232	0.232	0.232	0.212	0.212
	Circular lateral beams W dimension [m]	0.094	0.094	0.094	0.094	0.094	0.094	0.094	0.094	0.094	0.094	0.094	0.050
	Circular lateral beams H dimension [m]	0.230	0.230	0.230	0.230	0.230	0.230	0.230	0.230	0.230	0.230	0.230	0.180

Eigenfrequency 7 [Hz]	126.7	173.0	173.4	174.0	173.5	143.4	133.2	133.8	135.0	136.6	136.6	136.8
Eigenfrequency 8 [Hz]	148.3	179.6	181.3	185.7	181.9	169.5	159.2	160.5	162.6	164.9	164.6	166.8
Eigenfrequency 9 [Hz]	174.7	193.6	193.7	193.8	193.8	174.5	174.4	174.5	174.7	174.8	174.1	185.1
Eigenfrequency 10 [Hz]	194.6	201.0	204.5	207.8	205.9	193.9	193.8	193.8	194.1	194.1	193.8	194.4
Eigenfrequency 11 [Hz]	203.3					231.2	207.9	201.0	202.4	204.9	207.8	208.3
Eigenfrequency 12 [Hz]	244.5											280.0
Eigenfrequency 11 [Hz]												282.3
Eigenfrequency 14 [Hz]		313.5	300.7	288.2	289.3							
Eigenfrequency 15 [Hz]		318.0	disappeared	disappeared	disappeared				286.2			

Table 3.9: Complete gearbox: variation of parameters from the first to the second version. In the lower part the effects of each variation on the eigenfrequencies are reported. Each eigenmode is associated to a colour, in order to track their variations when their order changes. Each eigenmode has been identified by means of its mode shape, where possible.

A more complete list of all eigenfrequencies is given in table 3.10, and the results of the modal assurance criterion are shown in table 3.11 and figure 3.4, below.

Id	Full model [Hz]	Simplified model [Hz]	Difference from the full model [Hz]	Percentage of variation from the full model
	Natural frequencies [Hz]	Natural frequencies [Hz]		
1	126,3	136,8	10,5	8,3 %
2	161,0	166,8	5,8	3,6 %
3	192,1	185,1	-7,0	-3,6 %

4	212,4	194,4	-18,0	-8,5 %
5	225,1	208,3	-16,8	-7,5 %
6	289,6	280,0	-9,6	-3,3 %
7	295,4	283,5	-11,9	-4,0 %
8	298,2	296,5	-1,8	-0,6 %
9	313,6	309,2	-4,4	-1,4 %
10	331,7	354,7	23,0	6,9 %
11	363,2	368,5	5,3	1,5 %
12	385,3	407,4	22,1	5,7 %
13	417,4	414,4	-3,0	-0,7 %
14	440,6	416,8	-23,8	-5,4 %
15	456,7	429,2	-27,5	-6,0 %
16	466,9	443,7	-23,3	-5,0 %
17	469,3	458,2	-11,2	-2,4 %
18	490,3	464,0	-26,2	-5,4 %
19	493,1	464,9	-28,2	-5,7 %
20	513,6	470,4	-43,1	-8,4 %

*Table 3.10: Second version of complete gearbox: natural frequencies comparison between full and simplified model.*

Simplified model		Full model		MAC Value	Freq2-Freq1 (Hz)
Id1	Freq1	Id2	Freq2		
1	136.8	1	126.3	0.641	-10.5
2	166.8	2	161.0	0.607	-5.7
3	185.1	3	192.2	0.845	7.1
4	194.4	4	212.6	0.947	18.2
5	208.3	5	225.2	0.549	17
9	309.2	7	296.0	0.504	-13.2
11	368.5	11	364.3	0.626	-4.2
12	407.4	14	441.1	0.875	33.8

16	443.7	13	418.0	0.666	-25.7
17	458.2	18	490.8	0.509	32.6
20	470.4	15	457.2	0.760	-13.2

Table 3.11: Second version of complete gearbox: MAC results

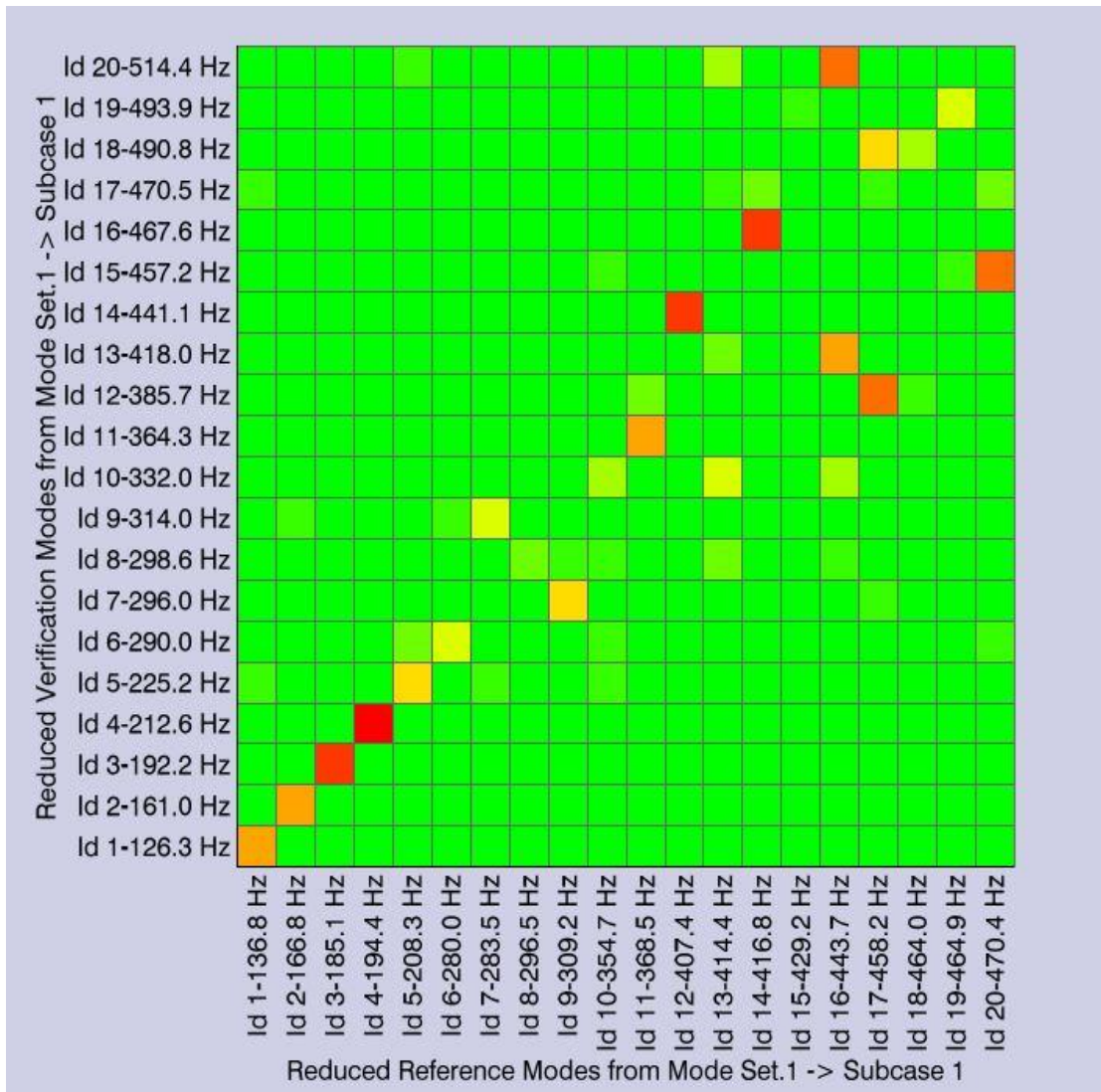


Figure 3.4: Second version of complete gearbox: MAC graphical representation.

In order to obtain good results by keeping the thickness of the bearing housing at realistic values, the change of the geometry of the high speed

stage housing had a key role. This last part of the gearbox is characterised by a considerable complexity, compared to the rest of the structure. A first version of the high speed stage housing, characterised by a heavy simplification by reducing it to almost a box, was created. Given the reached results described above, a greater grade of accuracy was needed in the reproduction of the last part of gearbox. The second version of the high speed stage housing was characterised by such higher grade of accuracy, as described in chapter 2.

However, by considering both the first and the second version, this is the part of the gearbox which undergoes the biggest geometrical simplification.

Although the 2 versions of high speed stage housing are both very simplified with respect to the full model, there is a considerable difference between the results achieved from the first and the second version. Indeed, by analysing the results of the second version it is possible to observe:

- The realistic thickness of the surfaces which compose the bearing housing.
- The correspondence of the vibrational modes extends to the 6<sup>th</sup> mode (a mode more than the first version).

The first point leads to an important approach to the effective behaviour of the gearbox structure, as already described in the paragraph.

The extension of the correspondence to the 6<sup>th</sup> mode allows to widen the range frequency correlation between the simplified and the full model from [0 Hz – 225 Hz] to [0 Hz - 290 Hz].

Although MAC values are lower than the ones achieved with the first version of the high speed stage housing, this is not an issue which compromises the faithfulness to the full model.

Once a good correlation between the two models is assured for the first 6 natural frequencies, an optimisation of the NVH behaviour phase is possible.

However, only the study of these first 6 natural frequencies has sense in the optimisation, because the two models are well-related in this frequency range. For other vibrational modes the correlation was considered null. For that reason, the vibrational modes subsequent to the 6<sup>th</sup> are not taken under consideration in the optimisation phase, which is described in chapter 5.

In figure 3.5 the first mode shape of the final version of the structure is reported.

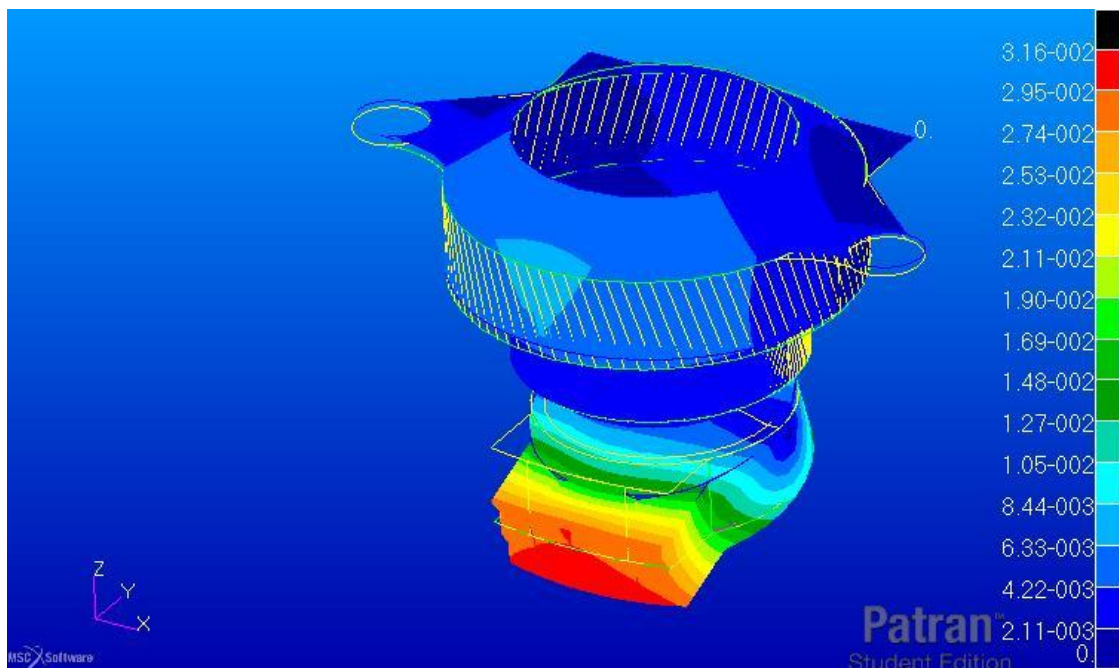


Figure 3.5: First mode shape of the structure. The yellow lines are the edges of the undeformed structure, while the colours from blue to red are related to the scale of deformation. The deformation values are not real: in modal analysis, Patran uses a certain scale factor for the deformation.



## 4 Sensitivity analysis of the torque arm

Once the step of the torque arm building was completed, and the comparison phase of such part was accomplished, a sensitivity analysis was performed on this part of the structure, in order to investigate the sensitivity of the first flapping mode is with respect to the design parameters. Given the frequency of such flapping mode at 80.5 Hz, if the excitation frequency of the gears is at about 80 Hz, this would bring the torque arm into resonance, causing high excitation to the wind turbine. Figure 4.1 illustrates the flapping mode.

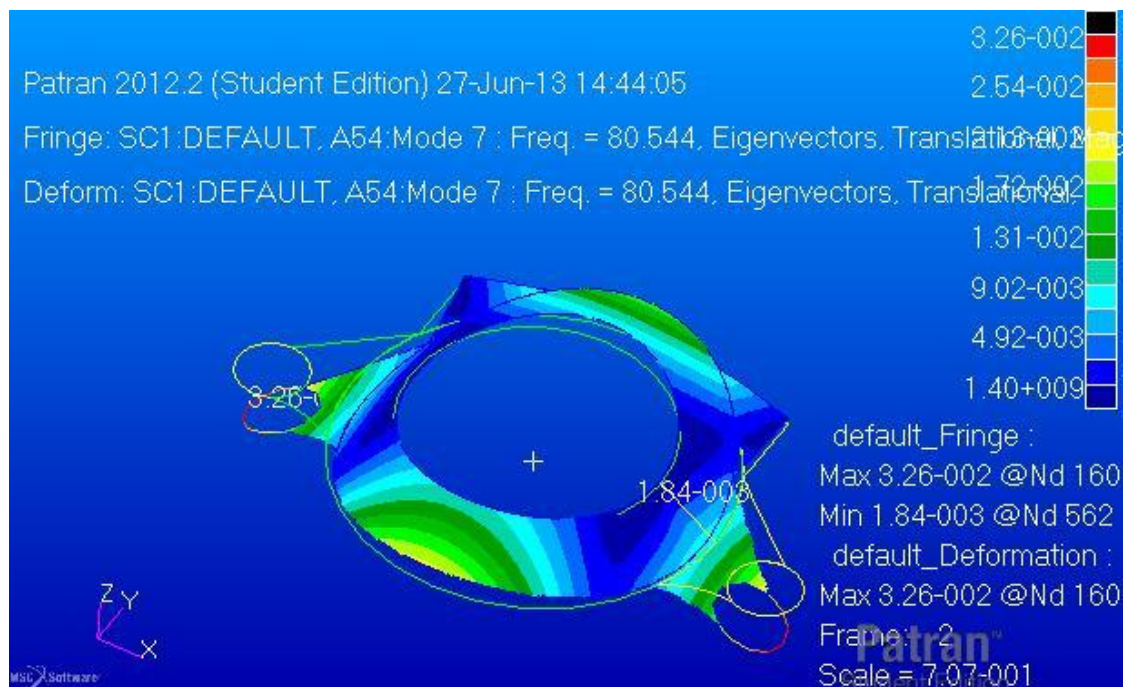


Figure 4.1: Shape of the flapping mode. The yellow lines are the edges of the undeformed structure, while the colours from blue to red are related to the scale of deformation. The deformation values are not real: in modal analysis, Patran uses a certain scale factor for the deformation.

Aim of the sensitivity study is the investigation of the easiness of shifting the flapping mode to higher or lower frequencies through some changes of the design parameters. By changing each parameter by 5%, it is possible to observe which parameter has the biggest effect on the natural frequency of the vibrational mode.

Variations were accomplished one at a time, and then the value of the parameter was brought back to the original, while another parameter was varied. This is in order to measure the effect that each single variation has on the natural frequencies.

Once the sensitivity analysis was performed, and its results were collected, the parameter which has the larger effect on the natural frequency was identified. Then, this parameter was changed such that the flapping mode was brought out of the frequency range [60 – 100 Hz].

Finally, the addition of mass to the lateral circular beams of the torque arm was tested. Such an investigation has the scope both to complete the sensitivity analysis with the addition of mass, which was not considered among the parameters to change, and to study the way the suspension system influences the flapping mode. Indeed, the positioning of the additional mass is so as to represent the mass of the suspension system.

#### **4.1 Sensitivity analysis of the torque arm**

The design parameters varied in the sensitivity analysis are the thickness for the surfaces, and the two dimensions of section and the offset for the beams. Results of the sensitivity analysis are collected in tables 4.1 and 4.2, where each design parameter is associated to its variation and the consequent variation of the flapping mode. In table 4.1 the effects of a 5% increase of the



parameters are shown, whilst in table 4.2 the consequences of a 5% decrease of the parameters are collected.

Changing parameter	Reference value [m]	5% increased value [m]	New flapping mode [Hz]	Variation of the flapping mode [Hz]
Central surface thickness	0,079	0,083	81,1	-0,5
Lateral surfaces thickness	0,129	0,135	80,6	0,0
High surfaces thickness	0,104	0,109	80,6	0,0
In central beam radial dimension	0,096	0,101	80,6	-0,1
In central beam z dimension	0,134	0,140	80,6	-0,1
In central beam offset	0,015	0,016	80,5	0,0
Out central beam radial dimension	0,158	0,166	82,6	-2,1
Out central beam z dimension	0,255	0,268	82,2	-1,7
Out central beam offset	-0,090	-0,086	80,2	0,4
Lateral circular beams radial dimension	0,128	0,134	79,9	0,7
Lateral circular beams z dimension	0,259	0,272	79,9	0,7
Lateral circular beams offset	-0,020	-0,019	80,6	0,0
Lateral beams radial dimension	0,066	0,069	80,6	-0,1
Lateral beams z dimension	0,209	0,219	80,6	-0,1
Lateral beams offset	-0,025	-0,024	80,5	0,0

Table 4.1: Result of sensitivity analysis with 5% increased parameters.

Changing parameter	Reference value [m]	5% decreased value [m]	New flapping mode [Hz]	Variation of the flapping mode [Hz]
Central surface thickness	0,079	0,075	80,1	0,5
Lateral surfaces thickness	0,129	0,123	80,5	0,1
High surfaces thickness	0,104	0,099	80,5	0,0
In central beam radial dimension	0,096	0,091	80,5	0,1
In central beam z dimension	0,134	0,127	80,5	0,1
In central beam offset	0,015	0,014	80,5	0,0

Out central beam radial dimension	0,158	0,150	78,4	2,1
Out central beam z dimension	0,255	0,242	78,8	1,7
Out central beam offset	-0,090	-0,095	80,9	-0,4
Lateral circular beams radial dimension	0,128	0,122	81,2	-0,7
Lateral circular beams z dimension	0,259	0,246	81,3	-0,7
Lateral circular beams offset	-0,020	-0,021	80,5	0,0
Lateral beams radial dimension	0,066	0,063	80,5	0,1
Lateral beams z dimension	0,209	0,199	80,4	0,1
Lateral beams offset	-0,025	-0,026	80,6	0,0

Table 4.2: Result of sensitivity analysis with 5% decreased parameters.

Reference value is the parameter's value of torque arm such that the flapping mode is at 80.5 Hz.

- > 2 Hz variation (in absolute value)
- > 1 Hz variation (in absolute value)
- > 0.5 Hz variation (in absolute value)

Results of the sensitivity analysis show the most influential parameters, underlined by different colours according to their grade of influence on the first natural frequency. The most influential one is the radial dimension of the outer central beam, followed by the other dimension of the section of the same beam. This outcome suggests that the outer central beam has a key role in the determination of the flapping mode frequency.

Besides, the achieved results show that the two section's dimensions of the lateral circular beams are both the third most influential parameter. At that part of torque arm the additional mass was placed afterwards. For that reason, such results lead to foresee that the additional mass in the lateral circular beams would have an important role in the shifting of the flapping mode.

Finally, the performed analysis shows that the positive variation of each design parameter leads to an effect on the flapping mode consistent with the effect of the negative variation of the same design parameter. Indeed, such effects are the same in absolute value, but they have opposite sign, so as to have specular variations of natural frequency caused by the two variations of +5% and -5% of the design parameters.

Then, given the results of sensitivity analysis, the radial dimension of outer central beam was modified in order to study how much such parameter has to be varied to bring the frequency of the flapping mode out from the frequency range [60 – 100 Hz]. The results of the study are collected in table 4.3 and figure 4.2.

<b>Parameter value [m]</b>	<b>Parameter per cent change</b>	<b>Eigenfrequency [Hz]</b>
0,0785	-50,3 %	60,0
0,0948	-40,0 %	63,8
0,1106	-30,0 %	67,9
0,1264	-20,0 %	72,0
0,1422	-10,0 %	76,3
0,1580	0,0 %	80,5
0,1738	10,0 %	84,7
0,1896	20,0 %	88,8
0,2054	30,0 %	92,8
0,2212	40,0 %	96,7
0,2351	48,8 %	100,0

*Table 4.3: Values of central beam radial dimension needed for bringing first natural frequency out from range [60 – 100 Hz].*

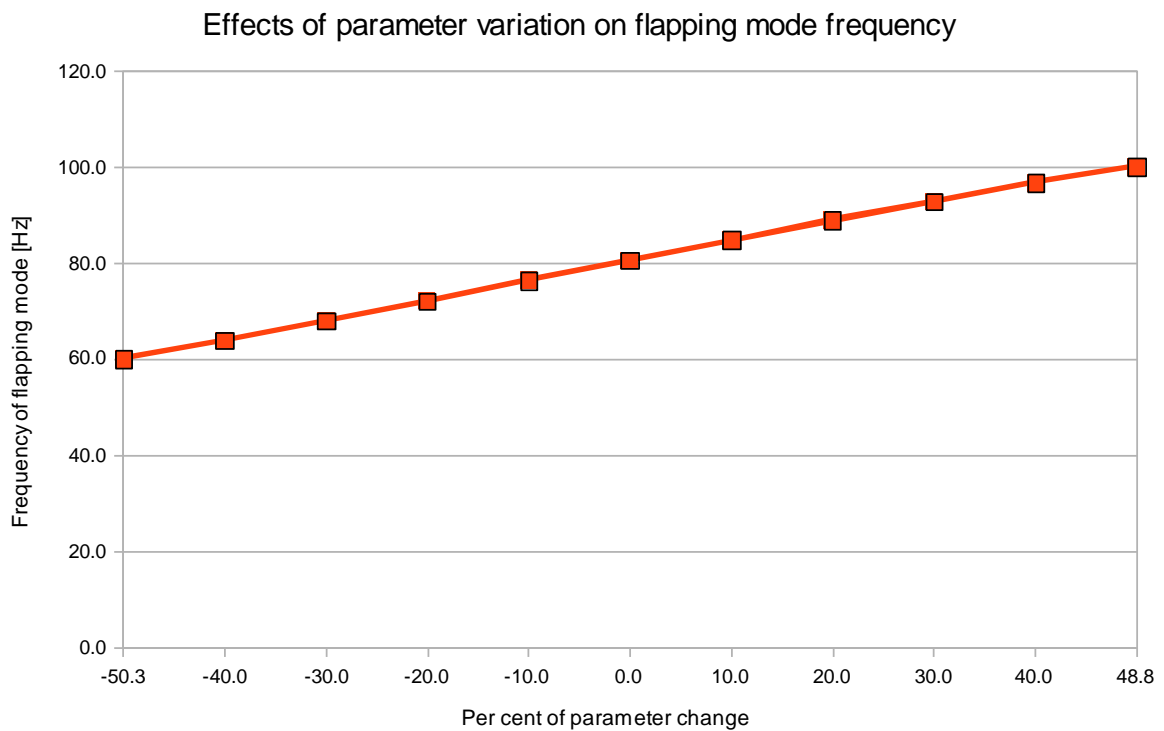


Figure 4.2: Graph of the effects on frequency of the flapping mode (y axis) caused by the per cent variation of the radial dimension of outer central beam (x axis).

The first line of the table reports the reference value of the parameter, and the subsequent ones show its percentage change and the effects on the flapping mode.

The needed percentage change of the parameter is about 50% of its first value in both cases to bring the first natural frequency out of the two bounds of the range [60 – 100 Hz]. However, percentage change is slightly lower in the case of increasing dimension of the parameter, by considering the absolute value of the change. Thus, shifting the flapping mode out from the frequency range [60 – 100 Hz] is slightly easier if its natural frequency is brought over the 100 Hz threshold.

The needed variation of the parameter denotes a quite marked sensitiveness of the flapping mode to the radial dimension of the outer central beam, considering that it is the only parameter changed to reach the goal.

## 4.2 Influence of the suspension system

Additional mass was added to lateral circular beams, in order to simulate the effect of the suspension system on the flapping mode of torque arm. The reference value of the mass is estimated considering the circular beam as a rectilinear beam with length equal to the axis of the beam, that is a circumference.

Being the radius of such a circumference equal to 0.19 m, the circumference is 1.19 m, and the volume of each beam is:

Beam volume = (circumference) x (radial dimension) x (z dimension) = 0.048 m<sup>3</sup>.

Given the density of 7100 kg/m<sup>3</sup> of the utilised material, the mass of each lateral circular beam is 341.5 kg before adding any additional mass. Then, such mass value was verified by a simple apart reproduction of the circular beam in Patran, with the same properties. The mass was extracted and it agreed with the datum calculated.

The entities of additional mass performed are in the first two columns of table 4.4, and in the last two columns the effects on the natural frequency of the flapping mode can be observed. The effects of additional mass on flapping mode frequency is shown in figure 4.3.

Simulations were accomplished for each 10% mass increase, until the exit from the [60 – 100 Hz] range was reached.

Percentage of mass to add	Additional mass [kg]	Total mass of each lateral circular beam [kg]	New natural frequency [Hz]	Variation of natural frequency [Hz]
0 %	0,0	341,5	80,5	0,0
10 %	34,2	375,7	78,6	-1,9

20 %	68,3	409,8	76,8	-3,7
30 %	102,5	444,0	75,1	-5,4
40 %	136,6	478,1	73,6	-6,9
50 %	170,8	512,3	72,2	-8,3
60 %	204,9	546,4	70,9	-9,6
70 %	239,1	580,6	69,7	-10,8
80 %	273,2	614,7	68,5	-12,0
90 %	307,4	648,9	67,5	-13,0
100 %	341,5	683,0	66,5	-14,0
110 %	375,7	717,2	65,6	-14,9
120 %	409,8	751,3	64,7	-15,8
130 %	444,0	785,5	63,9	-16,6
140 %	478,1	819,6	63,2	-17,3
150 %	512,3	853,8	62,4	-18,1
160 %	546,4	887,9	61,8	-18,7
170 %	580,6	922,1	61,1	-19,4
180 %	614,7	956,2	60,5	-20,0
189 %	645,0	986,5	60,0	-20,6

*Table 4.4: Effects on first natural frequency due to non-structural mass added to the two lateral circular beams in order to simulate the effects of the torque arm suspension system.*

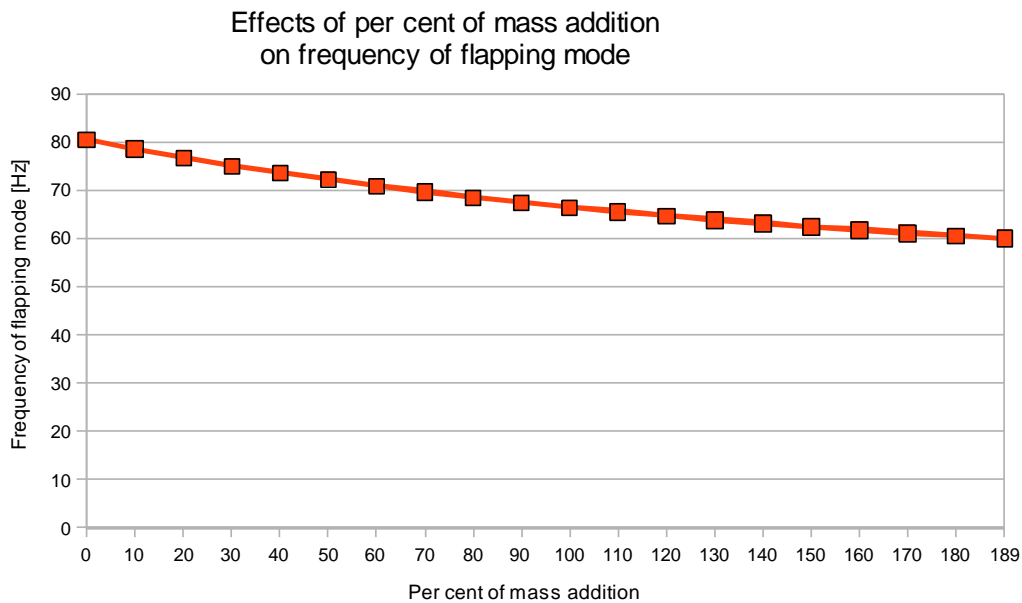


Figure 4.3: Graph of the effects on frequency of the flapping mode (y axis) caused by the per cent addition of mass (x axis).

The results show a decrease of frequency related to the addition of mass. Indeed, the additional mass located at the lateral circular beams makes the torque arm a structure characterised by great masses at the ends and a smooth transition at the centre. This aspect was predictable by observing the results of the sensitivity analysis as well, as regards the effect of a 5% increase of the circular lateral beams.

The sensitivity analysis does not imply exactly the same effect of the additional of mass. Indeed, while the performed sensitivity analysis adds material and so stiffness by increasing the dimensions of the object as well, additional mass is just a non-structural mass added to the object, and does not modify the stiffness. However, in this particular case the effects of the two different operations are quite similar with regard of the variation of the natural frequency.

A great amount of mass (almost the double of the mass of the singular circular lateral beam) has to be added at each circular lateral beam to shift the flapping mode below the 60 Hz threshold. Indeed, the second column of

table 4.4 shows that a great mass is needed to change significantly the first natural frequency.



## 5 Optimisation

The goal of the optimisation phase is to bring all the natural frequencies out of the range [70 – 150] Hz, by adding ribs or adjusting some existing geometrical properties. This implies a huge number of possibilities which could be investigated. For this reason, the accomplishment of a few ordered steps was necessary in order to give a strong simplification of the choice of the possibilities to investigate such an optimisation.

These steps are the following:

- 1) A sensitivity analysis was performed on the gearbox. It has the role of tracking the guide path for the optimisation phase: through the sensitivity analysis, the surfaces which show the greatest influence on the natural frequency were selected for the installation of the ribs.
- 2) A campaign of simulations was performed. with the ribs, in order to identify the direction we could follow to minimize the mass. The effects on the natural frequencies of some varying parameters of the ribs (dimensions, number, inclination and zone of positioning) were compared.
- 3) The effects on the natural frequencies of some error entities of the positioning and inclination of ribs were verified.
- 4) The different possibilities were compared each other as regard their saving of mass:

By observing the results achieved in the simulations, the configurations which reach the value of first natural frequency of 150 Hz were considered, and their mass extracted.

Then the masses were compared, as to finally get the most advantageous configuration in terms of mass, which reaches the goal of bringing all natural frequencies out of the range [70 – 150] Hz.

## **5.1 Sensitivity analysis of the gearbox**

The sensitivity analysis performed consists of sequentially varying the geometrical design parameters of the gearbox such as the thickness of surfaces and the dimensions of the beams, and observing the resulting changes in natural frequencies. The variations were accomplished one at a time, and then the value of the parameter was brought back to the original, while another parameter was varying. This is in order to measure the effect which each single variation has on the natural frequencies.

The variations for each parameter are: +5% and -5% of the original value.

Not all the parameters were submitted to the sensitivity analysis. According to the sensitivity experience gained in the phase of comparison with the full geometry, the changes of the beams' dimensions and of the thickness of little and marginal surfaces (like the 2 high surfaces of the torque arm and the 2 high surfaces of the bearing housing) have a negligible effect on the natural frequencies. For this reason, such parameters were not considered in the sensitivity analysis.

The first natural frequency has the mode shape represented in figure 3.5. This is the starting point for the sensitivity analysis, whose results gained with a variation of +5% of the parameters are shown in table 5.1.

Part of the gearbox	Changing parameter	Reference value [m]	5% increased value [m]	1 <sup>st</sup> natural frequency [Hz]	Variation of 1 <sup>st</sup> natural frequency [Hz]
1 <sup>st</sup> stage ring wheel	surface thickness	0,172	0,181	136,7	-0,1
2 <sup>nd</sup> stage ring wheel	surface thickness	0,093	0,098	137,1	0,3
Bearing housing	to 2 <sup>nd</sup> stage surface thickness	0,081	0,085	139,8	3,0
	to HV stage surface thickness	0,108	0,113	138,1	1,3
Intermediate bearing housing	inner surface	0,062	0,065	136,8	0,0
	outer surface	0,071	0,074	137,1	0,3
Torque arm	central surface thickness	0,095	0,100	136,7	-0,1
	lateral surfaces thickness	0,155	0,163	136,8	0,0
	lateral beams: W dimension	0,070	0,074	136,8	0,0
	lateral beams: H dimension	0,212	0,223	136,8	0,0
High speed stage housing	bottom greater surface thickness	0,067	0,070	136,5	-0,3
	bottom smaller surface thickness	0,033	0,035	136,7	-0,1
	front beams: W dimension	0,030	0,032	136,8	0,0
	front beams: H dimension	0,030	0,032	136,8	0,0
	internal circular surface thickness	0,170	0,179	137,4	0,6
	lateral circular surface	0,050	0,053	136,7	-0,1
	lateral square surface	0,090	0,095	135,9	-0,9
	top surface	0,152	0,160	136,7	-0,1


Table 5.1: Results of the sensitivity analysis with a variation of +5% of the parameters.




Table 5.2 shows the results of the sensitivity analysis gained with a variation of -5% of the parameters.

Part of the gearbox	Changing parameter	Reference value [m]	5% decreased value [m]	1 <sup>st</sup> natural frequency [Hz]	Variation of 1 <sup>st</sup> natural frequency [Hz]
1 <sup>st</sup> stage ring wheel	surface thickness	0,172	0,164	137,0	0,2
2 <sup>nd</sup> stage ring wheel	surface thickness	0,093	0,089	136,5	-0,3
Bearing housing	to 2 <sup>nd</sup> stage surface thickness	0,081	0,077	133,6	-3,2
	to HV stage surface thickness	0,108	0,103	135,4	-1,4
Intermediate bearing housing	inner surface	0,062	0,059	136,8	0,0
	outer surface	0,071	0,067	136,4	-0,4
Torque arm	central surface thickness	0,095	0,091	136,9	0,1
	lateral surfaces thickness	0,155	0,147	136,8	0,0
	lateral beams: W dimension	0,070	0,067	136,8	0,0
	lateral beams: H dimension	0,212	0,201	136,8	0,0
High speed stage housing	bottom greater surface thickness	0,067	0,064	137,1	0,3
	bottom smaller surface thickness	0,033	0,031	136,9	0,1
	front beams: W dimension	0,030	0,029	136,8	0,0
	front beams: H dimension	0,030	0,029	136,8	0,0
	internal circular surface thickness	0,170	0,162	136,2	-0,6
	lateral circular surface	0,050	0,048	136,9	0,0
	lateral square surface	0,090	0,086	137,7	0,9
	top surface	0,152	0,144	136,9	0,1

Table 5.2: Results of the sensitivity analysis with a variation of -5% of the parameters.

Reference value is the value of the parameter of the simplified gearbox such that the flapping mode is at 136.8 Hz

 >2Hz variation (in absolute value)

	>1Hz variation (in absolute value)
	>0.5Hz variation (in absolute value)
	>0.249Hz variation (in absolute value)

By observing the analysis 2 effects can be noted:

The first consists in an increase of thickness in some surface which can lead to an increase of the natural frequency. In this case, stiffness can be added by augmenting the thickness of the whole surface, or by placing some ribs on them.

The 2 parameters which show the greatest influence on the natural frequency in the sensitivity analysis, were identified: these are the thickness of the 2 surfaces which form the bearing housing.

1. The setting of some ribs in such surfaces was chosen.
2. The second effect consists in a thickness decreasing in some surfaces which can lead to an increase of the natural frequency.

It was chosen not to go deep into the strategy of decreasing the thickness of some surfaces in order to avoid to exceed any requirement of strength and stiffness of the gearbox. Indeed, as some surfaces already have a thickness of some centimetres, it was preferred to be sure to avoid some unwanted effects due to the lack of strength and stiffness, in the operational life of the structure.

## 5.2 Campaign of simulations

In the simulations campaign, the effects of some different configurations were investigated. Such configurations are characterised by different features of the added ribs, keeping the existing surfaces and beams at the thickness and

dimensions of the reference model. The goal of the simulations campaign is to investigate the most competitive configuration, aiming to the final comparison of the mass of the different studied possibilities.

Each configuration of ribs can have:

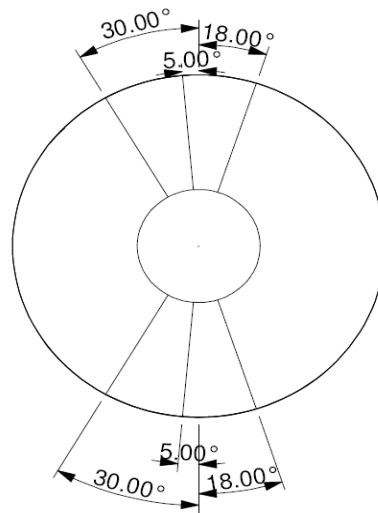
- varying dimensions (height and width) of the ribs
- a certain number of the ribs
- a certain inclination of the ribs

### **5.2.1 Illustration of the configurations**

Below the configurations used in the optimisation phase are illustrated and briefly described.

**1<sup>st</sup> layout: ribs in radial direction, 3 for each side.**

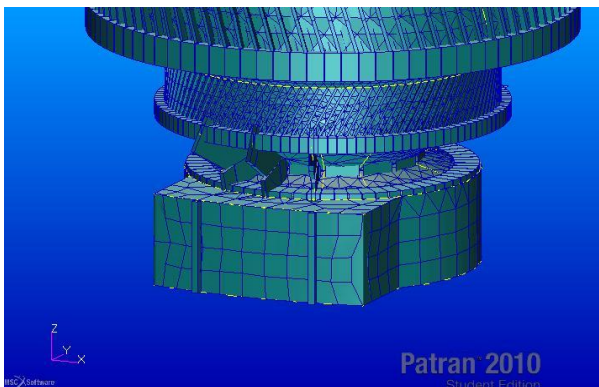
Back side



Front side

Figure 5.1: View of the ribs on the bearing housing from the top. The toroidal represents the bearing housing, and the radii are the ribs.

5.2/a. View of the front side



5.2/b. View of the back side

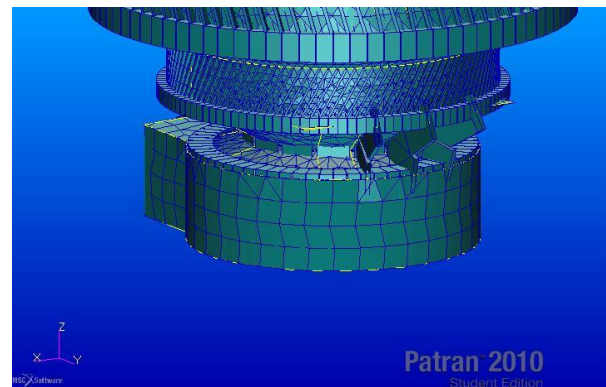
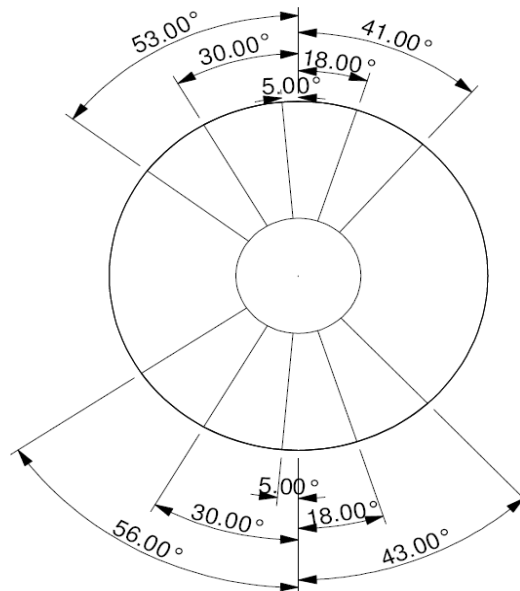


Figure 5.2: Views of the front (5.2/a) and back (5.2/b) side of the 1<sup>st</sup> layout of ribs. Pictures extracted from Patran.

**2<sup>nd</sup> layout: ribs in radial direction, 5 for each side.**

View of the ribs on the bearing housing from the top.

Back side



Front side

Figure 5.3: View of the ribs on the bearing housing from the top. The toroidal represents the bearing housing, and the radii are the ribs.

5.4/a. View of the front side

5.4/b. View of the back side

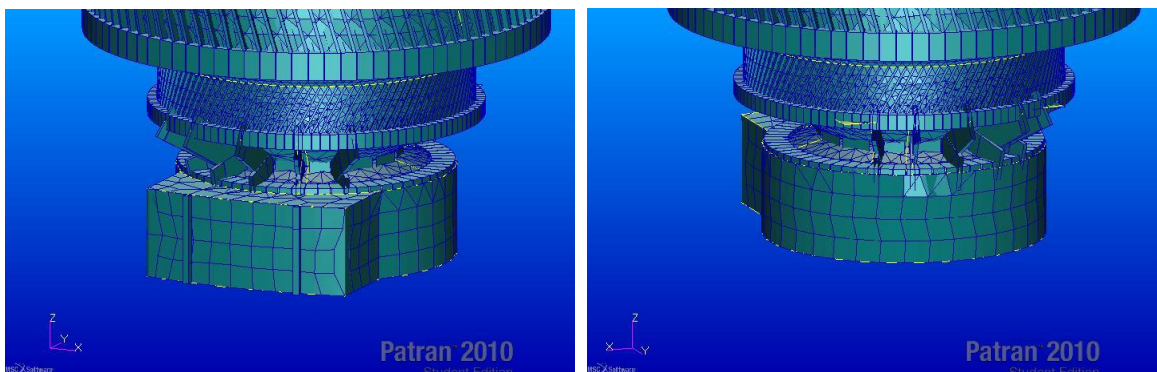


Figure 5.4: Views of the front (5.4/a) and back (5.4/b) side of the 2<sup>nd</sup> layout of ribs. Pictures extracted from Patran.

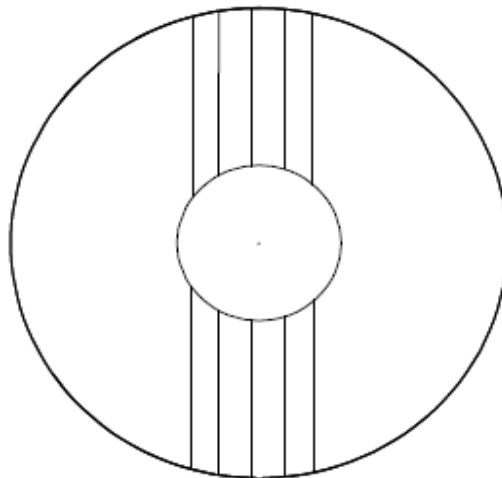


**3<sup>rd</sup> layout: ribs in y direction, 5 for each side.**

View of the ribs on the bearing housing from the top.

The angular positioning of the ribs is the same used in the configuration above. The change regards only the inclination of the ribs: they are all addressed toward the same direction (the y direction).

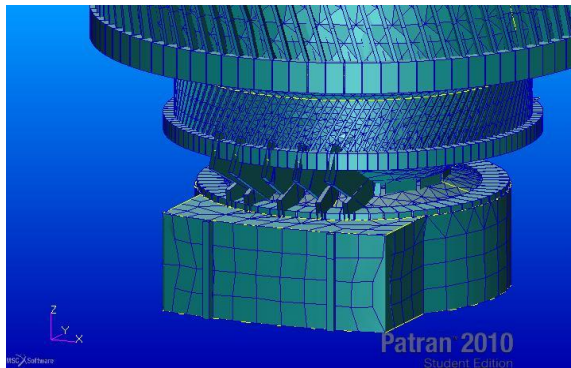
Back side



Front side

*Figure 5.5: View of the ribs on the bearing housing from the top. The toroidal represents the bearing housing, and the radii are the ribs.*

View of the front side



View of the back side

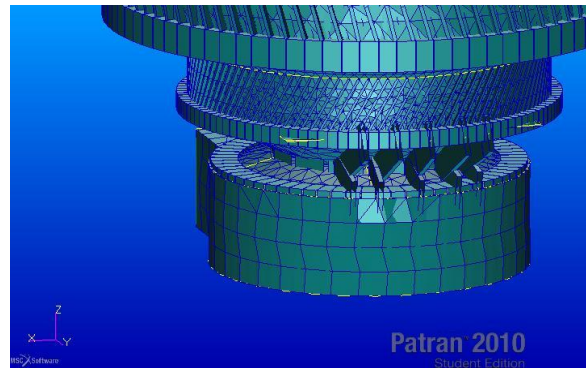


Figure 5.6: Views of the front (5.6/a) and back (5.6/b) side of the 3<sup>rd</sup> layout of ribs. Pictures extracted from Patran.

## 5.2.2 Results of the simulations

Below, results of the simulations of all configurations are collected.

**1<sup>st</sup> layout: ribs in radial direction, 3 for each side.**

Width of the ribs locked at 0.01 m

### 3 ribs for each side: radial direction

accuracy of positioning of ribs:  $\pm 0.05$  m and  $\pm 5^\circ$

Section's dimensions		Number of natural frequencies					
H [m]	W [m]	1 <sup>st</sup> [Hz]	2 <sup>nd</sup> [Hz]	3 <sup>rd</sup> [Hz]	4 <sup>th</sup> [Hz]	5 <sup>th</sup> [Hz]	6 <sup>th</sup> [Hz]
0	0	136.8	166.8	185.1	194.4	208.3	280.0
0.04	0.01	136.9	166.8	185.1	194.4	208.3	280.0
0.08	0.01	137.6	166.9	185.1	194.4	208.7	280.1
0.12	0.01	139.0	167.1	185.1	194.4	209.6	280.2
0.16	0.01	143.6	167.6	185.1	194.4	212.4	280.7
0.20	0.01	147.2	168.1	185.1	194.4	214.6	281.0
0.22	0.01	149.6	168.4	185.2	194.4	216.2	281.1
0.23	0.01	150.6	168.5	185.2	194.4	216.8	281.1

Mass	16770 kg
Volume	2.287 m <sup>3</sup>

Table 5.3: Results of simulations of 1<sup>st</sup> layout, with width of the ribs locked at 0.01 m.

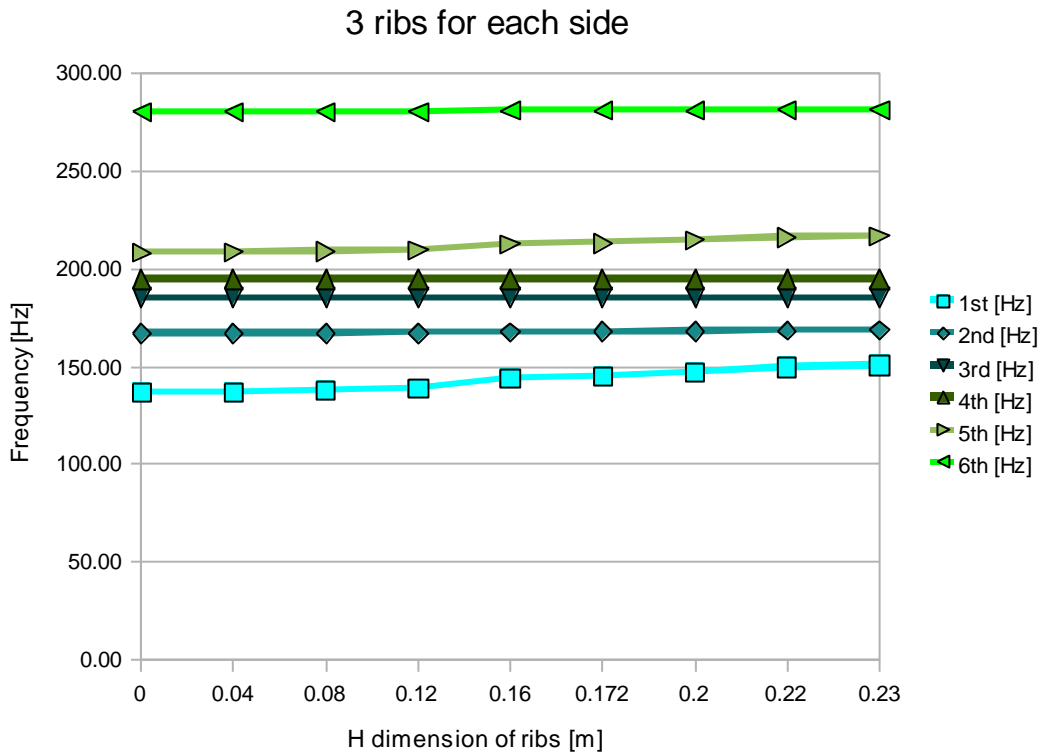


Figure 5.7: Natural frequencies resulting from simulations of 1<sup>st</sup> layout, in function of H dimension of ribs, with width of the ribs locked at 0.01 m.

W dimension locked at 0.02 m

**3 ribs for each side: radial direction**

accuracy of positioning of ribs:  $\pm 0.05$  m and  $\pm 5^\circ$

Section's dimensions		Number of natural frequencies					
H [m]	W [m]	1 <sup>st</sup> [Hz]	2 <sup>nd</sup> [Hz]	3 <sup>rd</sup> [Hz]	4 <sup>th</sup> [Hz]	5 <sup>th</sup> [Hz]	6 <sup>th</sup> [Hz]
0	0	136.8	166.8	185.1	194.4	208.3	280.0
0.04	0.01	136.9	166.8	185.1	194.4	208.3	280.0
0.08	0.01	137.6	166.9	185.1	194.4	208.7	280.1
0.12	0.01	139.0	167.1	185.1	194.4	209.6	280.2
0.16	0.01	143.6	167.6	185.1	194.4	212.4	280.7
0.172	0.01	144.7	167.7	185.1	194.4	213.1	280.8
0.20	0.01	147.2	168.1	185.1	194.4	214.6	281.0
0.22	0.01	149.6	168.4	185.2	194.4	216.2	281.1
0.23	0.01	150.6	168.5	185.2	194.4	216.8	281.1

Mass	16770 kg
Volume	2.287 m <sup>3</sup>

Table 5.4: Results of simulations of 1<sup>st</sup> layout, with width of the ribs locked at 0.02 m.

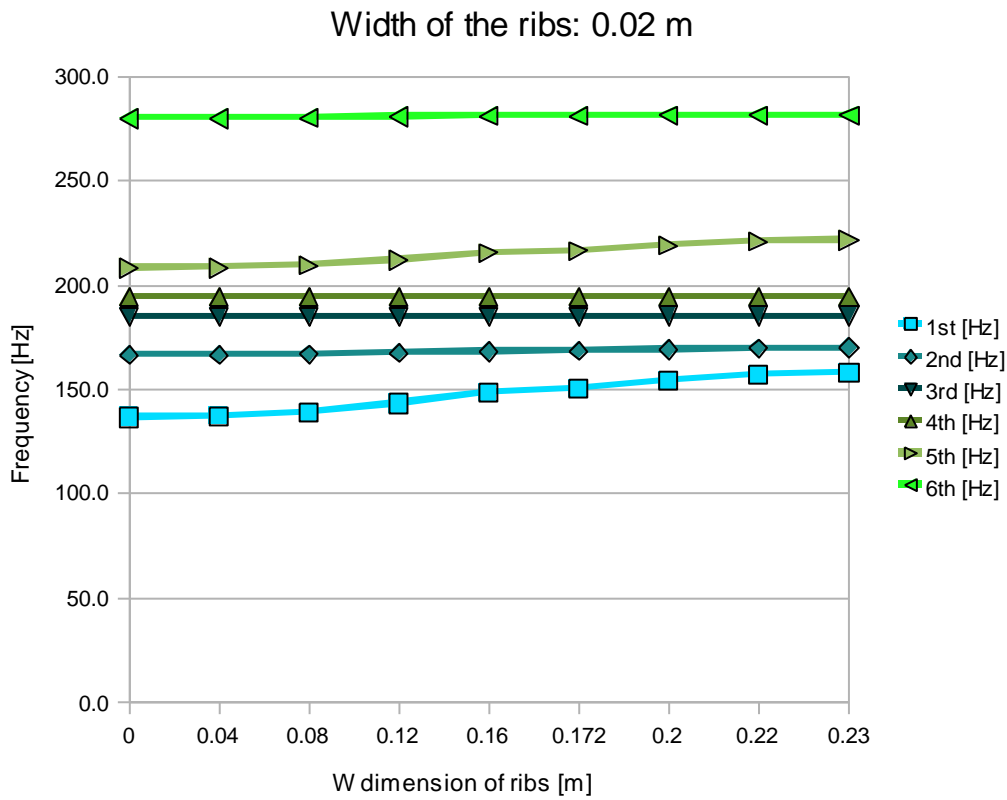


Figure 5.8: Natural frequencies resulting from simulations of 1<sup>st</sup> layout, in function of H dimension of ribs, with width of the ribs locked at 0.08 m.

**2<sup>nd</sup> layout: ribs in radial direction, 5 for each side.**

W dimension locked at 0.02 m

### 5 ribs for each side: radial direction

accuracy of positioning of ribs:  $\pm 0.05$  m and  $\pm 5^\circ$

Section's dimensions		Number of natural frequencies					
H [m]	W [m]	1 <sup>st</sup> [Hz]	2 <sup>nd</sup> [Hz]	3 <sup>rd</sup> [Hz]	4 <sup>th</sup> [Hz]	5 <sup>th</sup> [Hz]	6 <sup>th</sup> [Hz]
0	0	136.8	166.8	185.1	194.4	208.3	280.0
0.02	0.02	136.9	166.8	185.1	194.4	208.3	280.0
0.04	0.02	137.3	166.9	185.1	194.4	208.6	280.0
0.06	0.02	138.3	167.3	185.1	194.4	209.2	280.1
0.08	0.02	140.1	168.0	185.1	194.4	210.3	280.3
0.10	0.02	142.6	168.9	185.1	194.4	211.8	280.6
0.12	0.02	145.8	169.8	185.1	194.4	213.8	281.0
0.14	0.02	149.4	171.1	185.1	194.4	216.0	281.3
0.145	0.02	150.5	171.5	185.1	194.4	216.6	281.3
0.16	0.02	153.2	173.2	185.2	194.4	218.1	281.6
0.17	0.02	155.9	174.2	185.2	194.5	219.5	281.8
0.18	0.02	157.2	174.8	185.2	194.5	220.4	281.9
0.20	0.02	161.2	176.5	185.2	194.5	222.6	282.1
0.22	0.02	165.0	178.3	185.3	194.5	224.7	282.4

Mass	16840 kg
Volume	2.297 m <sup>3</sup>

Table 5.5: Results of simulations of 2<sup>nd</sup> layout, with width of the ribs locked at 0.02 m.

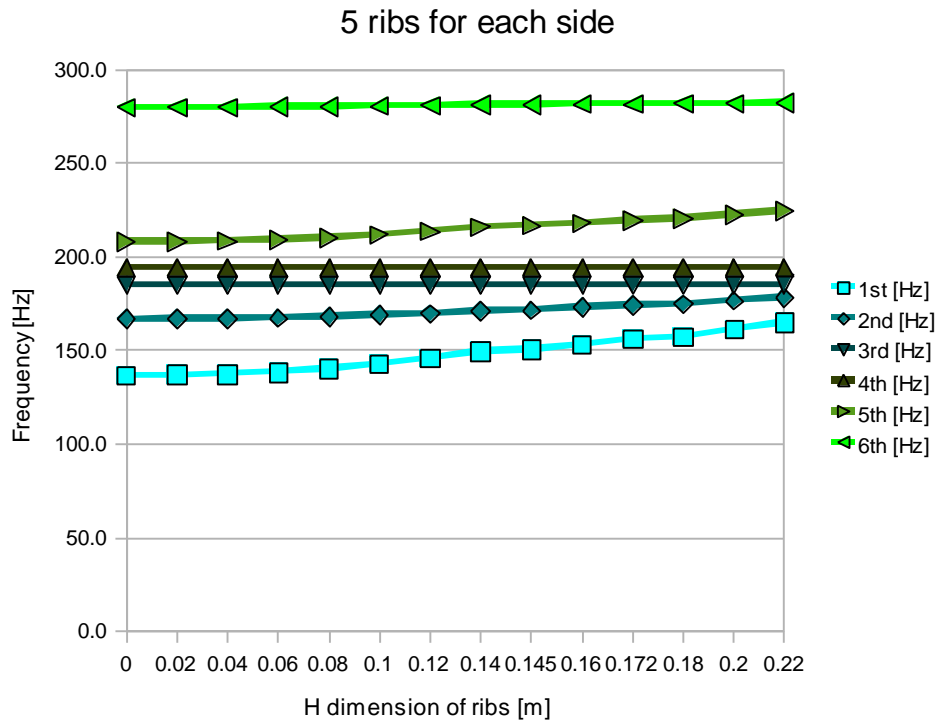


Figure 5.8: Natural frequencies resulting from simulations of 2<sup>nd</sup> layout, in function of H dimension of ribs, with width of the ribs locked at 0.02 m.

**3<sup>rd</sup> layout: ribs oriented in y direction, 5 at the back and 5 at the front side.**

W dimension locked at 0.02 m

**Ribs oriented in y direction**

accuracy of positioning of ribs: +-0.03 m and +-1°

Section's dimensions		Number of natural frequencies					
H [m]	W [m]	1 <sup>st</sup> [Hz]	2 <sup>nd</sup> [Hz]	3 <sup>rd</sup> [Hz]	4 <sup>th</sup> [Hz]	5 <sup>th</sup> [Hz]	6 <sup>th</sup> [Hz]
0	0	136.8	166.8	185.1	194.4	208.3	280.0
0.02	0.02	136.8	166.8	185.1	194.4	208.3	280.0
0.04	0.02	137.2	166.9	185.1	194.4	208.5	280.1
0.06	0.02	138.1	167.1	185.1	194.4	209.0	280.3
0.08	0.02	139.7	167.4	185.1	194.4	209.8	280.5
0.10	0.02	142.1	167.8	185.1	194.4	211.1	280.9
0.12	0.02	145.2	168.4	185.1	194.4	212.8	281.4
0.14	0.02	148.9	169.0	185.1	194.4	214.7	281.8
0.148	0.02	150.5	169.3	185.1	194.4	215.6	282.0
0.16	0.02	152.9	169.7	185.2	194.4	216.9	282.2
0.18	0.02	157.0	170.5	185.2	194.4	219.1	282.6
0.20	0.02	161.1	171.4	185.2	194.4	221.4	282.9
0.22	0.02	165.0	172.3	185.3	194.4	223.6	283.2

Mass 16860 kg  
Volume 2.299 m<sup>3</sup>

Table 5.6: Results of simulations of 3<sup>rd</sup> layout, with width of the ribs locked at 0.02 m.

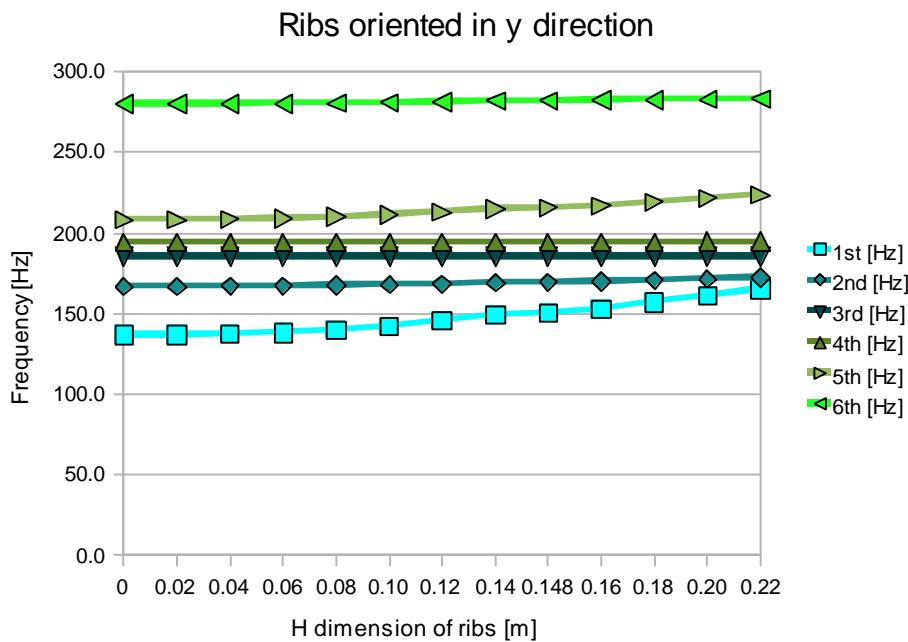


Figure 5.9: Natural frequencies resulting from simulations of 3<sup>rd</sup> layout, in function of H dimension of ribs, with width of the ribs locked at 0.02 m.

### 5.3 Verifications of the tolerance of any geometrical errors

It was considered not convenient to set the ribs at the exact position and inclinations, in order to have a perfectly symmetric geometry, as this would determine the building of a fine mesh to keep the geometry followed by the finite elements. By so doing, it would make the effective mesh slightly further from the need to have an accurate but light mesh. For that reason it was decided to accept to have not a perfect symmetry between the ribs, and to verify the effects of some entities of errors, both in the inclination and in the position of the ribs. These verifications showed the acceptability, in terms of natural frequency errors, of the imperfections which affect the position and inclination of the ribs.

2 kinds of error tolerances were verified. The first is the error of angular position of the ribs, and the second is the error of inclination of the ribs.

#### 5.3.1 First verification

The 4<sup>th</sup> layout, with 5 ribs at the front and 5 at the back side, was submitted to a variation of the angular positioning of its 5 front side ribs, in the quite pessimistic entities reported in the following table:

	<b>angular position of the 5 front side ribs</b>				
	<b>1<sup>st</sup> rib</b>	<b>2<sup>nd</sup> rib</b>	<b>3<sup>rd</sup> rib</b>	<b>4<sup>th</sup> rib</b>	<b>5<sup>th</sup> rib</b>
<b>Investigated layout</b>	-56°	-30°	-5°	18°	43°
<b>Verification layout</b>	-30°	-5°	18°	43°	65°

*Table 5.7: Comparison of angular position of the 5 front side ribs between the investigated and verification layout.*

Such verification values are greater than the errors committed in the performed simulations, and they were selected in order to be sure to have a correct interpretation of the attained results in the phase of optimisation.

Below, the views of the ribs on the bearing housing from the top are reported, for both layout. The toroidal represents the bearing housing, and the radii are the ribs.

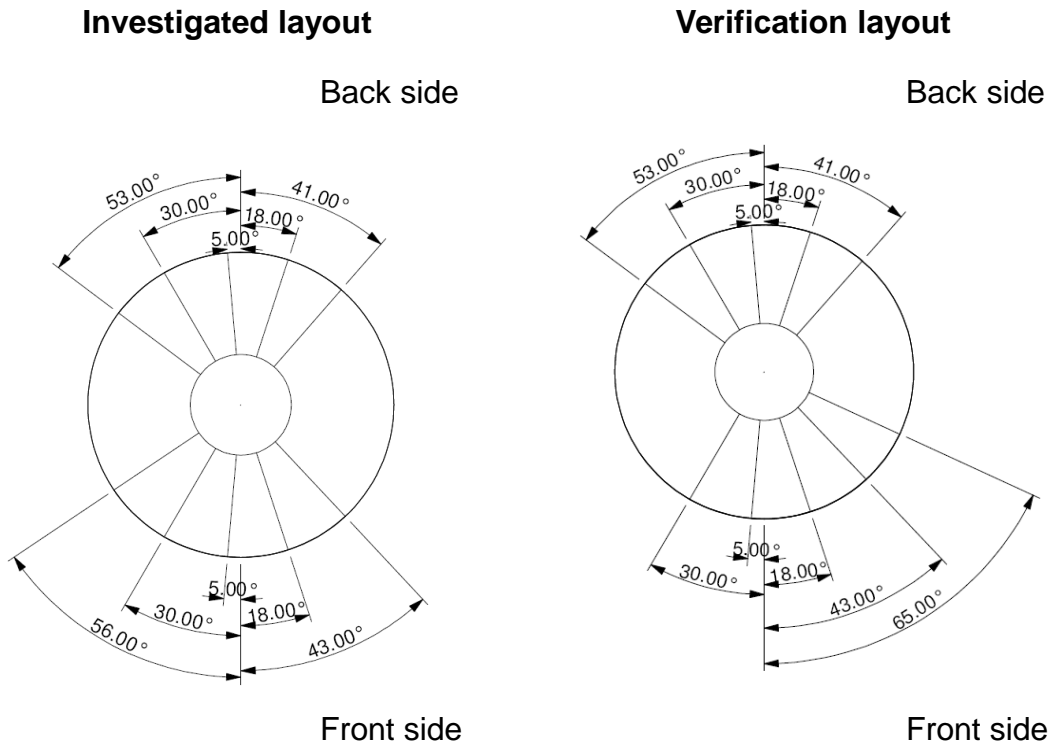


Figure 5.10: First verification: View of the ribs on the bearing housing from the top. The toroidal represents the bearing housing, and the radii are the ribs. On the left the investigated layout (5.10/a) is illustrated, and on the right the verification layout (5.10/b) is represented.

The following table shows the first natural frequency of the 2 configurations with 10 ribs (5 at the back and 5 at the front side) oriented in radial direction, with different angular position of the front side ribs. The difference, reported



also in the graphic, expresses the error in terms of first natural frequency induced by the angular positioning of the 2<sup>nd</sup> layout, compared to the values of the natural frequency gained with the first layout.

The width of the ribs is kept at 0.02 m

H [m]	1 <sup>st</sup> layout First natural frequency [Hz]	2 <sup>nd</sup> layout First natural frequency [Hz]	DIFFERENCE [Hz]
0	136,8	136,8	0,0
0,02	136,9	136,9	0,0
0,04	137,3	137,3	0,0
0,06	138,3	138,2	0,1
0,08	140,1	139,9	0,2
0,10	142,6	142,3	0,3
0,12	145,7	145,2	0,5
0,14	149,3	148,6	0,8
0,145	150,5	149,6	0,9
0,16	153,2	152,1	1,2
0,18	157,2	155,5	1,7
0,20	161,2	158,7	2,5
0,22	165,0	161,6	3,4

*Table 5.8: Error in terms of first natural frequency determined by the different angular position of ribs tested in the first verification.*

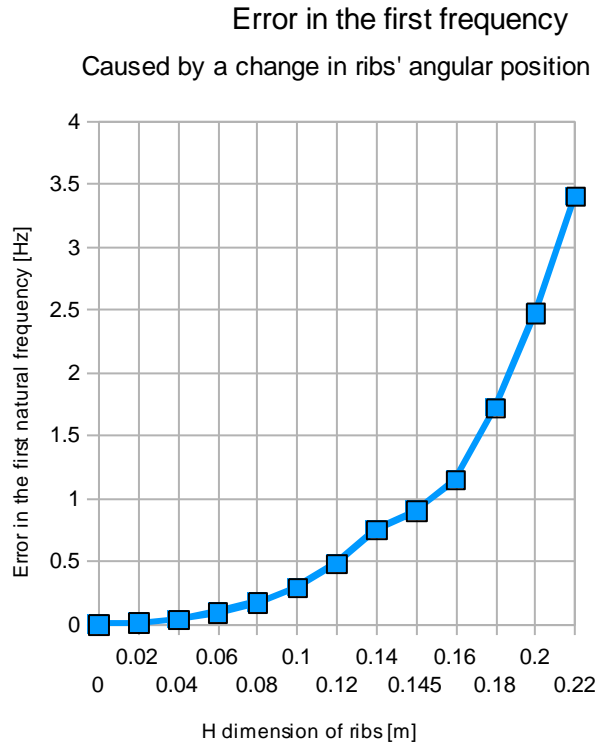


*Figure 5.11: Graphical representation of the error in terms of first natural frequency determined by the different angular position of ribs tested in the first verification, in function of H dimension of ribs.*

The results of this verification show a gap of slightly less than 1 Hz at the ribs' height values which make the natural frequencies of the structure exceed the 150 Hz. Thus, as a pessimistic entity of the errors was studied in this verification, it can be concluded that the errors of angular positioning of the ribs committed in the performed simulations can be neglected.

### **5.3.2 Second verification**

The second verification investigated the gap induced to the natural frequency

by some errors in the inclinations of the ribs. For this simulation the layout with ribs disposed in radial direction was taken, and the ribs were submitted to the angular change of the inclination listed in the following table and showed in the pictures below.

4 of the 10 ribs were changed in inclination, and they were selected casually. The entities of the inclination change were selected so as not to be greater than 10°, because in the investigated configurations there were not errors which exceeded this value.

The width of the ribs is kept at 0.02 m

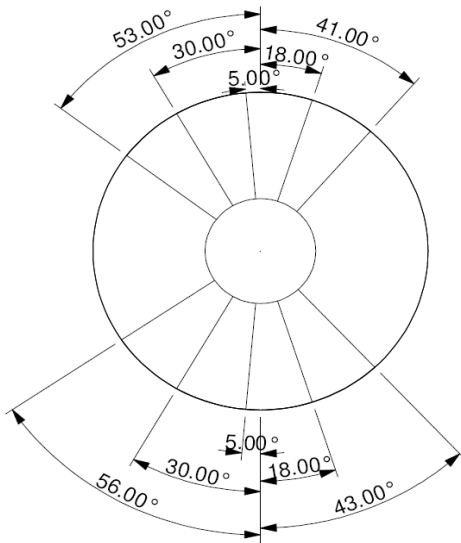
	<b>position</b>	<b>inclination change</b>
<b>1<sup>st</sup> rib</b>	back side	5° clockwise
<b>2<sup>nd</sup> rib</b>	back side	5° anticlockwise
<b>3<sup>rd</sup> rib</b>	back side	10° anticlockwise
<b>4<sup>th</sup> rib</b>	front side	5° anticlockwise

*Table 5.9: Inclination change of ribs for the second verification configuration.*

Views of the ribs on the bearing housing from the top, for both the compared layout. The toroidal represents the bearing housing, and the radii are the ribs.

**1<sup>st</sup> layout: ribs oriented in radial direction**

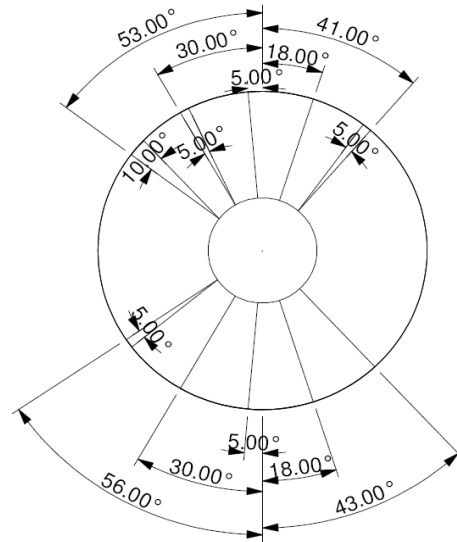
Back side



Front side

**2<sup>nd</sup> layout: Varied inclination of 4 of the 10 ribs**

Back side



Front side

*Figure 5.12: Second verification: View of the ribs on the bearing housing from the top. The toroidal represents the bearing housing, and the radii are the ribs. On the left the investigated layout (5.12/a) is illustrated, and on the right the verification layout (5.12/b) is represented.*

The following table shows the first natural frequency of the 2 configurations with 10 ribs (5 at the back and 5 at the front side) oriented in radial direction, with the differences in inclination collected in the table above. The difference, reported both in the table and in figure 5.13, expresses the error in terms of first natural frequency induced by the inclination of the ribs of the 2<sup>nd</sup> layout, compared to the values of the natural frequency gained with the first layout.

The width of the ribs is kept at 0.02 m

	<b>Ribs oriented in radial direction</b>	<b>Varied inclination of 4 of the 10 ribs</b>	
<b>H [m]</b>	<b>First natural frequency [Hz]</b>	<b>First natural frequency [Hz]</b>	<b>Difference [Hz]</b>
0,00	136,80	136,80	0
0,02	136,87	136,87	0
0,04	137,29	137,26	0,03
0,06	138,30	138,26	0,04
0,08	140,05	140,01	0,04
0,10	142,56	142,44	0,12
0,12	145,71	145,61	0,1
0,14	149,33	149,26	0,07
0,16	153,22	153,20	0,02
0,18	157,23	157,27	-0,04
0,20	161,20	161,27	-0,07
0,22	165,03	165,11	-0,08

*Table 5.10: Error in terms of first natural frequency determined by the different inclination of ribs tested in the second verification. Usually, frequency data do not need to be reported with two decimal places. In this case it has been done just for show the triviality of errors.*

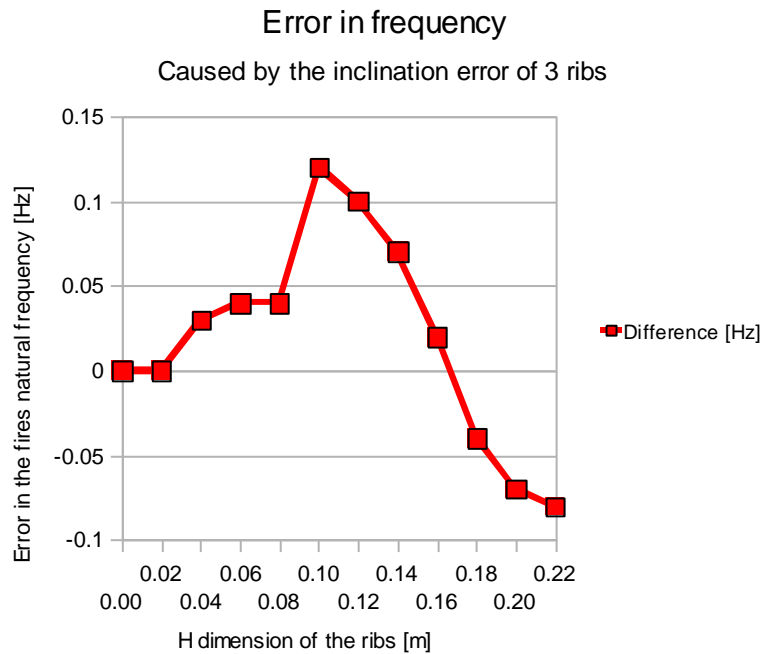


*Figure 5.13: Graphical representation of the error in terms of first natural frequency determined by the different inclination of ribs tested in the second verification, in function of H dimension of ribs.*

From the data collected, the errors in the first natural frequency induced by the changes of inclination of the ribs does not overcome the 0.15 Hz. Thus, this kind of error is totally negligible for the performed simulations.

## 5.4 Final comparison

The final step of the optimisation is the comparison of the gained results from the simulations, in order to determine what is the most convenient layout of ribs in terms of total mass.

To better appreciate the mass entity brought to the gearbox by the added ribs, another simulation is reported below: the reaching of the frequency goal was simulated with the only increase of a surface of the reference gearbox. The surface selected for testing the thickness variation was the one which in the sensitivity analysis showed the greatest influence on the natural frequency.

Gearbox without ribs and with only thickness variation of a surface: in table 5.11 the effects of a change of only the thickness of a surface of the bearing housing is shown. The value of the final thickness is the one which allows reaching the optimisation goal.

Configurati on	Initial thickness [m]	Final thickness [m]	1st natural frequency [Hz]	Total volume [m3]	Total mass [kg]	Added mass to the reference gearbox [kg]
a	0.081	0.103	150,5	2,309	16930	230

*Table 5.11: Features of the gearbox after undergoing a thickness increase at the surface of gearbox housing discussed above, in paragraph 5.4. This increase is made to bring all natural frequencies out from the [70 – 150 Hz] range.*

Gearbox with ribs: in the following table the investigated configurations are compared with regard to their total mass, as well as the mass saving they induce from the configuration a. This one is demonstrated to be inconvenient.

	Layout	Rib section [m] x [m]	1st natural frequency [Hz]	Total volume [m <sup>3</sup> ]	Total mass [kg]	Added mass to the reference gearbox [kg]	Mass saving from the configuration a [kg]
<b>b</b>	10 y-direction ribs	0.02 x 0.148	150,5	2,299	16860	160	70
<b>c</b>	10 radial ribs	0.02 x 0.145	150,5	2,297	16840	140	90
<b>d</b>	6 radial ribs	0.02 x 0.172	150,5	2,291	16800	100	130
<b>e</b>	6 radial ribs	0.01 x 0.23	150,6	2,287	16770	70	160

Table 5.12: Comparison between the tested solutions which bring all natural frequencies out from the [70 – 150 Hz] range. The better solution in terms of mass to add to the gearbox is underlined.

Given the frequency goal of the optimisation, the most competitive layout as regard the saving of mass is the one with 6 radial ribs, 3 at the front and 3 at the back side (indicated in yellow in table 5.12).

An observation of all the investigated configurations is interesting to track a path which can define which solutions should be followed in order to minimise the added mass.

If a stiffness-adding strategy is used to bring all the natural frequencies out of a frequency range, increasing the natural frequencies, and if a configuration which is optimised in terms of mass is searched, the following features should be approached:

- 1) ribs instead of surfaces with increased thickness
- 2) ribs oriented in a radial direction
- 3) low number of ribs
- 4) low width of ribs



# 6 Conclusions

## 6.1 Building a simplified model: considerations

The first goal of this thesis is to study an approach to get a simplified geometry of a wind turbine gearbox. Such a geometry has to represent the vibrational behaviour of the full gearbox model well, because it will support the second part of thesis, regarding NVH behaviour optimisation of the gearbox.

In order to obtain this simplified structure, at the beginning measurements of original gearbox dimensions were reproduced, where possible. In some areas of the structure, a precise ascertainment of parameters' measurement is difficult because of its marked geometrical irregularity. In these areas the values of parameters were approximated as well as possible to an average measurement of the original structure. After the modal analysis performed with Patran through SOL 103 solver and the comparisons by means of the Modal Assurance Criterion, geometrical parameters of beams and surfaces constituent the simplified gearbox were progressively varied until getting a model well-representing the full one in terms of modal behaviour. These variations are such as to keep the gearbox structure realistic. In chapter 3 parameters which determine a good correlation between the two models are defined.

The gearbox building process was divided into three steps, described in chapter 2. At each step, after completing a first version structure, changes of parameters of the overall gearbox were needed. Variations of parameters which belong only to that specific gearbox part were not sufficient to obtain a good modal correlation while keeping the structure realistic.

From the performed modal analysis and given the approximations made, it can be concluded that generally the large components of structure must necessarily be at least sketched. By large components it is intended beams and surfaces which clearly characterise the structure, or at least the structure building step. Such components in the simplified model can take a slightly different size, or they can slightly change their shape or offset from the original ones, if these variations benefit the modal correlation with the full model. These variations from the full model must be accounted by globally considering the whole structure or the structure part. Indeed, approximations and slight shape variations of an area should be considered in view of other areas which are adjacent to the first one, because often an approximation has to be compensated by another one.

As regards median dimension components, different considerations have to be taken into account. When considering the gearbox as a cylinder, and thus having an axial and radial dimension, then median dimension components are beams or surfaces which have a size that is non-negligible with respect to the radial or axial dimensions of the gearbox. In most cases these components have to be built, and their approximation can be more marked than the mentioned approximations of large components.

In some cases median dimension components may produce negligible effects on modal behaviour of the simplified structure. This is the case of the irregularities in the bottom surface of the high speed stage housing. Such irregularities were approximated to beams, but their presence produced negligible effects both on values of natural frequencies and on modal shapes of the first 10 vibrational modes. For that reason, they were not included in the simplified model.

Small components like holes and small irregularities could be approximated with shells or beams, but are negligible as their dimensions are less than a

tenth of axial and radial dimensions of the gearbox. In order to keep a general simplification of the structure, these features have not been built in this thesis. However, if they are densely present in an area, it is worth considering their presence globally. For example, the lateral and bottom surfaces of the high speed stage housing are full of small imperfections, holes and protrusions. They were taken into account in the simplified model and represented as additions or reductions of thickness of those surfaces.

Generally, It is necessary to understand if the detail, consisting in added or reduced mass respect to the surrounding area, can be represented in the simplified model as a variation of stiffness or a change of mass, (in the latter case emphasizing the modal shape and anticipating the natural frequency in question). Such a consideration is related to the modal shape and the modal mass of the case. Modal mass is the mass participating to the vibrational mode.

When building the simplified model with 1D and 2D elements, the time necessary for construction is certainly greater than the time a simple importation of the full model to FEM software would need. If the investigation of an optimisation strategy is required, several analysis of different configurations are necessary. Performing such a large amount of analysis through a 3D structure characterised by hundreds of thousands of nodes would be extremely demanding in terms of computational time and resources.

The choice of an optimisation strategy based on a simplified model is disadvantageous for eigenmodes after the first 5 – 10, depending on the extent of approximations made. However, the advantages of this choice consist of extremely short computational time and computational resources easily available for any modern calculator. Thus, such a kind of approach is particularly suitable for understanding what is the best optimisation strategy to

use. Moreover, a simplified model which well represents the real structure, is particularly suitable to perform innovative optimisation approaches, which are characterised by a poor background literature. Indeed, in case of unsatisfactory results obtained by the eventual innovative approach, the lost resources in terms of time will be trivial. Therefore, an optimisation approach through simplified model provides an incentive to the investigation of new configurations for NVH behaviour optimisation.

Thanks to global technological development, calculation possibilities are constantly improving as computational time decreases and large computational capacities are more and more easily within the reach of industries. Thus, likely 3D elements calculations will be less expensive in the future and more easily usable as well. However, nowadays and in the near future computations which are very demanding as for 3D structures characterised by a great amount of nodes, are affected by important disadvantages, as mentioned above. For that reason, structure simplification from 3D to 2D has an important role currently, and understanding where and how it can be improved and what kind of errors it can determine in different circumstances has a key role in its improvement.

## **6.2 Conclusions about comparison phase in three different building step**

The gearbox building process was divided into three steps, as mentioned above. This division has the purpose of facilitating the construction, which gradually proceeds in such a way, instead of being performed in a single act.

Furthermore, if structure development is divided in multiple steps, constructor becomes familiar with the structure sensitiveness. This is a considerable aspect, because at the final steps a variation of several parameters of the whole structure is likely required.

In the comparison phase, results of a good correlation were different for the three construction steps. At the first step, after some little corrections the simplified torque arm showed soon a good correlation with the full torque arm. In this case, geometry was still relatively simple. Indeed, at the end of this step it was obtained the best modal correlation between simplified and full model, among all steps.

At the second step geometry is more complex. After a first version of gearbox without high speed stage housing, it was necessary to perform a second version, without varying the geometry, but only modifying the already existing parameters like thickness of surfaces and section's dimensions of beams. In this case changing some parameters of the torque arm was necessary as well. This happened for the third step too. For that reason it can be concluded that in a simplified model approach with a building strategy divided into different steps, modal correlation reached at the end of each step could not definitively determine the already built geometry, but it is an approximate confirm of starting parameters for the next step.

At the third step, the geometrically most complex part was added. Given such complexity, it was decided to test a first approach in which a heavily simplified version of high speed stage housing was built. After the comparison phase for this step, it was concluded that a second version with more details was required. Thus, in this case the geometry was rebuilt, adding the details described in paragraph 3.4. Table 3.9 is important to understand the effects on eigenmodes brought by each change. The performed geometry changes

led to a shift of all eigenmodes of interest, and then changing many parameters was necessary in order to achieve the final good correlation.

With the progressive completing of the overall structure, the number of well related eigenmodes decreased. Indeed, while at the end of the second step the correlation regarded 9 eigenmodes, at the end of the third step there were 6 eigenmodes well related to the full model. For that reason it is important to get an as good as possible correlation since the beginning of the construction phase.

### **6.3 Considerations about optimisation results**

The other goal of this thesis is the optimisation of the simplified geometry obtained by the previous operations, in order to get optimal NVH features. This optimisation required to bring all natural frequencies out from the [70 – 150 Hz] range.

The investigation involves only the eigenmodes which were found well related to the full model. Thus, in this case the optimisation takes the first 6 vibrational modes into account.

The chosen optimisation strategy starts with a sensitivity analysis which indicates the ideal areas which have a big influence on the modeshapes. Options are adding or removing stiffness. The option of adding stiffness was preferred, so as to not remove material and to not approach the possibility of exceeding any strength or stiffness requirement of the gearbox. Two ways were investigated to add stiffness: addition of ribs and increase of thickness. Both possibilities were applied to surfaces indicated by the sensitivity analysis. Addition of ribs was tested in many configurations, as reported in chapter 5. For each configuration, once the frequency goal was reached, the

mass value was extracted by means of a quick calculation made by Patran. In such a way, the configuration which reaches the frequency goal with less mass could be found. Indeed, it was decided to perform the optimisation attaining the vibrational goal and minimising the mass, still keeping realistic dimensions and shape of the performed variations.

Inherently to the optimisation, two types of verification were performed. Such checks have the purpose of evaluating the error values that eventual geometrical imperfections in the simplified model determine to the natural frequencies. Verifications were made considering only the first natural frequency, because in every configuration only this natural frequency is within or close to the goal frequency range. Two kinds of error were submitted to this check: the angular position and the inclination of ribs. The first type can determine errors up to about 1 Hz, and the second kind up to about 0.1 Hz, as showed in paragraph 5.3. It can be concluded that the angular positioning leads to a larger error. However, both kinds of error can be neglected in the simulated configurations, because the error due to inclination is very small, and the error determined by angular positioning, despite it reaches about 1 Hz, is due to a large geometrical error, as illustrated in table 5.7 and in figure 5.10. For those reasons, all the performed simulations can be accounted free from considerable errors.

Usually, mass minimisation is wanted because it brings an economical saving which not only is due to the mere material saving, but to the facilitation in the handling of the structure as well. Furthermore, depending on the scope of the work, mass saving leads to reduction of system requirements, so as to allow further economical benefits.

In wind turbines, the support for the operating equipment is provided by the tower and the nacelle's bed plate. Therefore, at the starting phases of

optimisation, given the outlook of mass addition to reach the frequency goals, it was evaluated that the minimisation of mass has primary importance in order to attain an optimal set of features in achieving the NVH objectives.

The final comparison of paragraph 5.4 shows that the less expensive configuration in terms of mass is characterised by 6 radial ribs: 3 at the front and 3 at the back side, with 0.01 m of width.

Such data are considerable in order to identify this configuration as optimal. However, they are particularly useful to qualitatively determine that configurations characterised by ribs are better than an increase of thickness of a whole surface. Moreover, a radial rib layout is worth instead of a unidirectional rib layout, and having a few ribs and with small width is convenient.

Several configurations with ribs are possible and can be better than those investigated in this work. For that reason the optimisation results attained are particularly useful to indicate a good optimisation path.

Likely further investigations about different configurations with ribs could allow a final mass saving which would be less decisive than the ones studied in chapter 5. Indeed, tables 5.11 and 5.12 show that great amount of mass saving is allowed by the use of ribs instead of a thickness increasing on the whole surface, and by the use of a few radial tight ribs. The first choice determines from 70 to 160 kg saved, and the second choice leads up to 90 kg of mass saving. The best configuration needs 70 kg to add to the original gearbox. Thus, although there is still room for mass saving among these 70 kg, likely it would be small compared to the already reached mass savings which were investigated in this work.



However, it would be interesting to search a better configuration not only through other combinations of ribs, as for example considering different numbers of ribs at the front from the back side, as well as the use of ribs of different sizes from one another (while in this work all ribs have the same sizes at each simulation). It would be interesting to investigate other solutions with ribs characterised by other shapes as well, and with other devices which are different from ribs, or devices utilising different materials.

More generally, improving the wind turbines NVH behaviour compatibly to their functionalities is a very lively topic currently, and the development of new technologies and ideas as well as a strong believe in these efforts are a good hope for the future.



# Bibliography

[1.1] T. PRUGH ET AL. World Watch magazine. Volume 19, number 1. (January-February 2006)

[1.2] [www.iea.org](http://www.iea.org)

[1.3] A. ARSUFFI, G. ARENA. Energia eolica. Quaderni dell'ENEA.(July 2011)

[1.4] K. RAVE, S. TESKE, S. SAWYER. Global Wind Energy Outlook 2012. (November 2012)

[1.5] F. PONTA ET AL. Innovative Concepts in Wind-Power Generation: The VGOT Darrieus, Wind Turbines. Michigan Technological University, USA. April 2011.

[1.6] M. R. PATEL. Wind and Solar Power Systems.

[1.7] T. ACKERMANN. Wind Power in Power Systems. Royal Institute of Technology, Stockholm, Sweden. 2005.

[1.8] From [www.elek.com.au](http://www.elek.com.au): State-of-the-art Review of Wind Turbine Technologies. Technical Publication 2008-0502 ElectroTECHnic. Pty Ltd.

[1.9] P. W. CARLIN ET AL. The History and State-of-the-Art of Variable-Speed Wind Turbine Technology. Technical Report. National Renewable Energy Laboratory. February 2001.

[1.10] J. PEETERS. Simulation of Dynamic Drive Train Loads in a Wind Turbine. Katholieke Universiteit Leuven. PhD dissertation.

[1.11] Risø and DNV. Guidelines for Design of Wind Turbines. Det Norske Veritas (DNV) and Wind Energy Department, Risø National Laboratory. 2002.

[1.12] [www.renewable-energy-concepts.com](http://www.renewable-energy-concepts.com)

[1.13] S. MALHOTRA: Selection, Design and Construction of Offshore Wind Turbine Foundations. Wind Turbines. Chapter 10

[1.14] J. M. JONKMAN. Dynamics Modeling and Loads Analysis of an Offshore Floating Wind Turbine. Technical Report. National Renewable Energy Laboratory. November 2007.

[1.15] A. L. ROGERS ET AL. Wind Turbine Acoustic Noise. University of Massachusetts at Amherst. June 2002, amended in January 2006.

[1.16] H. STIESDAL. The Wind Turbine. Components and Operations. Bonus-Info-1998 newsletter.

[1.17] K. R. TILL. Design Overview of Large Ductile Iron Casting Wind Turbine Generator Components. Clipper Windpower. October 27<sup>th</sup>, 2010.

[1.18] J. HELSEN. The dynamics of high power density gear units with focus on the wind turbine application. Katholieke Universiteit Leuven. PhD dissertation. February 2012.

[1.19] J. HELSEN ET AL. Insights in wind turbine drive train dynamics gathered by validating advanced models on a newly developed 13.2MW dynamically controlled test-rig. *Mechatronics*, Volume 21, Issue 4, June 2011, Pages 737-752. Copyright 2011 Elsevier Ltd. Pay access: 31.50 \$

[1.20] [www.sandvik.coromant.com](http://www.sandvik.coromant.com)

[1.21] R. Citarella, L. Federico, A. Cicatiello: Modal acoustic transfer vector approach in a FEM–BEM vibro-acoustic analysis.

[1.22] A. F. SEYBERT ET AL. Acoustical Analysis of Gear Housing Vibration. NASA Technical Memorandum 103691. Prepared for American Helicopter Society Technical Specialists Meeting Philadelphia, Pennsylvania, October 15-16, 1991.

[1.23] F. VANHOLLEBEKE ET AL. Combining multibody and acoustic simulation models for wind turbine gearbox NVH optimisation. ZF Wind Power Antwerpen NV. Belgium.

[1.24] [www.people.bu.edu](http://www.people.bu.edu)

[1.25] A. L. ROGERS. Wind Turbines Noise Issues. Renewable Energy Research Laboratory. June 2002. Amended March 2004.

[2.1] B. G. FALZON, U. GALVANETTO. Finite elements. 2007-2011.

[3.1] M. PASTOR. Modal Assurance Criterion. 2012. Procedia Engineering 48 (2012) 543–548.



# Ringraziamenti

La presente tesi ed il conseguimento del relativo traguardo sono stati possibili grazie agli insegnamenti, al supporto ed agli sforzi dei miei genitori e di mio fratello Alessandro. A voi dedico questa tesi.

Thanks to Frederick, whose patience and kindness were proportional to the distance which kept us away during the development of this work.

Ringrazio il prof. Zaccariotto per i suoi sforzi e per la sua cortesia, che hanno reso possibile il conseguimento della mia laurea nella data prefissata.

Ringrazio mio zio Angelo, per il suo grande affetto e sostegno.

Ringrazio i miei amici Daniele, Matteo, Enrico, Alessandro, Riccardo, Filippo, Davide e Marco per questi anni trascorsi insieme che rimarranno per sempre nel mio cuore, come la nostra grande e sincera amicizia.

Ringrazio i miei compagni di avventure universitarie Giacomo, Alessandro, Stefano, Riccardo, Sara e Pierantonio per gli indimenticabili momenti passati insieme e per la loro incredibile capacità di ravvivare qualsiasi situazione. Un grazie particolare a Laura, con cui ho trascorso giornate e notti intense, il cui pensiero susciterà sempre in me un sorriso.